Utah Geological Survey

LONG RECURRENCE RECORDS FROM THE WASATCH FAULT ZONE, UTAH

Program Element II.5: Identify active faults, define their geometry, and determine the characteristics and dates of past earthquakes

Final Technical Report

Contract 99HQGR0058
National Earthquake Hazards Reduction Program
U.S. Geological Survey

Principal Investigator:
James P. McCalpin
GEO-HAZ Consulting, Inc.
P.O. Box 1377, 1221 Graves Ave.
Estes Park, CO 80517
OFFICE: (970) 586-3217
FAX: (970) 577-0041
www.geohaz.com/geohaz

Co-PI
Craig V. Nelson
URS Corporation
Salt Lake City, UT 84102-1959
craig_nelson@urscorp.com

May 24, 2000

This report was prepared under contract to the U.S. Geological Survey and has not been reviewed for conformity with USGS editorial standards and stratigraphic nomenclature. Opinions and conclusions expressed herein do not necessarily represent those of the USGS. Any use of trade names is for descriptive purposes only and does not imply endorsement by the USGS.

TABLE OF CONTENTS

1. ABSTRACT 4
2. INTRODUCTION 5
3. GEOLOGIC AND GEOMORPHIC SETTING OF THE MEGATRENCH SITE 5
3.1 Location and Local geology 5
3.2 Site Geomorphology 9
3.3 Previous Trenching Study of Woodward-Clyde Consultants (1979) 9
4. STRATIGRAPHY, SOILS, AND GEOCHRONOLOGY 12
4.1 Mapping conventions 12
4.2 Lacustrine units 12
4.3 Loess 19
4.4 Alluvial units 21
4.5 Colluvial units 22
4.5.1 Colluvium in the eastern and central parts of the trench 22
4.5.2 Colluvium in the western end of the trench 23
5. STRUCTURE 25
5.1 Overview 25
5.2 Fault zone F1 26
5.3 Fault zone F2 26
5.4 Fault zone F3 26
5.5 Fault zone F4 26
6. SEQUENCE OF FAULTING EVENTS 26
7.1 Overview 26
7.2 Fault zone F1 27
7.3 Fault zone F2 29
7.4 Fault zone F3 29
7.5 Fault zone F4 31
7. CONCLUSIONS 36
7.1 Comparison of Previous Paleoearthquake Chronologies 36
7.2 Physical Causes of Variable Earthquake Recurrence 38
7.3 Implications of the Megatrench Results for Probability Estimates of Future Earthquakes on the SLC Segment 39
8. REFERENCES 41
9. APPENDICES 42
9.1 Appendix 1; Trench unit descriptions 42
9.2 Appendix 2; Graphs showing calibration of radiocarbon age to calendar years 47

List of Figures **Page**

Fig. 1. Location map of study area 6
Fig. 2. Geologic map of the central Cottonwood section of the SLC segment. (a) Insert Map from Personius and Scott, 1992; (b) Enlargement showing location of the megatrench in relation to the four 1979 trenches 7
Fig. 3. 3-dimensional perspective map of the megatrench site; contour interval 20 ft 10
Fig. 4. Photograph of the megatrench, looking from toe to head 11
Fig. 5. Log of the megatrench 13
Fig. 6. Enlarged trench logs. (a) Eastern 1/3 of trench; (b) Central 1/3 of trench; (c) Western 1/3 of trench 15
Fig. 7. Schematic cross-sections before, during, and after Event T at ca. 16 ka 16
Fig. 8. Retrodeformation sequence for fault zone F1 28
Fig. 9. Elevation of the shoreline of Lake Bonneville as a function of time (uncalibrated radiocarbon years before present, in thousands). All elevations have been corrected for isostatic rebound. Because both faulting and rebound have affected the elevation of the shoreline at our site, we merely plot the time interval (vertical dashed box) within which the lake shoreline was less than 25 m below the highstand shoreline (horizontal dashed box). From Oviatt, 1997 30
Fig. 10. Retrodeformation sequence for fault zone F4 32
Fig. 11. Simplified retro sequence for the entire megatrench, from 17 ka to present. (a) Steps 1-8, 17 ka to 14.5 ka; (b) Steps 8-15, 14.5 ka to ca. 7 ka; (c) Steps 16-21, ca. 7 ka to present 33
Fig. 12. Space-time diagram of paleoearthquakes dated in previous studies, and in the Megatrench 37

List of Tables

Table 1. Radiocarbon samples collected and dated in this study 20
Table 2. Summary of age constraints on the latest four faulting events in fault zone F1 27
Table 3. Summary of age constraints on the latest four faulting events in fault zone F4 36
Table 4. Age estimates for paleoearthquakes on the SLC segment from Black et al. (1996) 36
Table 5. Probability estimates of M>7 earthquakes in the next 100 years for the SLC segment 39

1. ABSTRACT

The Wasatch fault "megatrench" was excavated in Sept. 1999 across an 18 m-high double-scarp of the Salt Lake City segment of the Wasatch fault zone (WFZ), 1 km north of the mouth of Little Cottonwood Creek. The trench and accompanying auger hole exposed 26 m of vertical section, roughly 4 times that of the typical trench on the WFZ. Each of the two fault scarps transected were underlain by normal faults with 7-9.5 m of vertical displacement measured on the top of Bonneville-age lake beds (ca. 15,500 years old). Each fault was fronted by 3-4 colluvial wedges, indicating 3-4 post-Bonneville faulting events on each fault. The one surprise in the trench was the existence of a thick buried soil developed atop the lake beds and underlain by scarp-derived colluvium. This soil argues for a long period of fault inactivity between ca. 9,000 years ago and 15,500 years ago. That time span is roughly 4 times as long as the typical intervals between major earthquakes on this segment of the WFZ. The quiescent interval could be either an irregularity typical of the long-term behavior of the WFZ, or a response to the drying up of Lake Bonneville between 15,000 years ago and ca. 11,000 years ago, which relieved a huge weight on the downthrown fault block of the WFZ. If it was an unloading effect, it died out by the time of Event W, and that it has not affected the regular 1300-1400 year recurrence cycle since that time. Therefore, we do not propose to favor or disfavor any of McCalpin and Nishenko's recurrence models based on the long recurrence times observed while the lake was drying up.

However, we can apply the results of some more recent recurrence studies to the likelihood of the various recurrence models. For example, the highest 100-year conditional probability calculated by McCalpin and Nishenko (1996) was 57%, based on a Weibull model of recurrence with a mean of 1328 years and a COV of only 0.04. By comparison, conditional probabilities based on lognormal models with COVs of 0.21 and 0.5 indicated probabilities of 22% and 11%, respectively (Table 5). So, is the COV of long-term recurrence on the SLC segment closer to 0.04, 0.21, or 0.5?

McCalpin and Slemmons (1998) inventoried all published paleoseismic chronologies that contained 3 or more well-dated events. They found that, as a group, worldwide normal faults with a large span of slip rates and mean recurrences tended to have an average COV of recurrence of 0.35. The same data set for all fault types yielded an average COV of recurrence of 0.36. In addition, the more paleoearthquakes that had been dated at a local trench site, the closer the COV of that local recurrence series approached 0.36. McCalpin and Slemmons argued that a relatively short recurrence series at a site (say, containing only 3-4 events, or 2-3 recurrence intervals) could yield a wide possible range of recurrence COVs, ranging from ca. 0.04 to 0.8. However, the site chronologies with successively more events tended to have COVs that converged on the value 0.36. They further argued that, for the purposes of making conditional probability estimates, it would be preferable to use the value COV=0.36 rather than use an "apparent" COV value from a short (3-4 event) recurrence series.

Their conclusions suggest that we should probably not lend much weight to the probability estimate of 57% in Table 5, which is based on a COV=0.04 from only 4 events on the SLC segment. Instead, we should probably assume a long-term recurrence COV of 0.36 for the SLC segment. Note that 0.36 falls almost exactly halfway between the COVs of 0.21 and 0.5, which resulted in probability estimates of 22% and 11%, respectively, for the next 100 years. If we assume that conditional probability varies linearly with COV over this relatively small range, then an assumed recurrence COV=0.36 would imply a conditional probability of 16% for M>7 earthquakes in the next 100 years.

2. INTRODUCTION

Our goal is to excavate a deep enough trench into the Wasatch fault zone to expose evidence of all (8-12?) paleoearthquakes that postdate the abandonment of the Bonneville Shoreline (ca. 14.5 ka). We would then attempt to date these paleoearthquakes to define a series of 7-11 recurrence intervals at a single site. The mean and variability of recurrence would then be compared to the recurrence values deduced previously for that fault segment, by shallower trenches and/or the ergodic substitution for the whole WFZ (McCalpin and Nishenko, 1996). If the variability of the long records is similar to that predicted by the ergodic substitution, then we will not only have more confidence in applying ergodic results to the WFZ, but to other faults as well.

In order to capture the post-Bonneville paleoearthquakes on the WFZ we have to trench a Bonneville-age (or older) geomorphic surface, rather than the mid-Holocene alluvial fans traditionally trenched by prior investigations. Our trench site is located about 1 km north of the mouth of Little Cottonwood Canyon, on the north flank of the latest glacial moraine (age ca. 20 ka). This site had previously been trenched by Woodward-Clyde Consultants in 1979, when 4 trenches about 3 m deep were excavated. However, due to the shallowness of those trenches, the unstratified nature of graben fill, multiple fault strands that were not trenched, and the lack of datable material, few firm conclusions could be made about the chronology of Holocene faulting at the site. This site is unique in that it encompasses transition zones in both geomorphology and structure, as described below.

The megatrench was excavated from Sept. 13-17, 1999 across the two subparallel scarps that compose the main scarp of the WFZ; together these scarps have 18 m of vertical relief. The trench was a excavated in a benched style, with two 1.5 m-high walls leading down to two 1 m-wide bench levels, and then a 3-4 m-deep inner slot 1 m wide (Fig. 1). Altogether the trench exposed 23 m of vertical exposure. An additional 3 m of vertical "exposure" was gained by drilling a 3 m-deep hollow-stem auger hole at the toe of the trench.

3. GEOLOGIC AND GEOMORPHIC SETTING

3.1 Location and Local geology

The Salt Lake City (SLC) segment of the Wasatch fault zone (WFZ) extends for about 46 km at the base of the Wasatch Mountains from the Traverse Mountains on the south to the Salt Lake salient on the north (Fig. 1). The SLC segment displays abundant geologic and geomorphic evidence for multiple surface-faulting earthquakes during Holocene time (Schwartz and Coppersmith, 1984). Fault scarps on Bonneville-age (ca. 15 ka) deposits tend to be 20-25 m high, on Provo-age (ca. 13 ka) deposits are 10-15 m high, on early Holocene alluvial fans 5-8 m high, and on late Holocene alluvial fans 2-5 m high. Personius and Scott (1992) subdivide the SLC segment into a southern Cottonwood section, a shorter central East Bench fault, and an even shorter northern Warm Springs fault (Fig. 1). The megatrench was located in the center of the Cottonwood section. Most of the fault scarps in the Cottonwood section displace geomorphic surfaces formed by shoreline processes in Lake Bonneville near its highstand (Fig. 2), while a smaller proportion displace alluvial fans of Holocene age.

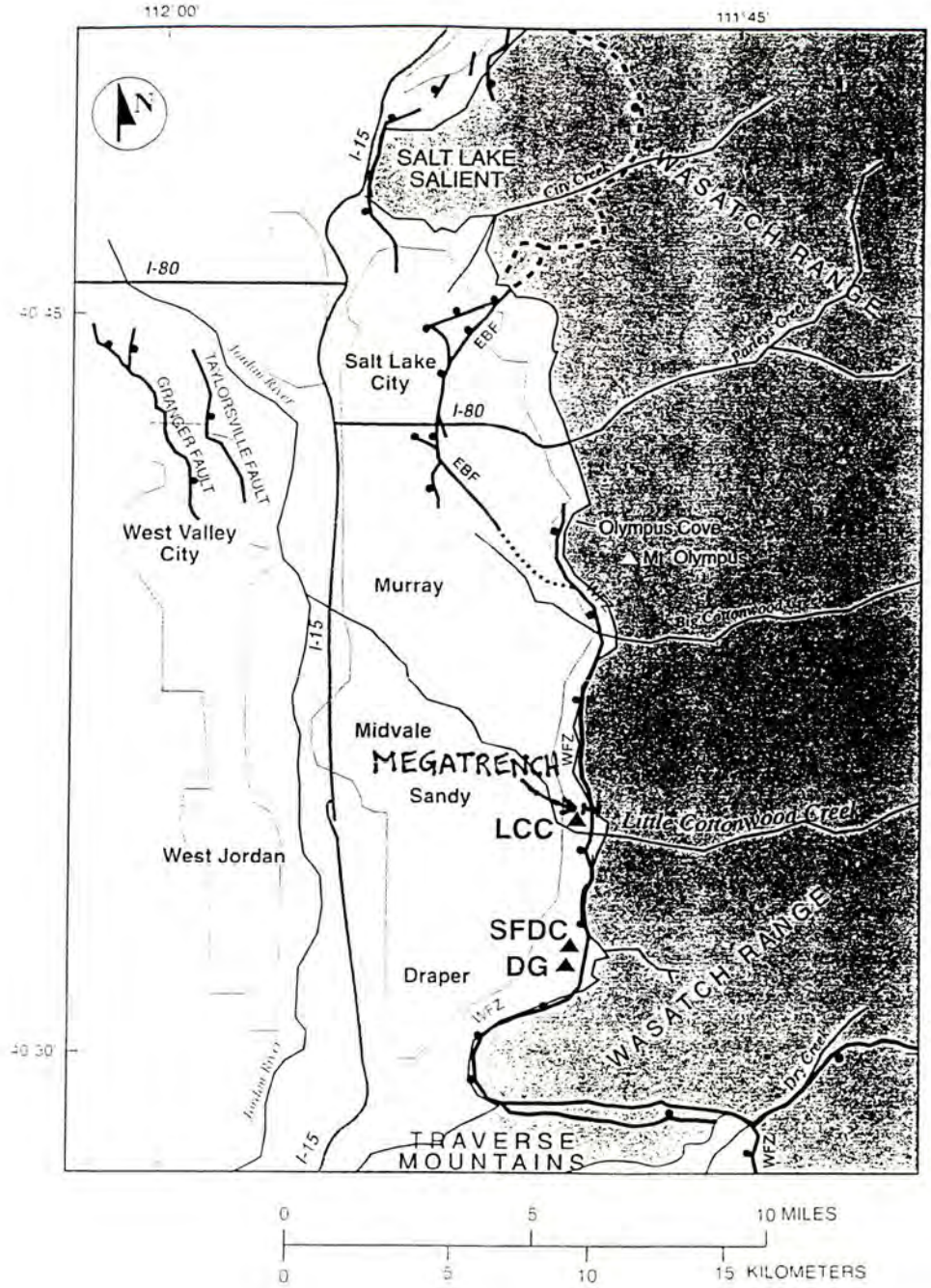

Fig. 1. Location map of megatrench study area, showing the SLC segment of the WFZ. Fault traces are thick black lines, ball on downthrown side. EBF, East Bench fault; LCC, Woodward-Clyde Little Cottonwood Canyon trench site; SFDC and DG, trench sites at S. Fork Dry Creek and Dry Gulch (Black et al., 1996).

Fig. 2. Geologic map of the central Cottonwood section of the SLC segment. (a) Insert Map from Personius and Scott, 1992;

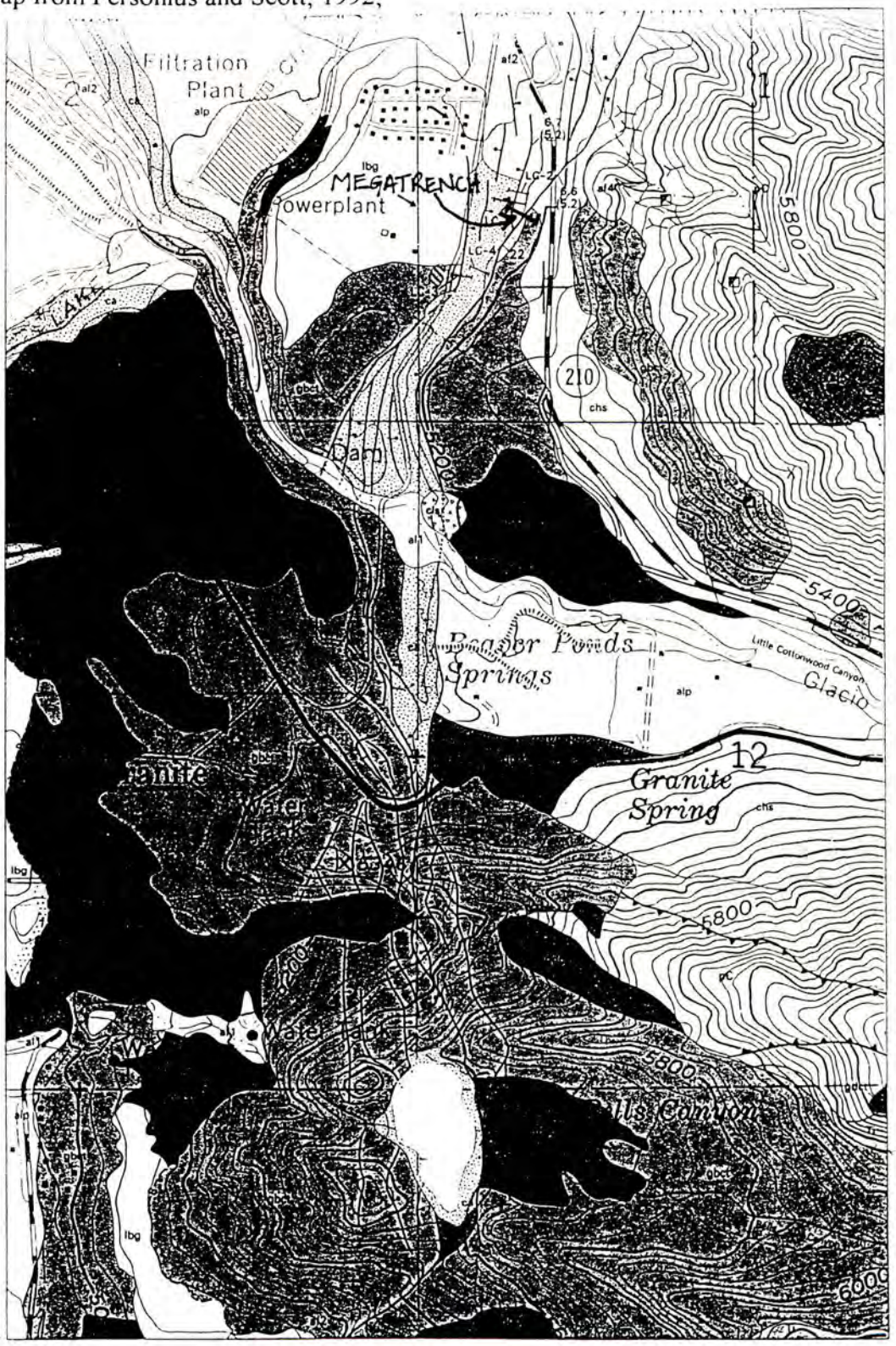

Fig. 2(b) Enlargement showing location of the megatrench in relation to the four 1979 trenches.

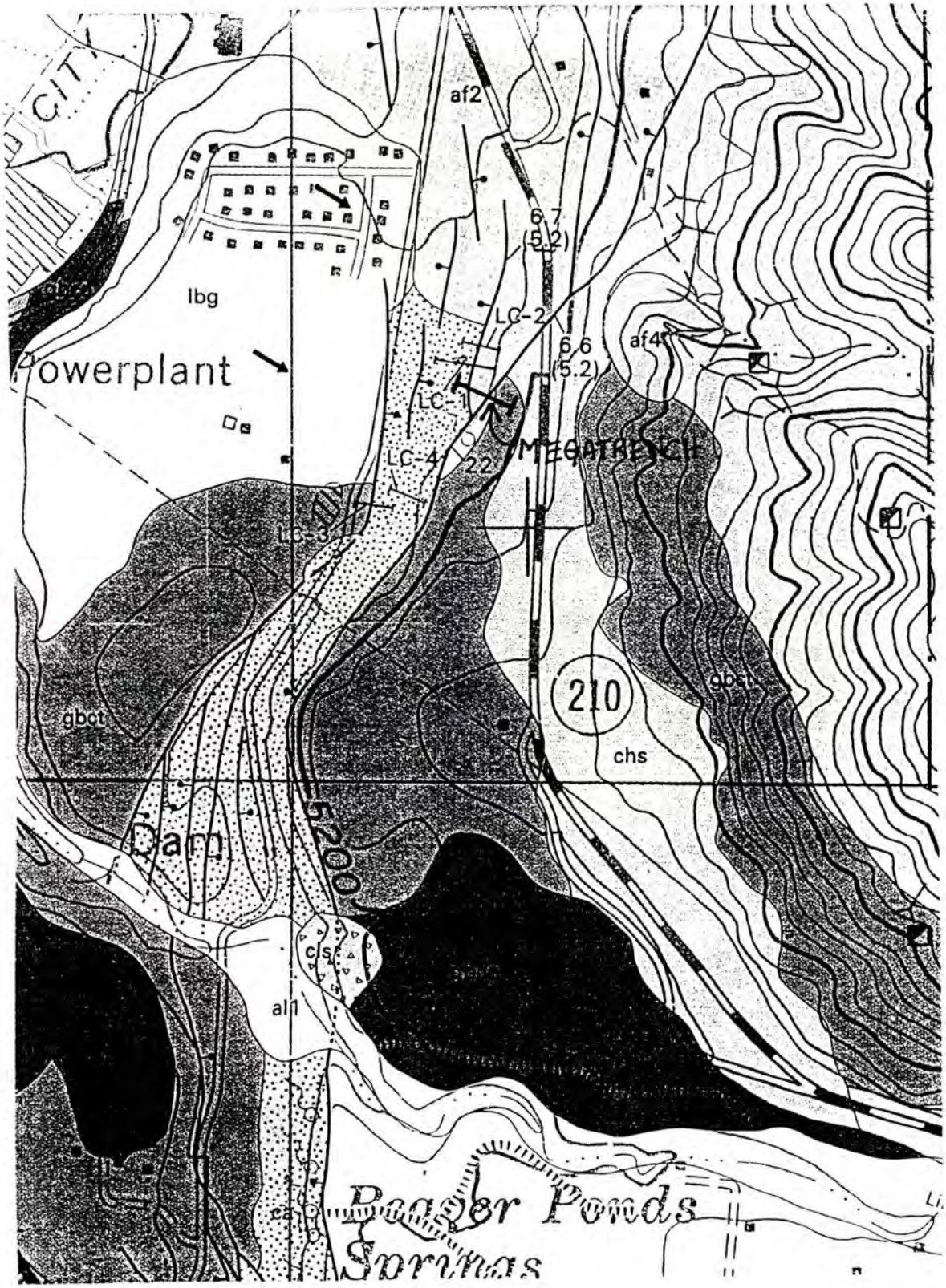

3.2 Site Geomorphology

The megatrench was located on the north flank of the latest glacial (Bells Canyon) lateral moraine complex, where the moraine is thinning. The moraine surface south of the trench was planed off by the transgression of the Bonneville Shoreline (Fig. 3), so we expected to find thin shoreline gravels (or perhaps merely a boulder lag) overlying very bouldery till. In addition, the trench site is also overlapped by the south edge of a large alluvial fan (map unit af2 on Fig. 2) emanating from a range-front drainage to the north. Thus, although the bulk of the faulted deposit here is till, the surface should be underlain by an interfingering complex of Bonneville shoreline deposits and/or younger locally derived fan gravels. In the 50 m-wide graben at the base of the scarps, a thick sequence of sandy graben fill was expected (based on the prior trenching of Woodward-Clyde Consultants in 1979). The northern part of the graben is occupied by planted blue spruce trees and is locally known as the "Christmas Tree Farm", owned by Robert V. Despain of Sandy, Utah.

The trench site also occupies a transition in the morphology and structure of the Wasatch fault zone. South of the trench the fault zone is a rather narrow graben, bounded by a 25 m-high west-facing scarp on the east (the main scarp), and a ca. 10 m-high east-facing scarp on the west (Figs. 2, 3). As the main scarp approaches our megatrench site it begins to separate into 3 subparallel scarps, each roughly 5-7 m high. At the latitude of our trench only two of these scarps have completely separated, by about 30 m horizontally, forming a gently-sloping bench (Fig. 4). The trackhoe excavators took advantage of this bench to situate themselves while digging the trench; they could not have reached the scarp midpoint on the steep face of the 25 m-high main scarp farther south.

3.3 Previous Trenching Study of Woodward-Clyde Consultants (1979)

The graben at the Christmas Tree Farm was the site of a 4-trench study by Woodward-Clyde Consultants in 1979 (Swan et al., 1981). Two of the WCC trenches were excavated across the westernmost of the three west-facing scarps on the eastern side of the graben (Fig. 2b). The third trench was excavated across the antithetic (east-facing) scarp on the western margin of the graben. The fourth trench was excavated at the toe of the 22 m-high main scarp south of the branching pint, but it did not extend far enough up the scarp face to intersect the fault plane.

Swan et al. (1981) recognized stratigraphic evidence for only two surface-faulting events, due to the poor differentiation of colluvial wedges and graben strata. The older event occurred shortly after 8000-9000 C-14 years BP. No datable organic material was found to constrain the age of the younger event. Given the limitations of these trenches, Swan et al. (1981) used an indirect method of calculating paleoearthquake recurrence. That is, they compute an average slip rate of 0.9 mm/yr based on a net vertical tectonic displacement of 13.5 m across the graben developed on Bonneville-highstand (14.5 ka) deposits. They then assumed that paleoearthquakes displayed a typical vertical displacement of 2 m per event. The average recurrence interval of 2200 years was then derived by dividing the displacement per event (2 m) by the average slip rate (0.9 mm/yr).

Fig. 3. 3-dimensional perspective map of the megatrench site; contour interval 20 ft .

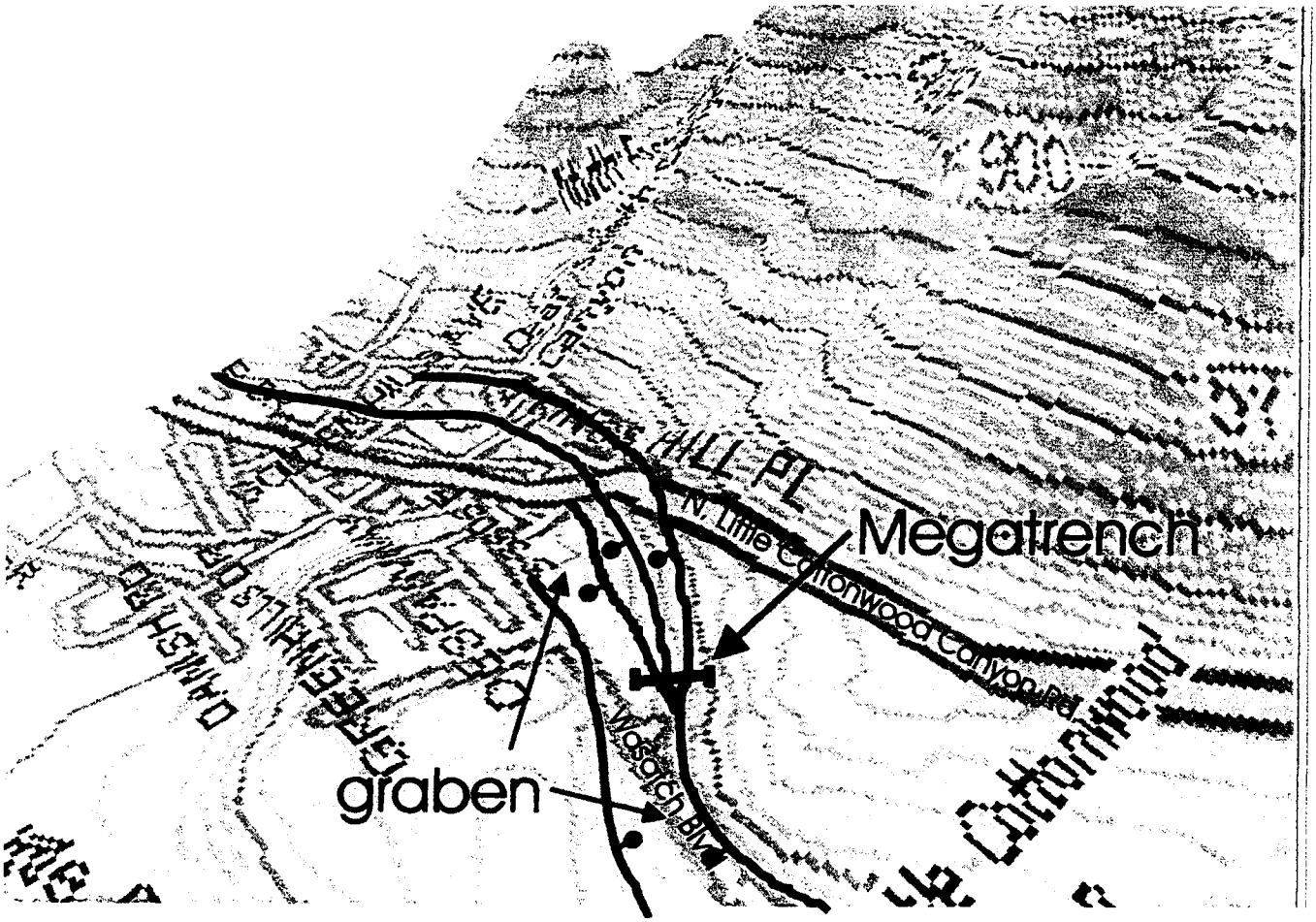

4. STRATIGRAPHY AND SOILS

The stratigraphy exposed in the trench was not exactly the thin veneer of alluvium/ beach gravels over till that we expected. On the upthrown blocks of the upper and lower fault strands, we never encountered Bells Canyon till, even though we exposed up to 7.5 m of stratigraphic thickness in each block (Fig. 5). Instead, the upthrown blocks exposed only Bonneville lake sediments, which varied in facies from well-laminated clays, to massive sands, to well-stratified (beach?) gravels, to diamictons composed of huge granite boulders in a matrix of lacustrine silt. In general the upper 2 m of the lake beds coarsened upward, indicating a regressive sequence. Our failure to expose till in the trench is not critical, because we only needed to expose the top of the Bonneville lake beds to capture all the post-Bonneville faulting events. From that standpoint much of the trench was deeper than necessary; e.g., we exposed up to 7 m of lake sediments in some places, when 1 m would have been sufficient.

4.1 Mapping conventions

The unconsolidated map units defined in this trench include both parent materials unaffected by soil formation (e.g., unit 7a), and parent materials that have been affected by soil formation (e.g., unit 6Btb4). In the latter group the map units are soil horizons defined by changes in soil horizon properties, rather than by a change in parent material sedimentology. Horizons were recognized and named according to the definitions of SCS (1994) and Birkeland (1999). In each map unit abbreviation the parent material number (1=oldest) forms the first part of the unit designation and the soil horizon abbreviation forms the next part of the map unit designation. The final part of the map unit designation indicates whether the soil horizon is part of a buried soil (i.e., not the surface soil) and if so, the number of the buried soil, with "b1" indicating the uppermost (youngest) buried soil. Thus, the map unit designation "6Btb4" indicates that the parent material is unit 6 (loess), the soil horizon is a Bt horizon (textural B horizon defined by clay accumulation), and the Bt horizon is part of the 4th buried soil counting down from the ground surface. This same naming convention is used throughout the trench.

The unconsolidated deposits exposed in the trench fall into four distinct genetic groups, which also form an age sequence. These groups are, from oldest to youngest: 1) lacustrine sediments deposited in shallow water near the time of the Bonneville highstand, ca. 14.5 ka, comprising units 1-5; 2) loess deposited in the early Holocene after Lake Bonneville desiccated, around 9.5-10.5 ka, unit 6; 3) alluvial gravels and sands of the mid-Holocene alluvial fan north of the trench, which includes graben-fill sediments, deposited between ca. 5 ka and 9 ka, unit 7; and 4) colluvial wedges and crack fills deposited in response to surface-faulting events, generally since 5.5 ka, units 8-12. Below, we describe each stratigraphic group separately.

4.2 Lacustrine units

Units 1-5 were deposited under water and compose a transgressive-regressive sequence punctuated by a slope failure episode. Based on the location of the trench below the Bonneville highstand shoreline but above the Provo Shoreline, the lacustrine units must have been deposited between the last phase of transgression up to the Bonneville highstand and the rapid fall to the Provo Shoreline accompanying the Bonneville Flood (ca. 14.5 ka). Detailed descriptions of units are given in Appendix 1.

Wasatch fault "Megatrench"

Salt Lake City segment, 1 km north of Little Cottonwood Canyon, at the Despain Christmas tree farm

NOTES: 1) Trench logged by J. McCalpin, A. Jones, C. Nelson, B. Black, G. McDonald, D. Batatian, B. Solomon; Sept. 16-Oct. 8, 1999.
2) Auger hole at W end of trench was drilled Oct. 5 with a Giddings hollow stem auger rig. Only cuttings were logged, and rig hit refusal at a depth of 15 ft.
3) Trench unit abbreviations begin with E (for the eastern 50 m of the trench) or W (for the western 15 m). The next number represents the major parent material package (1 = oldest), followed by lower-case letters for parent material subunits. If the parent material is affected by soil format ion the horizon abbreviation is next, followed by the number of the buried soil (counting from the surface soil downward). Thus, unit E5cAb5 is in the eastern part of the trench, parent material 5 (lacustrine), subunit c (regressive sand), soil horizon A, belonging to the 5th buried soil beneath the surface.

GEO-HAZ Consulting, Inc.

LONG RECURRENCE RECORDS FROM THE WASATCH FAULT ZONE, NEHRP GRANT 99HQGR0056

LITTLE COTTONWOOD CANYON "MEGATRENCH", S. WALL

DATE May 23, 2000 | FIGURE 5

DWG. NO. F:\GEOHAZ\USGS\NEHRP-99\WFZ99\LOG.CDR

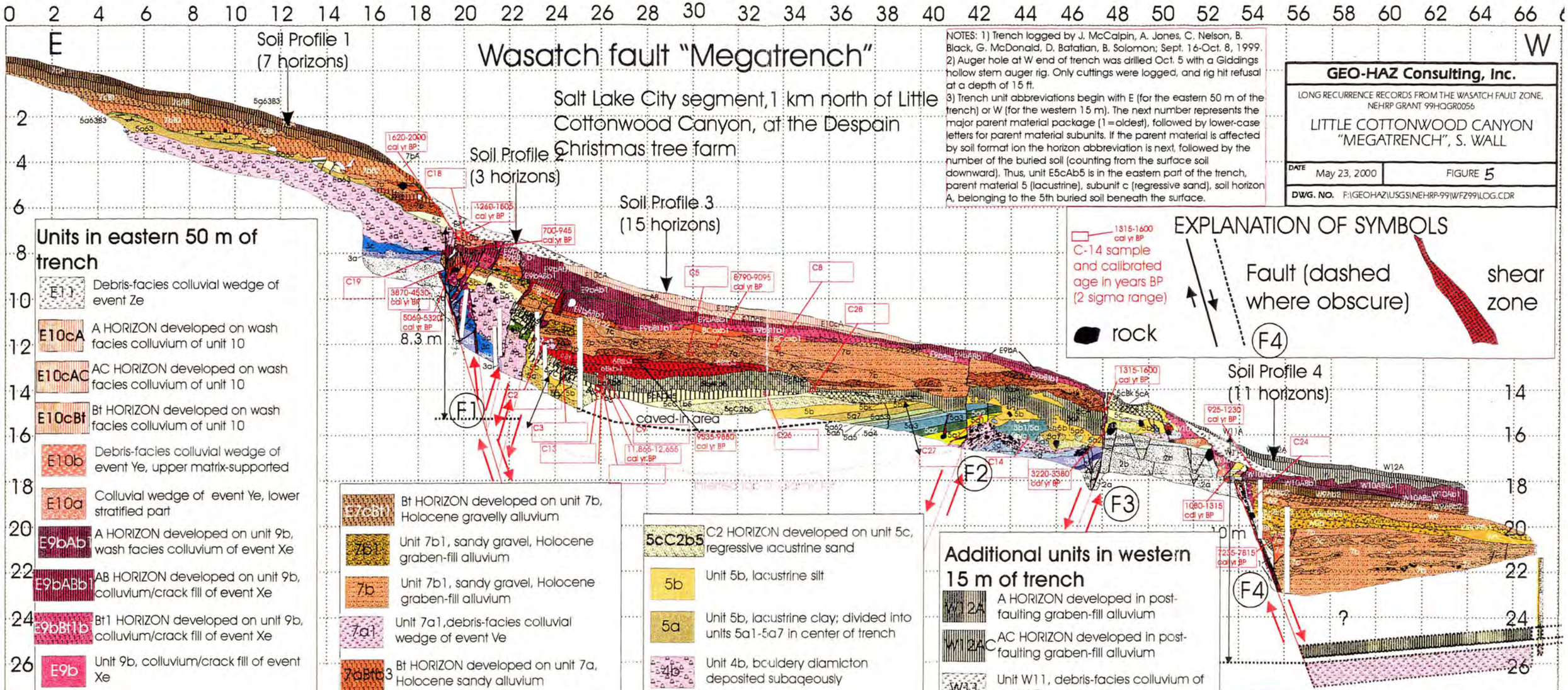

Units in eastern 50 m of trench

- E11 — Debris-facies colluvial wedge of event Ze
- E10cA — A HORIZON developed on wash facies colluvium of unit 10
- E10cAC — AC HORIZON developed on wash facies colluvium of unit 10
- E10cBt — Bt HORIZON developed on wash facies colluvium of unit 10
- E10b — Debris-facies colluvial wedge of event Ye, upper matrix-supported
- E10a — Colluvial wedge of event Ye, lower stratified part
- E9bAb1 — A HORIZON developed on unit 9b, wash facies colluvium of event Xe
- E9bABb1 — AB HORIZON developed on unit 9b, colluvium/crack fill of event Xe
- E9bBt1b — Bt1 HORIZON developed on unit 9b, colluvium/crack fill of event Xe
- E9b — Unit 9b, colluvium/crack fill of event Xe
- E8Ab2 — (A horizon?)Organic crack fill of event We
- E8ACb2 — (AC horizon?)Organic crack fill of event We
- E8Btb2 — Bt HORIZON developed on wash facies colluvium of event We
- E8b — Unit 8, sandy wash facies colluvium of event Xe
- E8a — Unit 8, gravelly wash facies colluvium of event Xe
- E7cA — A HORIZON developed on unit 7b, Holocene gravelly alluvium
- E7cAB — AB HORIZON developed on unit 7b, Holocene gravelly alluvium
- E7cBt1 — Bt HORIZON developed on unit 7b, Holocene gravelly alluvium
- 7b1 — Unit 7b1, sandy gravel, Holocene graben-fill alluvium
- 7b — Unit 7b1, sandy gravel, Holocene graben-fill alluvium
- 7a1 — Unit 7a1, debris-facies colluvial wedge of event Ve
- 7aBtb3 — Bt HORIZON developed on unit 7a, Holocene sandy alluvium
- 7a — Unit 7a, sand, Holocene graben-fill alluvium
- 6Btb4 — Bt HORIZON developed on unit 6, early Holocene loess (9.5-9.9 ka)
- 6Bkb4 — Bk HORIZON developed on unit 6, early Holocene loess
- 5cAKb5 — Ak HORIZON developed on unit 5c, regressive lacustrine sand
- 5cAb5 — A HORIZON developed on unit 5c, regressive lacustrine sand
- 5cACb5 — AC HORIZON developed on unit 5c, regressive lacustrine sand
- 5cC1b5 — C1 HORIZON developed on unit 5c, regressive lacustrine sand
- 5cC2b5 — C2 HORIZON developed on unit 5c, regressive lacustrine sand
- 5b — Unit 5b, lacustrine silt
- 5a — Unit 5b, lacustrine clay; divided into units 5a1-5a7 in center of trench
- 4b — Unit 4b, bouldery diamicton deposited subaqeously
- 4a — Unit 4a, gravelly diamicton liquefied during faulting
- 3d — Unit 3d, well-sorted sand of the Bonneville transgression
- 3c — Unit 3c, silt and clay of the Bonneville transgression
- 3b — Unit 3b, well-sorted sand of the Bonneville transgression
- 3a — Unit 3a, silt and clay of the Bonneville transgression
- 2b — Unit 2b, sand of the Bonneville transgression
- 2b — Unit 2b, sand of the Bonneville transgression

Additional units in western 15 m of trench

- W12A — A HORIZON developed in post-faulting graben-fill alluvium
- W12AC — AC HORIZON developed in post-faulting graben-fill alluvium
- W11 — Unit W11, debris-facies colluvium of event Zw
- W10Ab1 — A HORIZON developed on colluvium of event Yw
- W10ABb1 — AB HORIZON developed on colluvium of event Yw
- W10 — Unit 10, debris-facies colluvium of event Yw
- W9Ab2 — A HORIZON developed on colluvium of event Xw
- W9Btb2 — Bt HORIZON developed on colluvium of event Xw
- W9 — Unit W9, wash-facies colluvium of event Xw
- W8bBtb3 — Bt HORIZON developed on colluvium of event Ww
- W8b — Unit W8, wash-facies colluvium of event Ww
- W8a — Unit W8, debris-facies colluvium of event Ww
- W8c — Unit W8, massive silt (loess or fluvial overbank deposit?)
- A HORIZON developed on unit 7f, loess atop crack fill of event Vw
- 7e — Sandy gravel, disturbed; crack fill of event Vw?
- 7d — Sand, backtilted, disturbed; crack fill of event Vw?
- 1 — Unit 1, alternating lacustrine sand and clay of the Bonneville transgression

The oldest unit in the trench (unit 1) is exposed only in the footwall of fault zone F4 (Fig. 5). This unit is composed of laminated to thin-bedded fine to coarse sand with occasional cross beds, representing a nearshore (swash zone) environment. Unit 2 is found in the footwalls of both fault zone F1 and F4. The lower part of the unit (unit 2a) is a subangular, cobbly sandy gravel with a clean medium-coarse sand matrix. The angularity of the gravels, their large size (mean diameter=10 cm), and the lack of granitic clasts from the Little Cottonwood stock suggest they represent shoreline gravels being transported southward by longshore drift. The upper part of the unit (unit 2b) is a gray coarse sand with rare clasts, very well sorted and well stratified in planar beds. The decrease in grain size from unit 2a to 2b implies a local increase in water depth, probably associated with continued transgression to the Bonneville highstand, a trend which continues with the deposition of unit 3.

Unit 3 is found only in the footwall of fault zone F1. Presumably it also once existed atop unit 2b in the horst block between faults F3 and F4, but was later eroded. Unit 3 is a fine-grained sequence divided into four parts. Units 3a (oldest) and 3c are well-stratified, well-sorted silts, with planar beds ranging from 1-2 cm thick to mm-scale laminations. These units were deposited from suspended load and represent quiet (deep?) water conditions. Units 3b and 3d (youngest) are clean coarse sands. The bedding in unit 3d has been contorted into folds, either by liquefaction or by soft-sediment loading of the overlying diamicton (unit 4).

Unit 4 is an anomalous deposit in the lacustrine sequence. It is found in the hanging wall and footwall of fault zone F1 and in the footwall of fault zone F2. In general unit 4 is a matrix-supported diamicton containing granitic boulders up to 1 m in diameter. The larger part of unit 4 (unit 4b) is exposed on the footwall of fault zone F1 (Figs. 5, 6a), where it overlies (and deforms) unit 3 and underlies attenuated sections of units 5a and 5c (regressive sand, described later). The deposit is a diamicton composed of a pale yellow-white silt matrix (resembling units 3 and 5) containing clasts up to 1 m in diameter. Almost all the clasts larger than 30 cm diameter are well-rounded granitic clasts derived from the Little Cottonwood stock, whereas the smaller clasts are a mix of granitic and Paleozoic rocks. From the soft-sediment deformation of the underlying unit, and the fact that unit 4 is overlain by more lacustrine deposits, it is clear that this diamicton was deposited subaqeously. Our preferred interpretation is that a landslide occurred on the outer slope of the lateral moraine and shed morainic boulders into the lake and onto the soft silt of the lake floor, where they became mixed into a diamicton. There is no direct evidence that this landslide was seismically triggered; instability is common on the flanks of fresh moraines. The remainder of unit 4 (unit 4a) contains less silt matrix and more clasts, but is also clearly plastically deformed, particularly in fault zone F2. This more clast-supported gravel may have experienced liquefaction from a later faulting event.

The largest granitic boulders in the trench were not found in unit 4b, however; they were found in unit 5 between fault zones F2 and F3. Typically unit 5 does not contain any clasts at all, so finding granitic boulders >1 m in diameter was surprising. These boulders had clearly pressed downward into the soft silt of units 3 and 5 and deformed them. Our interpretation is that a faulting event ruptured the lake floor and "daylighted" unit 4b in the footwall of fault zone F1 (Fig. 7). This faulting event was also accompanied by slip on antithetic fault zone F3, which formed an east-facing subaqeous scarp that formed a "backstop" for sediments being transported from the east. The subaqeous free face atop fault zone F1 failed in a slump and transformed into a turbidite, which carried silt and granitic boulders downslope (westward) until they encountered

Fig. 6. Enlarged trench logs. (a) Eastern 1/3 of trench.

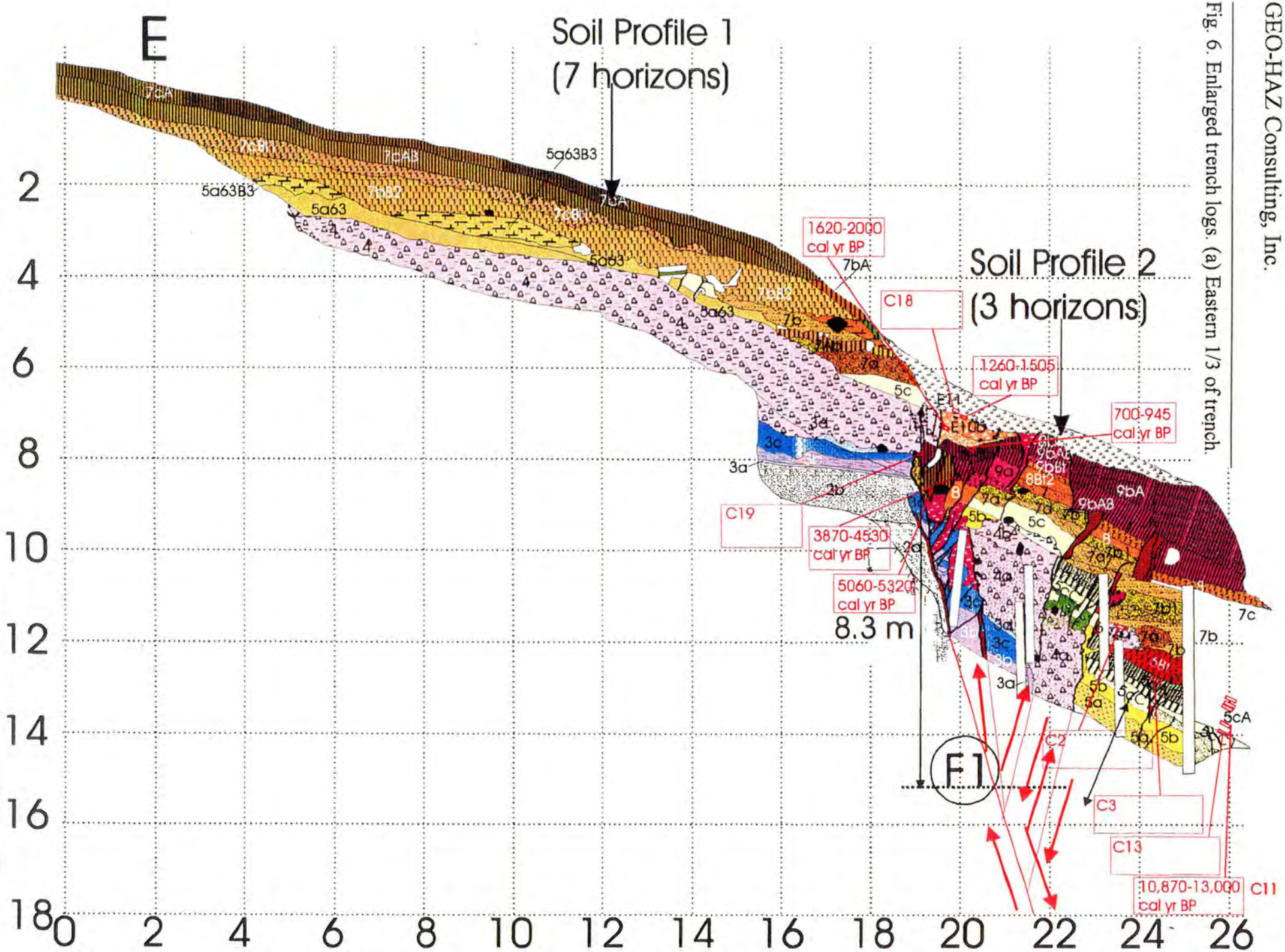

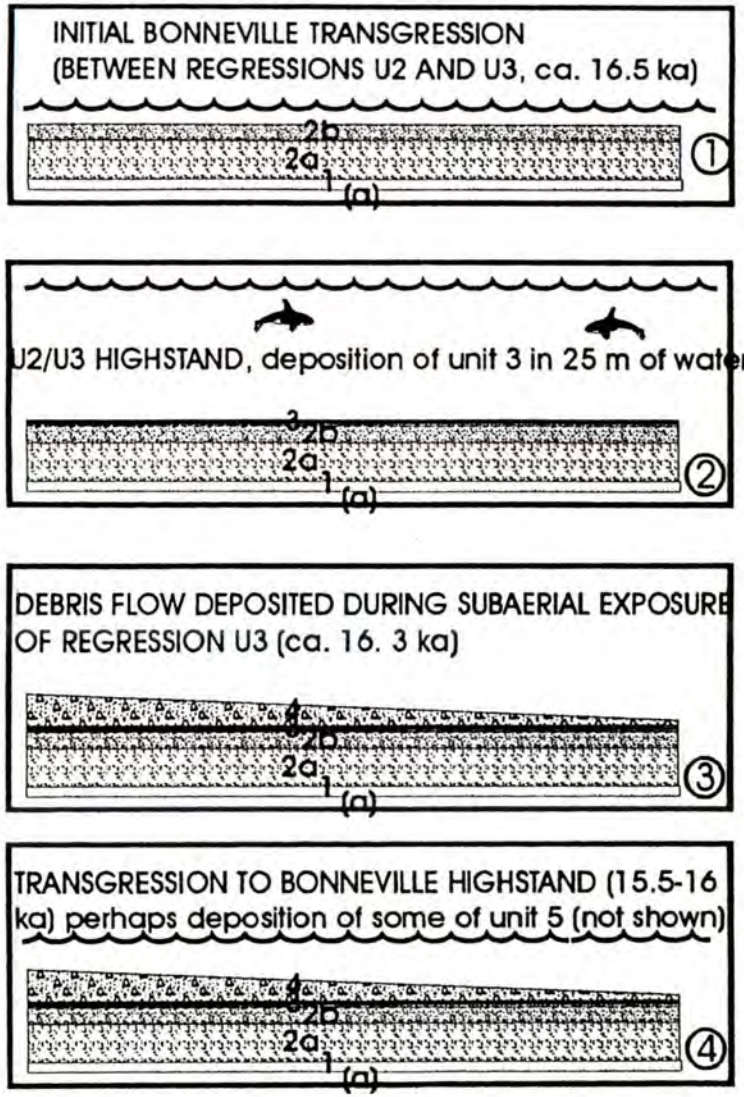

Fig. 7a Sequence of schematic cross-sections showing the inferred evolution of the megatrench area near the time of the Bonneville highstand. This sequence incorporates the dated shoreline curve of Oviatt (1997), and stratigraphic details such as the greater thickness of unit 5 between faults F1 and F3.

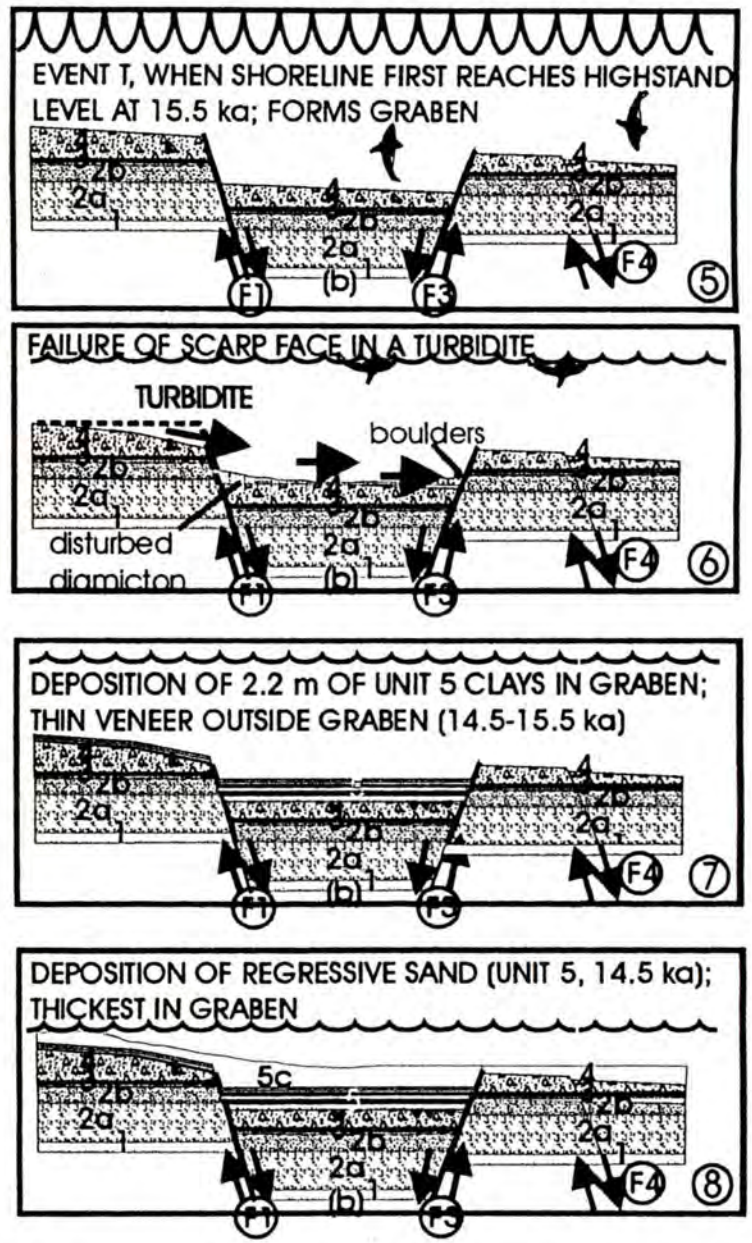

Fig. 7. Schematic cross-sections before, during, and after Event T at ca. 16 ka

the backstop formed by fault F3. The heavy boulders were deposited against the scarp. Subsequent to this faulting event (Event T in our composite chronology, as explained later), the regressive sands of unit 5 were deposited ca. 14.5 ka.

The youngest lacustrine package in the trench is defined as unit 5, but it is a complex unit including both deep-water silts and clays and the regressive sand of the Bonneville Flood, so perhaps it should have been divided into two major units. Unit 5 is composed of three major subunits. Subunit 5a is mainly pale yellow to olive (reduced?) lacustrine clay and silt, very well sorted and laminated, representing deep-water deposition. In the center of the trench subunit 5a is further subdivided into cm-scale beds 5a1-5a7 (see Figs. 5, 6b, and Appendix 1). Subunit 5b is a lacustrine silt, considerably coarser, more massively bedded, and more oxidized than subunit 5b. Subunit 5c is a yellow (oxidized) massive, medium-coarse sand with low-angle foreset beds dipping 5-6 degrees west. All deposits above unit 5 are terrestrial in origin. Unit 5 thus comprises a coarsening-upward sequence that probably records the shallowing of water depths associated with the fall of Lake Bonneville from the Bonneville highstand to Provo shorelines. A long period of subaerial exposure of unit 5 is indicated by the strong soil profile (5cA/5cAk/5cAC/5cCox) developed on unit 5c. Unit 5c is the oldest unit for which we defined map units based on soil horizons, although that practice will be common in overlying units 6-12. Counting down from the surface, the soil developed on unit 5 is the 5th buried soil beneath the present ground surface (b5).

The soil profile developed on unit 5 plays an important role in the reconstruction of tectonic history, so we describe it herein in some detail. First, like many soil profiles in fault zones, the soil and its component horizons are not exactly parallel to the boundaries of the parent material subunits in which the soil is developed. This angular discordance, seen particularly between 34 m and 40 m H (34-40 m on the horizontal scale of Figs. 5 and 6b), results when parent materials are folded or tilted, then eroded to a gently-sloping surface, upon which the soil profile forms. In such a case the soil horizons tend to forms at a constant depth below the ground surface, which brings a given horizon into varying stratigraphic levels of the tilted parent materials along a dip section, such as the trench. For example, soil horizon 5cAb5 is developed on the uppermost part of parent material 5c between 26-28 m H, but traced westward this soil horizon is developed on successively deeper parts of unit 5c, until at 40 m H the horizon is developed on unit 5b. This cross-cutting relationship indicates that soil formation postdates the folding of unit 5. In contrast, the soil horizons in unit 5 between 22-24 m H appear to be folded along with the parent materials, indicating that this drag along the fault postdates both the parent material and the soil developed on it.

A second phenomenon that might confuse the reader is the overprinting of one soil's properties onto a lower soil. The best example of this is the overprinting of calcium carbonate from buried soil "b4" (developed in unit 6) onto the uppermost part of buried soil b5. The uppermost soil horizon in buried soil b5 is horizon 5cAkb5, that is, a black, organic A horizon that contains stringers and blebs of white calcium carbonate. Calcium carbonate is much too soluble to normally occur in a well-developed A horizon, which is well-leached by infiltrating rainwater and has an acid pH from breakdown of organic matter. The calcium carbonate contained in horizon 5cAkb5 is actually derived from overlying soil b4, which has as its lowest horizon unit 6Bkb4, a B horizon containing pedogenic calcium carbonate. In other words, carbonate was infiltrating the ground surface formed by the top of unit 6Btb4 and traveling downward until it was precipitated at a depth below the ground surface dictated by the average

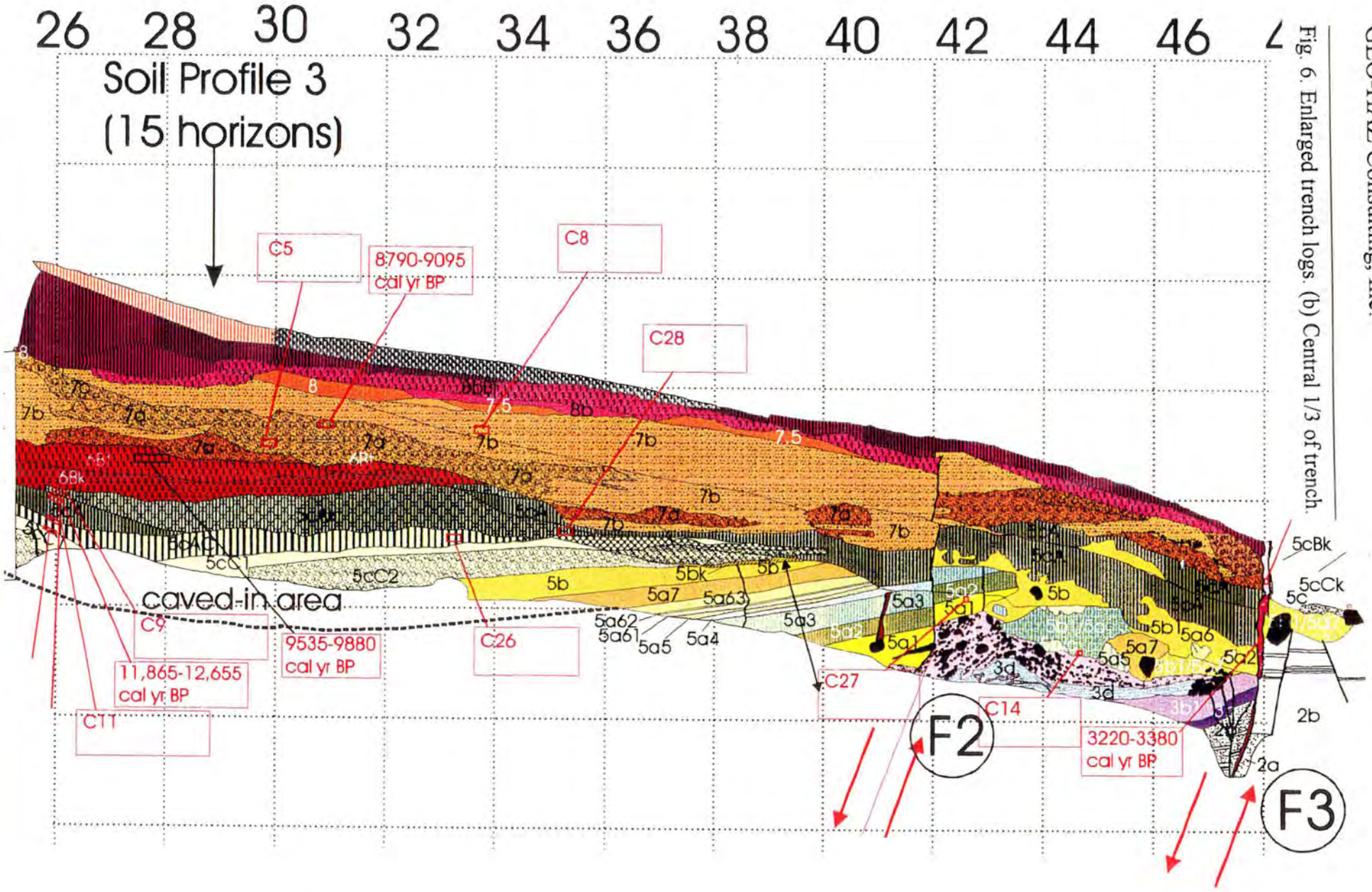

Fig. 6. Enlarged trench logs. (b) Central 1/3 of trench.

depth of wetting events. This depth just happened to coincide with the A horizon of the earlier soil b5.

Buried soil 5 is the oldest unit that yielded datable material. Carbon from the top of horizon 5cA yielded a calibrated radiocarbon age of 11,865-12,655 calendar years Before Present (cal. yr BP) (see Table 1 for a list of all C-14 dates and Appendix 2 for the calibration curves). A slightly deeper sample from the bottom of the 5cAC horizon yielded an age of 10,870-13,000 cal. yr BP. These two ages are considerably younger than the inferred age of the 5c parent material, interpreted as the regressive sand laid down during the Bonneville Flood ca. 14.5 ka. However, it should be noted that buried soil 5 developed over a long period of subaerial exposure, and the bulk carbon dated in horizons 5cAb5 and 5cACb5 contained carbon that began accumulating upon exposure of unit 5c (ca. 14.5 ka?) and continued until the soil was buried by unit 6 (ca. 10 ka?). Previous radiocarbon dating of thin buried soils in WFZ trenches by many workers (see Machette et al., 1992 for a synthesis; also McCalpin and Nishenko, 1996) concluded that the bulk organic material in those A horizons has a mean residence age of ca. 200 years. That is, a typical 5-10 cm-thick sample of A horizon contained carbon of various ages that would yield an apparent age of 200 years even for the modern (living) soil. However, the radiocarbon ages from horizons 5cAb5 and 5cAC b5 span a larger time range than 200 years and suggest that very thick soils may contain a mean residence age much longer than 200 years.

4.3 Loess

Unit 6 is comprised of a massive silt that lies unconformably on buried soil b5, and is buried by alluvium of unit 7. Its stratigraphic position atop a well-developed soil indicates it is a subaerial deposit, but its grain size and lack of clasts or stratification indicate it is not a fluvial deposit. We have therefore interpreted unit 6 as a loess, although it fact it may be loessial silt retransported into a topographic depression such as an ephemeral sag pond. Given the degree of postdepositional soil formation in this unit we cannot be more specific about its depositional environment. However, its stratigraphic position does coincide with that of early Holocene loess deposits exposed in trenches across the WFZ at American Fork (Forman et al., 1991) and at Brigham City (McCalpin and Forman, 1991).

A relatively strong soil profile is developed in unit 6, composed of horizons 6Btb4 (textural B horizon) and 6Bkb4 (B horizon with carbonate). In addition the parent material in both horizons has abundant small angular vesicles, which is typical of loess deposits.

Unit 6 pinches out to the east and west and thus has the shape of a lens. However, this shape is partly the result of faulting of the eastern margin of the unit and erosion of the western margin of the unit by alluvial unit 7. Unit 6 does occupy the axis of a syncline developed in the top of buried soil 5, so some of its lenticularity may be a primary depositional feature.

A small piece of charcoal from unit 6Btb4 was dated by the AMS radiocarbon method and yielded an age of 9535-9880 cal yr. BP. This age could either date the deposition of the upper part of parent material 6 (if the charcoal was detrital) or the later development of buried soil b4 on unit 6 (if the charcoal was intrusive). We believe it is unlikely that a piece of charcoal blew in with the loess, so an intrusive origin is more likely. Thus, the age 9.5-9.9 ka more closely dates the burial of buried soil b4 by unit 7 alluvium, than it dates the deposition of parent material 6.

Table 1. Radiocarbon samples collected and dated in this study. Only 14 of the 30 samples collected could be dated due to budgetary constraints.

Field No.	Unit	X coord.	Y coord.	Material	Lab. No. Beta-xxxxxx	Lab. C-14 age (C-14 years BP)	Calibrated Age (+/- 2 sigma, calendar years BP)	Event Constraint
C1	6Bt	28.5	-12.9	charcoal	139254	8680+/-60	9535-9880	6 soil, upper
C2	7c wedge	23.5	-11.6	charcoal				Ve, far Minimum
C3	5cA	24.2	-12.8	charcoal				5 soil, close Minimum
C4	6Bt	27.5	-12.7	charcoal				6 soil, upper
C5	7c	29.9	-12.4	charcoal				7 alluv., lower
C6	7c	30.8	-12.1	charcoal	139253	8070+/-50	8790-9095	7 alluv., middle
C7	7c	31.8	-12.3	Charcoal+ root				7 alluv., middle
C8	7b	33.51	-13.12	charcoal				7 alluv., upper
C9	6Bk	26.0	-13.3	A horiz.				5 soil, v. close Minimum
C10	5cAk	26.0	-13.3	A horiz.	139255	10,320+/-60	11,865-12,655	5 soil, v. close Minimum
C11	5cA	26.0	-13.4	A horiz.				5 soil, close Minimum
C12	5cA	25.8	-13.8	A horiz.	139256	10,260+/-330	10.870-13,000	5 soil, middle
C13	5cAC	25.8	-14.1	AC horiz.				5 soil, bottom
C14	5b1 w/blocks	44.8	-16.2	charcoal				Um, Maximum?
C15	APE-A	20.3	-7.8	A horiz.	139244	920+/-60	700-945	Xe, close Maximum
C16	PE wedge, lower	19.7	-7.4	Org. gravel	139243	1890+/-80	1620-2000	Ye, close Maximum
C17	PE wedge, upper	20.2	-7.1	A horiz.	139242	1440+/-70	1260-1505	Ze, close Maximum
C18	MRE wedge	20.2	-7.0	A horiz.				Ze, close Minimum
C19	APE-A cf	19.2	-8.0	A horiz.				Xe, average
C20	AAPE-A, cf	19.5	-8.7	A horiz.	139246	4560+/-40	5060-5320	We, average
C21	APE-A, cf?	20.0	-8.4	A horiz.	139245	3820+/-120	3870-4530	We, close Minimum
C22	W9Ab2	53.5	-18.0	A horiz.	139249	1310+/-60	1080-1315	Yw, close Maximum
C23	W10Ab1	54.6	-17.5	A horiz.	139248	1130+/-70	925-1230	Zw, close Maximum
C24	W9Ab2	54.6	-18.9	A horiz.				Yw, close Maximum

C25	W7.5Ab	55.5	-20.3	A horiz.	139250	6640+/-180	7235-7815	Ww, close Maximum
C25a	Fissure fill	48.05	-15.9	A horiz.	139252	3090+/-40	3220-3380	Ym, close Maximum
C26	5cAC	33.0	-14.14	charcoal				5 soil, middle
C26a	Fissure fill	48.0	-15.0	A horiz.	139251	1570+/-70	1315-1600	Zm, close Maximum
C27	5a1 (5cAC?)	42.72	-15.15	charcoal				5 soil, middle
C28	5cAk	34.8	-14.0	charcoal				5 soil, middle

4.4 Alluvial units

The most laterally extensive unit exposed in the trench is a sequence of alluvial sandy gravels and gravelly sands that are herein included in unit 7. Actually, during the initial logging of the trench the alluvial deposit sequences in the eastern, central, and western thirds of the trench were all given different unit numbers, because their correlation across the major faults was unclear. By the end of logging, however, it became apparent that all the alluvium belonged to a single, albeit dismembered, blanket of alluvial fan sediments shed from the mid-Holocene alluvial fan mapped by Personius and Scott (1992) north of the megatrench site.

Instead of meticulously numbering all the sand and gravel beds in this section in stratigraphic order, we used a simplified scheme of labeling sandy beds unit 7a and gravelly beds 7b. This expediency was suggested by the lenticular nature of the alluvial beds (e.g., between 56-66 m H) and their repetition in vertical section. However, this texture-based labeling scheme did not facilitate the correlation of unit 7 across the major fault zones, as described later.

One small part of unit 7 is a colluvial wedge (unit 7a1) shed from fault zone F1 at 23.5 m H. This small wedge lies atop unit 6 and interfingers with the basal alluvium of unit 7. It might be argued that this small pocket of poorly-sorted gravel is merely a channel of poorly-sorted alluvium (debris flow?) exposed in cross-section. However, retrodeformation analysis of fault zone F1 will demonstrate that there must have been a faulting event post-unit 6 and pre-unit 7 to account for stratigraphic relations in F1.

Although the alluvium assigned to unit 7 throughout the trench is all derived from the same alluvial fan north of the trench site, it is probable that the exposed strata are older in the eastern part of the trench than in the central part, and older in the central part than in the western part. Our reasoning for this is that fan deposition will be restricted to the topographically lowest parts of the terrain. Once faulting creates a scarp, deposition should be restricted to the downthrown block. Following this logic, the part of unit 7 that has been uplifted the most (i.e., in the eastern 1/3 of the trench, on the footwall of fault zone F1) should represent only the oldest part of the alluvial fan sequence. By this same logic, unit 7 in the central 1/3 of the trench contains both these oldest fan deposits and somewhat younger deposits, but not the youngest fan deposits, which should only be found in the western 1/3 of the trench, which is currently at grade with the graben floor. Thus, it is possible that the part of the mid-Holocene alluvial fan section exposed in the eastern 1/3 of the trench correlates with fan deposits that are beneath the floor of the far western part of the trench. The way to test this hypothesis is to radiocarbon date unit 7 throughout the trench. Unfortunately, datable material was only collected from unit 7 in the

central part of the trench, and due to fiscal constraints only 1 of 3 samples was dated. That charcoal sample yielded an AMS date of 8790-9095 cal. yr BP. Because this charcoal is not from a soil horizon it is probably not intrusive, so we favor a detrital origin and believe it dates the deposition of the middle of unit 7.

4.5 Colluvial units

Colluvial deposits are present at fault zones F1 and F4, and include colluvial wedges and crack fills. Because these two sequences of colluvial deposits are not in physical contact their correlation is uncertain, so they are labeled E8-E11 at fault zone F1 and W6-W12 at fault zone F4. In the following discussion we first describe colluvial units in the eastern and central parts of the trench, and then in the western end.

4.5.1 Colluvium in the eastern and central parts of the trench

At fault zone F1 the youngest colluvial wedge (unit E11) overlies the fault trace and is in depositional contact with the footwall, thus it must postdate the most recent event (MRE) on fault F1 (Event Ze). Unit E11 contains organic material throughout, probably derived from erosion of the surface A horizon on the scarp face. The unit E11 wedge extends about 7 m downslope from fault F1 where it pinches out. The age of unit E11 is constrained by a date on the top of unit E10b, discussed below.

Underlying this wedge is a faulted colluvial wedge (unit E10) composed of a matrix-supported gravelly upper half (unit E10b) and a better-stratified, darker (more organic), clast-supported lower half (unit E10a). This wedge predates the MRE (Event Ze) and postdates the penultimate event (PE), or Event Ye. The proximal part of unit E10 is much smaller in volume than unit E11, extending only about 2 m downslope from fault F1. However, a more distal (wash-facies) equivalent to Unit E10 (unit E10A) extends from 24.5-40 m H (Fig. 5). These two facies are inferred to be parts of the same colluvial deposit, a portion of which was eroded away between 21.5-24 m H. Note that the "missing" part of unit E10 between 21.5-24 m H coincides with a structurally uplifted domain in which subjacent units (such as 8Bt2) are uplifted as much as 1 m relative to outside the domain. Thus, we interpret units E10a, E10b, and E10A as being part of a single colluvial wedge that extends nearly 20 m downslope from fault F1 before pinching out. Organic material from the uppermost part of unit E10b yielded an AMS date of 1260-1505 cal. yr BP. This date indicates that the surface of unit E10b was buried by the deposition of unit E11 at that time, so the date constrains Event Ze to be about 1260-1505 cal. yr BP. A second sample from the E10a/E10b contact yielded a date of 1620-2000 cal. yr BP. This date shows that the base of unit E10 is older than 1.6-2 ka, and thus the penultimate event (Event Ye) must be older than 1.6-2 ka.

The next oldest colluvial deposit (unit E9) contains a strong buried soil (horizons E9A/E9AB/E9Bt). Due to the strong soil development (mainly the accumulation of organic matter) and the faulting of unit E9 by down-to-the-east strands of fault zone F1, we could not define the facies contact between proximal (debris-facies) and distal (wash-facies) colluvium in this unit. Unit E9 predates Event Ye and postdates Event Xe. An AMS date on the uppermost part of the strong A horizon (E9Ab1) yielded a date of 700-945 cal. yr BP. This date is younger than the two overlying dates previously cited, and is assumed to be contaminated with younger (intrusive?) carbon. A second sample was collected from the bottom of horizon E9ABb1, which yielded an age of 3870-4530 cal. yr BP. Strict reliance on this date would indicate that Event Ye

occurred after 3.8-4.5 ka, and before the 1.6-2 ka date from unit E10. In addition, it implies that Event Xe occurred before 3.4-4.5 ka. However, due to the extensive deformation of units E8 and E9, and the possible overprinting of buried soil 1 onto either unit E9 or E8, it is not clear that the carbon dated at 3.8-4.5 ka actually was derived from parent material E9, as opposed to E8.

The oldest colluvial deposit in fault zone F1 is unit E8, which is mainly interpreted as crack fill, although some of the material may be parts of a scarp-derived wedge that has been downfaulted along fault F1. Because unit E8 has been subsequently faulted three times (Events Ze, Ye, and Xe), its original geometry is somewhat difficult to establish. Unit E8 predates Event Xe and post-dates Event We. A sample from the stratigraphically lowest part of unit E8A yielded an AMS date of 5060-5320 cal. yr BP. If this date is uncontaminated, it implies that Event We occurred slightly before 5.1-5.3 ka, and that Event Xe occurred sometime between 3.8-4.5 ka and 5.1-5.3 ka. Colluvial unit E8 grades into a stratified, fluvial equivalent unit that extends discontinuously as far west as 40 m H. The fluvial part of unit E8 is transitional downward to the top of alluvial unit 7.

4.5.2 Colluvium in the western end of the trench

Colluvial deposits in the western end of the trench are scarp-derived colluvial wedges and cracks fills associated with fault zone F4. The youngest two deposits are W11 (proximal, debris-facies colluvium deposited after Event Zw) and unit W12, which is finer-grained, better stratified, and overlies unit W11. During initial logging we interpreted unit W12 as post-Event Zw graben-fill alluvium. However, the westward slope of the top of unit W12 and its position slightly above the graben floor suggest it is more likely wash-facies colluvium. Unit W1w carries a weak (A/AC) soil and is composed of map units W12A and W12AC. No radiocarbon samples were obtained from units W11 or W12.

The next older colluvium has both a proximal, debris-facies part (unit W10, on the footwall of fault F4) and a finer, wash-facies part (between 54 m H and the western end of the trench) affected by soil formation. The latter part is divided into map units W10Ab1, W10ABb1, and W10Abkb1 (Figs. 5, 6c). The proximal and distal parts of unit W10 are separated by a zone of fault-bounded blocks of footwall stratigraphic units, indicating that this colluvium has been faulted at least once. A radiocarbon sample from the top of soil horizon W10Ab1, directly beneath unit the W11 colluvial wedge, yielded an AMS age of 925-1230 cal. yr BP. This age suggests that Event Zw is slightly younger than 0.9-1.2 ka. Unit W11 postdates Event Yw, but no datable material was found in the lower part of the unit that would provide a close constraint on that event.

Beneath unit W10 is a similar-looking, poorly sorted colluvial deposit shed after Event Xw. This deposit (unit W9) carries an even better-developed soil than does unit W10, being composed of horizons W9Ab2, W9ABb2, and W9Btb2. Only the part of unit W9 within about 2 m of the fault plane is scarp-derived colluvium (unit W9a). West of that point unit W9 becomes moderate-to-well stratified and must represent a fluvial facies. A small piece of A horizon in the F4 fault zone, correlated with unit W9Ab2, was AMS dated and yielded an age of 1080-1315 cal. yr BP. Either our correlation of this small chunk of soil with W9Ab2 is incorrect, or the sample is contaminated with modern carbon.

The next oldest colluvial unit is a complex unit (unit W8) composed of three facies. Nearest to the fault plane this deposit is coarse debris-facies colluvium (unit W8a) that contains blocks of footwall material. Most of the lateral extent of unit W8 is a matrix-supported gravelly

Fig. 6. Enlarged trench logs. (c) Western 1/3 of trench

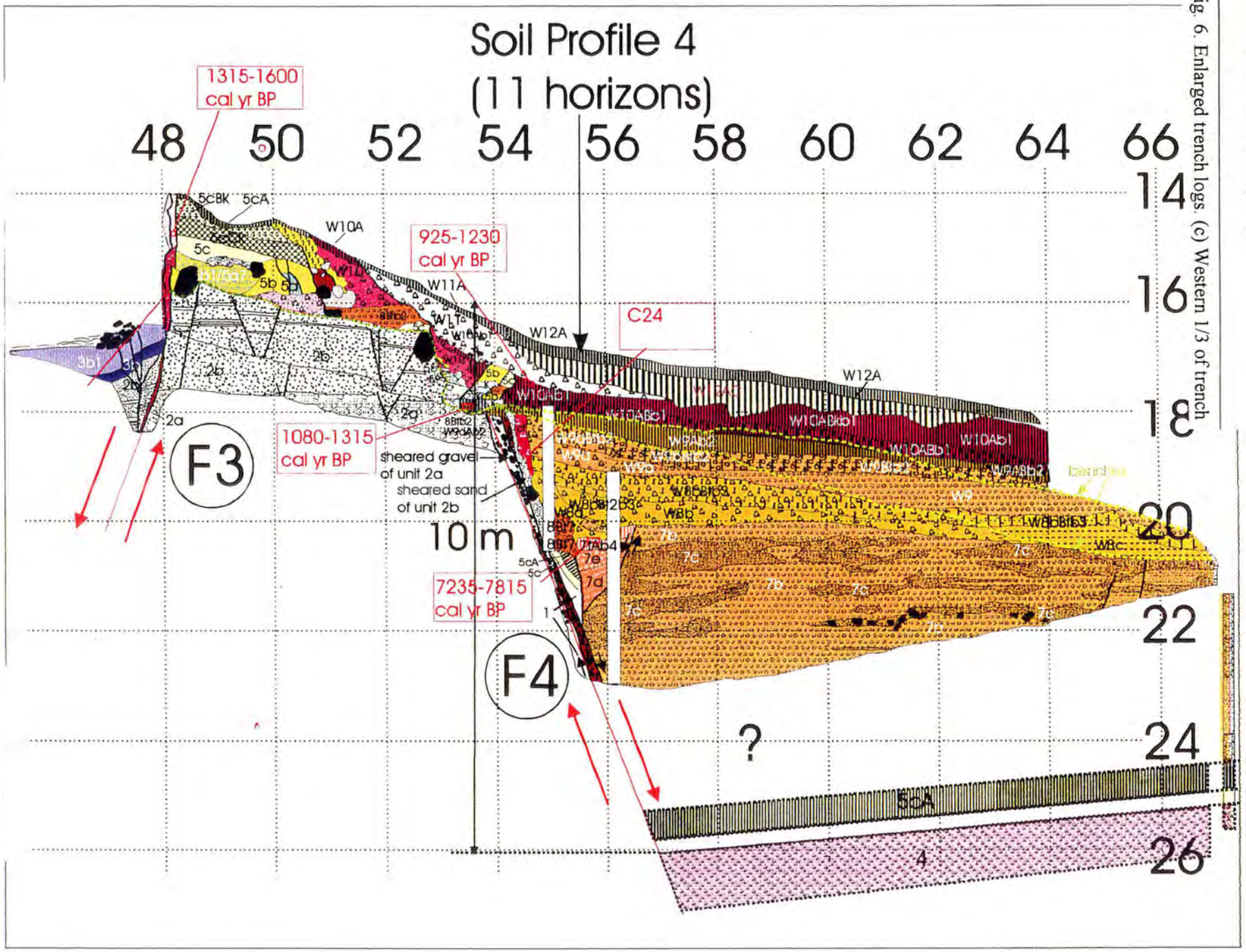

sand, probably wash-facies colluvium (unit W8b). The farthest west part of unit W8 is a massive silt, either a fine-grained alluvial swale fill (overbank facies?) or reworked loess. The soil developed on unit W8 is the third buried soil beneath the surface (b3) and is missing it's A or AB horizon. Instead, the uppermost horizon is the BT horizon (unit W8bBtb3), with a lower Bt2 horizon (unit W8bBt2b3) developed between 55-56 m H.

The oldest colluvial deposit associated with fault F4 forms a downward-tapering wedge adjacent to the fault plane. We have numbered this deposit "7", the same number used for the Holocene alluvium, for several reasons: 1) the two lower units (7d and 7e) resemble units 7c and 7b, respectively, that is they are fluvial sands and gravels; 2) however, their fabric and texture suggest they may be disturbed correlatives of units 7b and 7c that fell down into a tension fissure; and 3) the uppermost unit (7f) is a massive silt that has no counterpart within alluvial unit 7, although it does resemble the massive silt of unit W8c. Clearly, this crack fill deposit and its soil (unit 7fAb4) must postdate alluvial unit 7 and predate the deposition of the proximal colluvial wedge of unit W8 (unit W8a). An AMS date on bulk matrix of unit 7fAb4 yielded an age of 7235-7815 cal. yr BP.

5. STRUCTURE

5.1 Overview

As we expected from the presence of two separate fault scarps along our trench line, there are major normal faults beneath the eastern scarp (fault zone F1; Fig. 5, 6a) and the western scarp (fault zone F4; Fig. 5, 6c). In addition, there are two fault zones (F2, F3) that did not have topographic expression. Each fault zone contains one or more faults and is described below.

5.2 Fault zone F1

Fault zone F1 underlies the eastern, 7 m-high scarp transected by the megatrench. Because this eastern scarp is higher and steeper than the western scarp cut by the trench, we expected it to be the larger fault and have the most throw. Actually, fault zone F1 has 8.3 m of throw measured on the top of unit 4, or about 1.3 m more throw than scarp height. The decreased scarp height in relation to throw was caused by the deposition of colluvial units E8-E11 on the hanging wall that are not present on the footwall. By comparison, the gentler, 3.5 m-high western scarp is underlain by a fault with 10 m of throw! (described later).

Fault zone F1 has a rather unusual structure, containing both the expected west-dipping normal fault, but also two 1-1.5 m-wide forward-toppled "domino" blocks bounded by apparent reverse faults. These domino blocks are composed of intact stratigraphic sections of units 3-9 that broke off the footwall, slid down along fault F1 and toppled westward. The domino blocks farthest west have slid downward the most. The rotation of the dominoes has two results: 1) a large tension crack opened between the normal fault F1 and the closest domino, into which various blocks and pieces of unit 3 fell (Figs., 5, 6a), and 2) the bounding faults of the dominoes, which are generally down-to-the-west, dip east and have the appearance of reverse faults, but they do not represent the effects of compressional tectonics. The westward toppling of the dominoes has evidently continued up to Event Z, if our interpretation of proximal unit E10 being preserved in a graben overlying the pull-away zone is correct. More detail on the sequence of faulting events is given in Sec. 6.2.

5.3 Fault zone F2

Fault zone F2 is a minor, subvertical, down-to-the-east antithetic fault at 42 m H (Figs. 5, 6b). Total throw is 0.4 m measured on the top of unit 5cA.

5.4 Fault zone F3

Fault zone F3 bounds the western side of the prominent horst between 48-54 m H and contains several down-to-the-west (antithetic) faults. We dug a small pit in the floor of the trench along the main fault in zone F3 (Figs. 5, 6c). Down-to-the-west throw measured on the top of unit 2b is 1.6 m on the main fault and 2.0 m across the entire fault zone. The upper part of fault F3 is marked by a 10-15 cm-wide fissure filled with organic material.

5.5 Fault zone F4

Fault zone F4 underlies the relatively subdued, 3.5 m-high western scarp. However, the slope and height of this scarp are deceiving. The slope angle is evidently gentle because the footwall is composed mainly of the loose sand of units 5 and 2, not due to the absence of recent faulting. The scarp height is small because the lower part of the scarp was buried by deposition of up to 5 m of Holocene graben-fill alluvium. In fact, this 3.5 m-high scarp is underlain by a normal fault with 10 m of throw, measured on the top of unit 4 (diamicton).

Unlike fault zone F1, fault zone F4 does not contain structural complexities such as domino blocks. Instead, the zone is dominated by a single, planar normal fault that dips 75 degrees west (Fig. 6c). The fault is defined by a 10-15 cm-wide zone where gravel clasts of unit 2a have been rotated parallel to the fault (shear fabric). A few blocks of footwall material are found, for example a block of units 5cA/5cC, as well as one undifferentiable crack fill higher up (unit cf). As the fault approaches the surface its expression changes to include several antithetic (east-dipping) faults that disrupt unit W10. The main normal fault is difficult to trace within 2 m of the modern ground surface, either due to human disturbance associated with old mining activities, or because the soft sands of unit 2b on the footwall collapsed during the last 2 faulting events. However, the upward transition from fault contact to depositional free face contact at the base of the MRE wedge (unit W11) is well preserved.

The total throw across fault zone F4 was reconstructed by projecting unit contacts in the auger hole at the western end of the trench back to the main normal fault plane at a dip angle of 6 degrees east. This dip angle mimics that of "backtilted" lenticular sand beds within unit 7, and is a minimum value, because it assumes that backtilt angles do not increase with depth to the top of unit 4.

7. SEQUENCE OF FAULTING EVENTS

7.1 Overview

We reconstruct the sequence of faulting events on fault zones F1 and F4 by use of graphic retrodeformation sequences, in which a series of cross-sections are generated "back in time" by progressively removing, step by step, the youngest deposits and then reversing movement on the fault planes to achieve the pre-faulting geometry. For faults F2 and F3 the small number of displacement events was directly inferred without a retro sequence.

7.2 Fault zone F1

The common interpretational paradigm used on normal faults assumes that each faulting event is followed rapidly by deposition of a crack fill and/or colluvial wedge deposit. Past trenching investigations on the WFZ (Machette et al., 1992) have shown that soils typically have sufficient time (1000-3000 years) to form on one colluvial deposit before it is buried by the next one. Therefore, merely counting the colluvial deposits and their associated soils should yield the number of faulting events. In fault zone F1 we have four colluvial deposits (from top to bottom, E11, E10, E9, and E8). Unit E11 has the typical wedge-shape of a scarp-derived colluvial wedge, while the other units becomes progressively deformed due to their sagging down into the depression created by domino blocks pulling away from the footwall. The radiocarbon age constraints on the last four events are listed below:

Table 2. Summary of age constraints on the latest four faulting events in fault zone F1.

Event	Colluvial Unit Formed	Min. Age	Max. Age (all ages in cal. yr BP)
Ze	E11	NA	1260-1505
Ye	E10	1620-2000	bad date
Xe	E9	3870-4530	5060-5320
We	E8	5060-5320	NA

Only one colluvial wedge exists farther down in the section below unit E8; it is unit 7a1, interbedded with the basal part of alluvial unit 7 (at 23.5 m H; Figs. 5, 6a). If we rely only on the presence of colluvial wedges to detect paleoearthquakes then we have evidence for only one event between ca. 14.5 ka (age of unit 5) and ca. 5 ka. Fortunately, there is another independent line of evidence for vertical displacements in fault zone F1, and that is the attenuation of the stratigraphic section on the domino blocks in relation to farther west. A cursory examination of Figs. 5 and 6a shows that, in the center of the trench clayey units 5a and 5b reach an aggregate thickness of 2.2 m, unit 5c is 1.9 m thick, unit 6 is 1 m thick, and alluvial unit 7 is 1.9 m thick. In contrast, some of these units are entirely missing atop the dominoes, while others exist but at reduced thicknesses. For example, unit 5c is only 0.6 m thick atop the western domino but contains soil horizons 5cA, 5cAC, and 5cC, whereas atop the adjacent domino to the east, only 0.4 m of unit 5cC exists. In order to explain this difference in deposit and soil thickness we can postulate that unit 5c and its soil once existed atop both dominos, but at some time before the deposition of alluvial unit 7 the eastern domino was elevated by faulting with respect to the western domino, and the upper part of unit 5c and its soil were eroded. The basic assumption here is that, since units 5b and 5c exist in the farthest eastern part of the trench, they also existed at one time across the entire length of the trench.

Following this line of reasoning, we constructed a series of schematic cross-sections that progress backward in time from the present trench geometry in fault zone F1 (Fig. 8). We simplified the diagrams by straightening out the domino-bounding faults and removing the forward rotation of the dominos. Because the differential erosion of the domino tops was caused by differential vertical displacement on their bounding faults, we felt that neglecting the rotation was justified, as long as we preserved the vertical displacements. To move backwards in time with our sequence, we started with the present (schematic) geometry of the dominoes and removed the youngest deposit. We then reversed the movement on the faults until the base of the youngest remaining unit was horizontal. We then increased the stratigraphic thickness of that unit on any

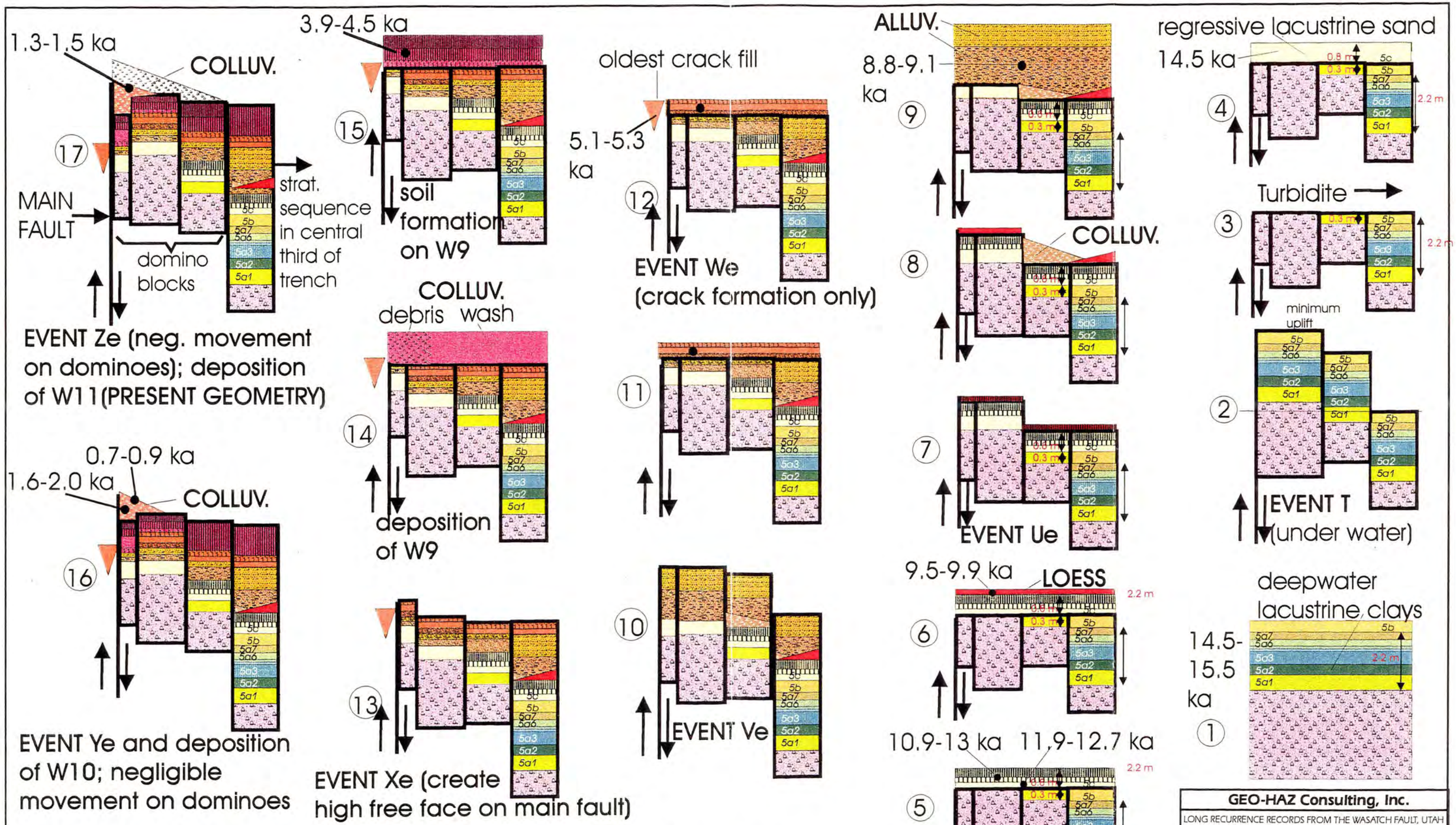

RETRODEFORMATION SEQUENCE FOR FAULT ZONE F1, 1999 WASATCH FAULT MEGATRENCH (rotation of dominos is not portrayed); Note that most inter-domino displacement occurred in Events T, U, and V, with small or no shifting in Events W-Z. In the latest 4 events (particularly Xe) most displacement has occurred on the main normal fault.

GEO-HAZ Consulting, Inc.	
LONG RECURRENCE RECORDS FROM THE WASATCH FAULT, UTAH	
LITTLE COTTONWOOD MEGATRENCH- S. Wall	
NEHRP Grant 99HQGR0056	
DATE April 5, 2000	FIGURE 8
DWG. NO. F:\GEOHAZ\USGS\NEHRP-99\WFZ\LOG.CDR	

structural block where the present thickness is less than the thickness outside of fault zone F1. This step is equivalent to assuming that each deposit and soil horizon originally covered the fault zone with constant thickness. The stratigraphic thickness added in this step also defines, by definition, the vertical displacement of the fault blocks in the preceding step.

The retrodeformation sequence relies on both colluvial wedges, crack fills, and differences in thickness of units E9 and E8 to reconstruct the latest four faulting events (Events Ze, Ye, Xe, We). Differential thickness of unit 7 across the dominoes requires a significant displacement event (Event Ve) between units 7 and 8. The absence of unit 6 on the dominoes, and the existence of colluvial wedge 7a1, requires an event following deposition of unit 6 (Event Ue). Finally, the absence of units 5a and 5b on the dominoes requires an event between units 5b and 5c (Event Te), an event that must have occurred underwater, which was responsible for the turbidite-emplacement of the large granite boulders described previously. Inclusion of these three displacement events within the time period 16 ka to ca. 5 ka satisfies all the present geometric constraints, without the need for additional displacement events. Using the principle of parsimony, our interpretation is that as few as 7 displacement events can adequately explain the present geometry of fault zone F1, and that there is no need to postulate additional events.

The timing of these three pre-5 ka displacement events is constrained by sparse radiocarbon dates. **Event Ve occurred after 8.8-9.1 ka but before 5.1-5.3 ka**, i.e. late during the deposition of alluvial unit 7. **Event Ue occurred shortly after the formation of buried soil 4 on unit 6, dated at 9.5-9.9 ka**. Event Te must have occurred while this site was still submerged beneath Lake Bonneville. The center of the trench is presently at an elevation of 5160 ft (1573 m), or roughly 80 ft (25 m) below the Bonneville highstand shoreline as carved on the north lateral moraine of Little Cottonwood Canyon. According to Oviatt (1996) the lake shoreline was within 25 m of the highstand elevation only for a short time between ca. 14.5 ka (Bonneville Flood) and 17 ka, if one accounts for the U2 excursion (Fig. 9). However, this excursion was followed by brief subaerial exposure, and there is no evidence of subaerial exposure within the lacustrine sequence. Therefore, if the U2 excursion is neglected the shoreline was only within 25 m of the highstand **between 14.5 ka and 16 ka, which form tight age brackets on Event Te**.

7.3 Fault zone F2

Fault zone F2 has a total throw of 0.4 m measured on the top of unit 5cA. Throws measured on units higher and lower are essentially identical, and there are no colluvial wedges preserved along the fault. This geometry suggests that the entire 0.4 m of throw occurred in a single event that must postdate unit 8b. Two events (Event Ze, Ye) fall into this time interval on fault zone F1, so the displacement on F2 may be contemporaneous with either event. No radiocarbon samples were collected to try and constrain the age of this event, because the fault is such a minor structure, and it was deemed unlikely that a surface-rupturing event would cause movement on this fault without also causing movement on the major fault zones F1 or F4, the chronologies of which were dated in detail.

7.4 Fault zone F3

Fault F3 does not contain any colluvial wedges from which to infer the number of events that have contributed to its 2 m of throw. However, the upper part of the fault is marked by a 10-15 cm-wide fissure filled with organic material. We identified a higher, looser, younger, more organic fissure fill in the upper 1 m of the crack, underlain by a lower, denser, and less organic

Fig. 9. Elevation of the shoreline of Lake Bonneville as a function of time (uncalibrated radiocarbon years before present, in thousands). All elevations have been corrected for isostatic rebound. Because both faulting and rebound have affected the elevation of the shoreline at our site, we merely plot the time interval (vertical dashed box) within which the lake shoreline was less than 25 m below the highstand shoreline (horizontal dashed box). From Oviatt, 1997

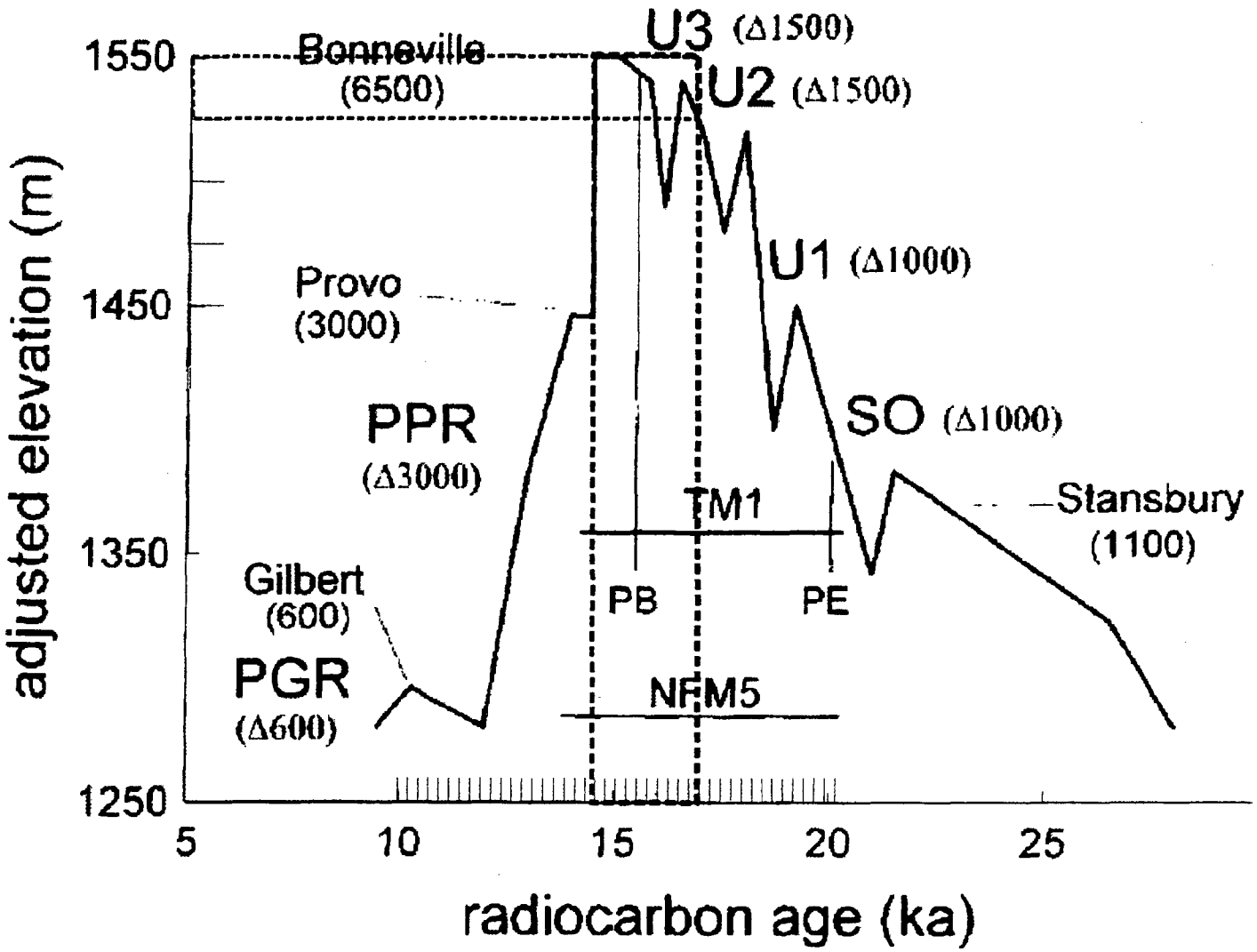

crack fill. Our inference was that each crack fill deposit accumulated rapidly after a faulting event from A or AC horizon soil material falling into the crack from the surface soil. Accordingly, we dated the lowest parts of the upper and lower crack fill deposits. The upper crack fill deposit yielded an AMS age of 1315-1600 cal. yr BP. This age is quite similar to the closely-limiting maximum age of 1260-1505 cal. yr BP on Event Ze on fault zone F1, and suggests that this fissure may have opened during that event. The older crack fill unit yielded an AMS date of 3220-3380 cal. yr BP. This date does not exactly coincide with any date from fault zone F1.

7.5 Fault zone F4

Due to the simple geometry of fault zone F4, the chronology of all displacement events younger than alluvial unit 7 can be reconstructed from colluvial wedge evidence. However, the trench was not deep enough on the hanging wall of F4 to expose the stratigraphic levels at which evidence for the three pre-5 ka events might be found (i.e., the base of unit 7 and lower). The retrodeformation sequence (Fig. 10) is based on several assumptions: 1) the free face created during each event W-Z had to be at least as high as the thickness of the colluvium deposited after the event (units W8-W11, respectively), 2) the free faces created during Events Ww and Xw were composed only of unit 7 alluvium, i.e. unit 5 did not daylight, 3) the free faces of Events Yw and Zw did daylight unit 5 in the free face, and 4) by the present time, erosion has removed all of unit 7 from atop the F3/F4 horst. As shown by the retrodeformation sequence (Fig. 10), removal of colluvial units W11, W10, E9, and W8, and reversal of displacement according to the rules listed above only removes 7.5 m of the 10 m of total throw on this zone, or about 1.8 m per event. This amount of throw is somewhat less than the 2 m per event that is typical of paleoearthquakes on the WFZ, but if the same events simultaneously ruptured fault zone F1 by an additional 1 m, then the net down-to-the-west displacement would have summed to about 2.8 m per event. By comparison, the total throw of 18.3 m on faults F1 and F4, if divided among 7 events, averages 2.6 m per event.

Notably, after "removal" of the latest four events (Zw, Yw, Xw, Ww) there is still 2.5 m of throw that must be accounted for by pre-5 ka events on fault zone F4, according to the retro sequence. This 2.5. m of throw must be attributed to Events Vw, Uw, and Tw, but the relative proportions to assign to each event are unknown, because the direct evidence for these events (colluvial wedges, crack fills) is beneath the trench floor. Based on the schematic retrodeformation sequence of Fig. 11 , Event T may not have ruptured fault F4. If true, this scenario leaves the "missing" 2.5 m of throw to be partitioned between Events Uw and Vw, at roughly 1.25 m per event; that value is similar to the displacement values inferred for all other Events in the trench.

Obviously, many other scenarios are also possible, given the limited constraints posed by the reconstruction of the latest four events (Fig. 10) on the one hand and the projection of auger hole contacts to fault F4 on the other hand. We cannot even prove that there were not additional events besides Tw, Uw, and Vw in the time period 7-15 ka, since we did not expose that part of the stratigraphic section. However, because we have only 2.5 m of "missing" throw to account for, and already three candidate events (Tw, Uw, Vw) that could have caused that throw, there is not a compelling need for an additional faulting event in addition to the three already recognized.

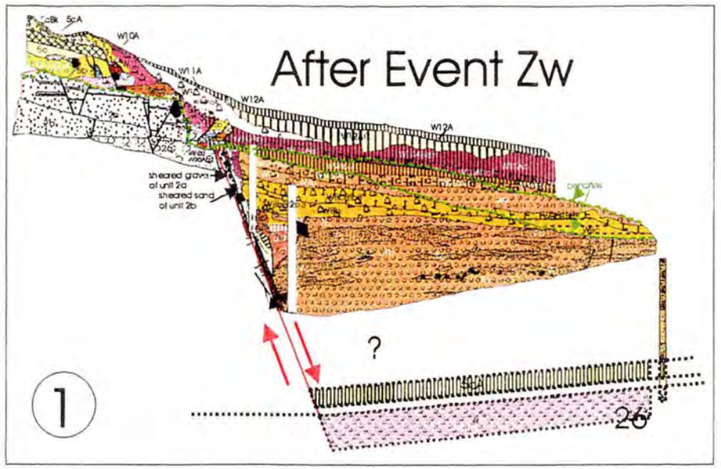

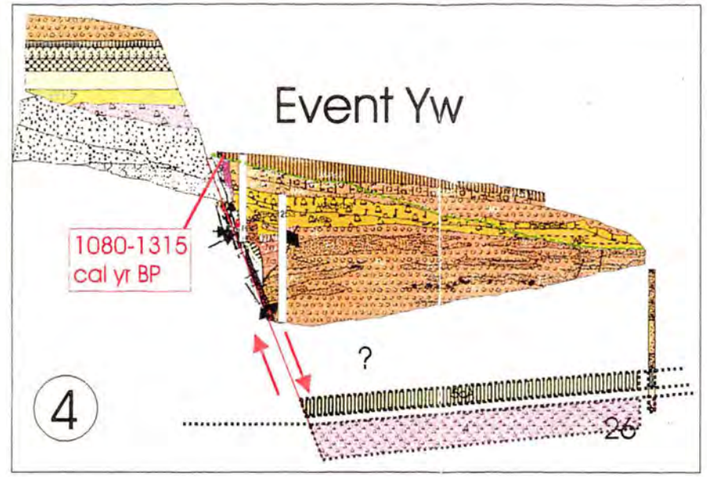

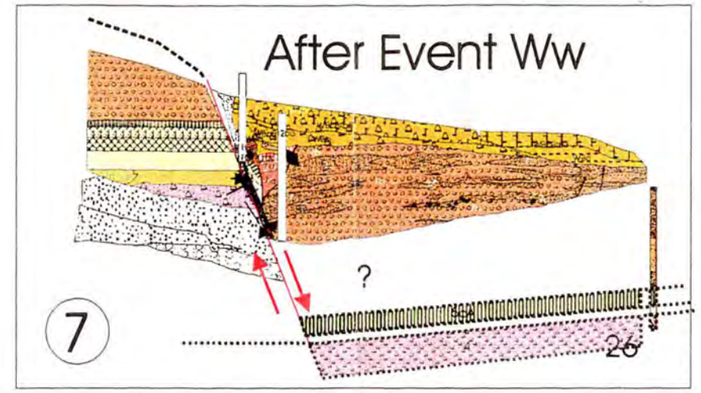

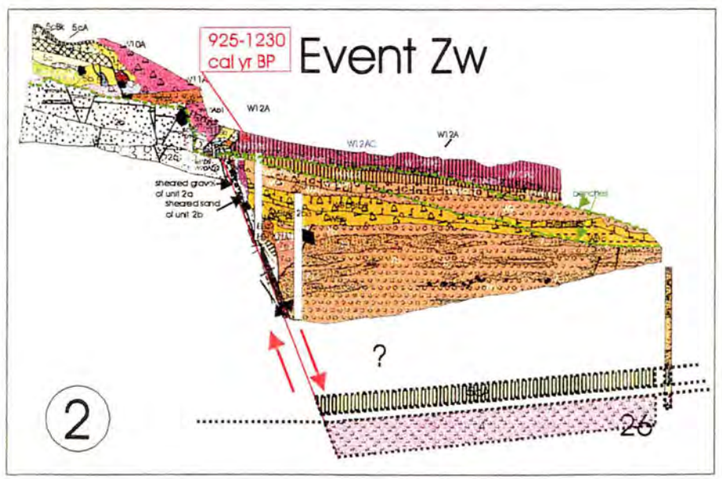

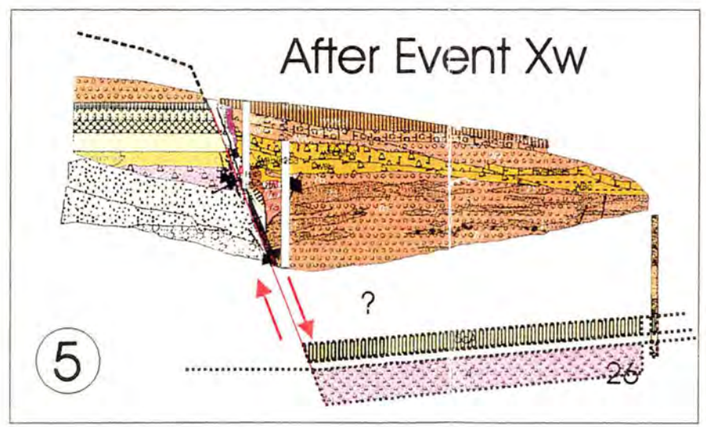

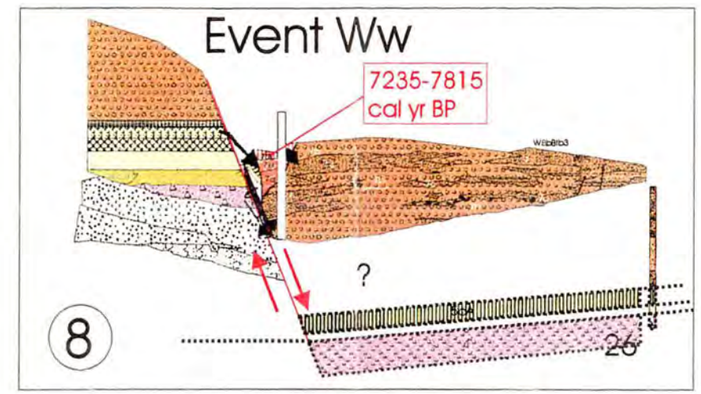

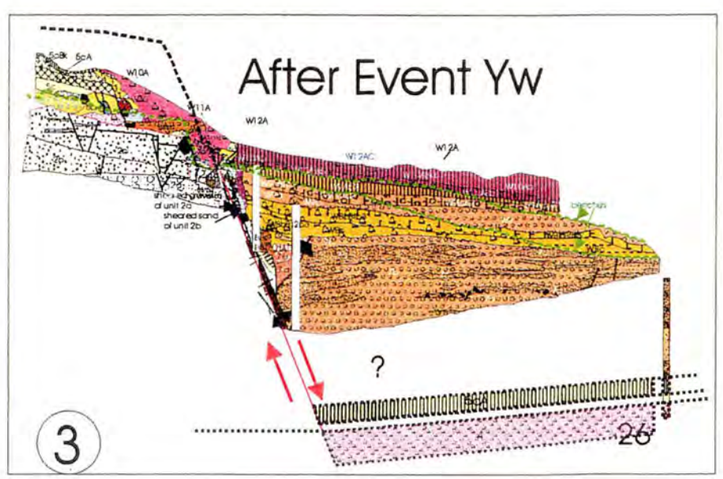

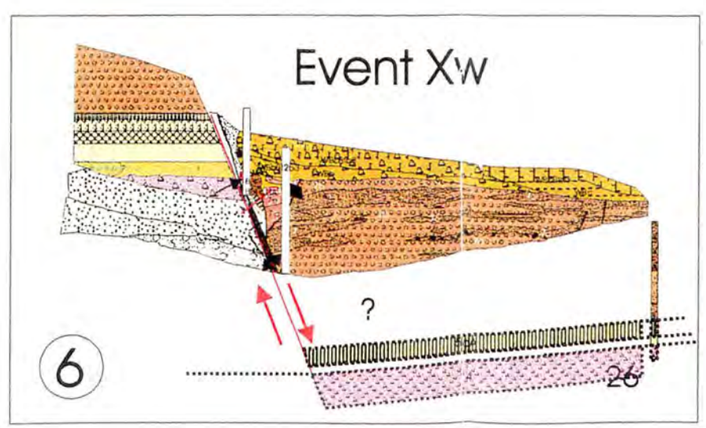

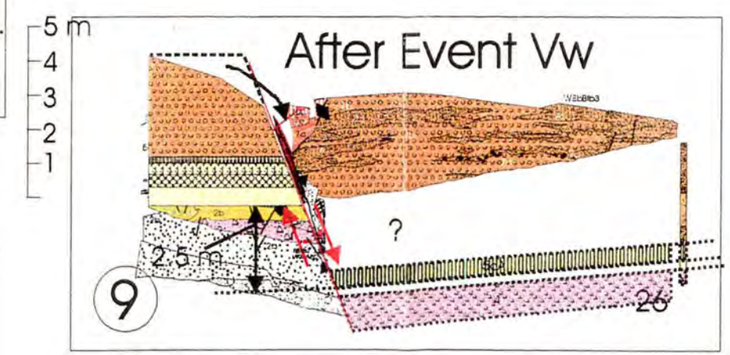

Notes: 1) Dashed lines show the top of the footwall from the previous step.
2) The sum of restored displacements in events Ww and Xw is the maximum permitted without daylighting unit 5 in the free face.

GEO-HAZ Consulting, Inc.

LONG RECURRENCE RECORDS FROM THE WASATCH FAULT ZONE, NEHRP GRANT 99HQGR0056

RETRODEFORMATION SEQUENCE, FAULT ZONE F4, MEGATRENCH

DATE	May 20, 2000	FIGURE 10
DWG. NO.	F:\GEOHAZ\USGS\NEHRP-99\WFZ99\W_RETRO.CDR	

Fig. 11. Simplified retro sequence for the entire megatrench, from 17 ka to present. (a) Steps 1-8, 17 ka to 14.5 ka.

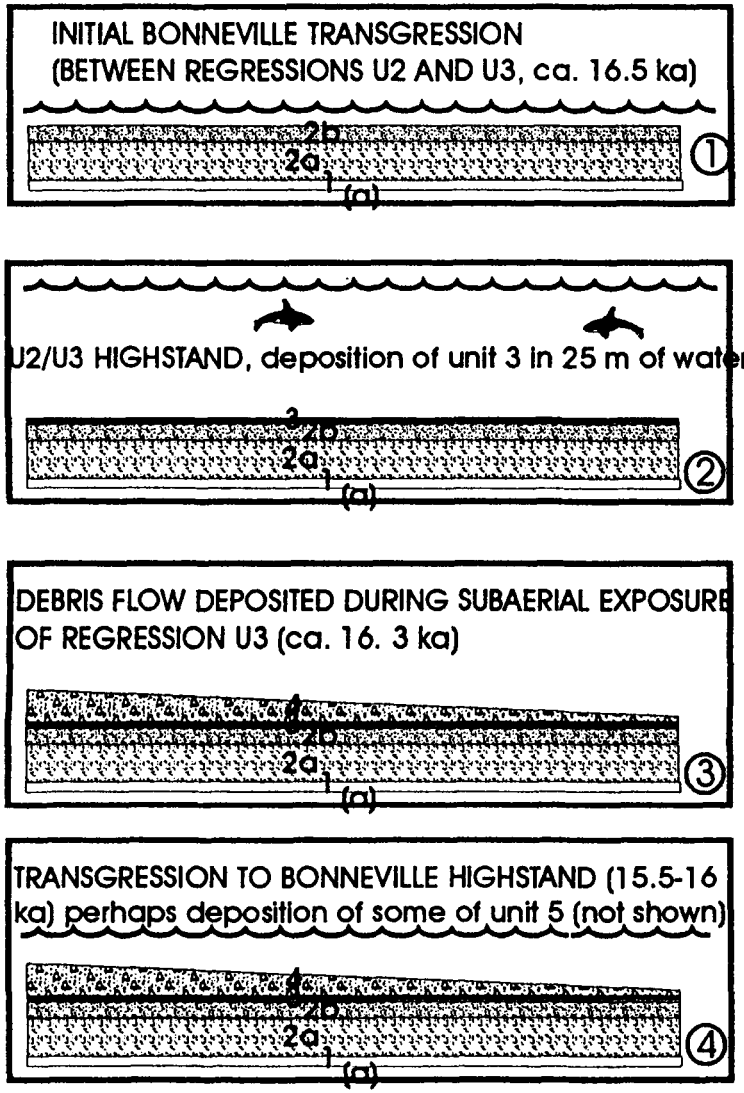

Fig.11a Sequence of schematic cross-sections showing the inferred evolution of the megatrench area near the time of the Bonneville highstand. This sequence incorporates the dated shoreline curve of Oviatt (1997), and stratigraphic details such as the greater thickness of unit 5 between faults F1 and F3.

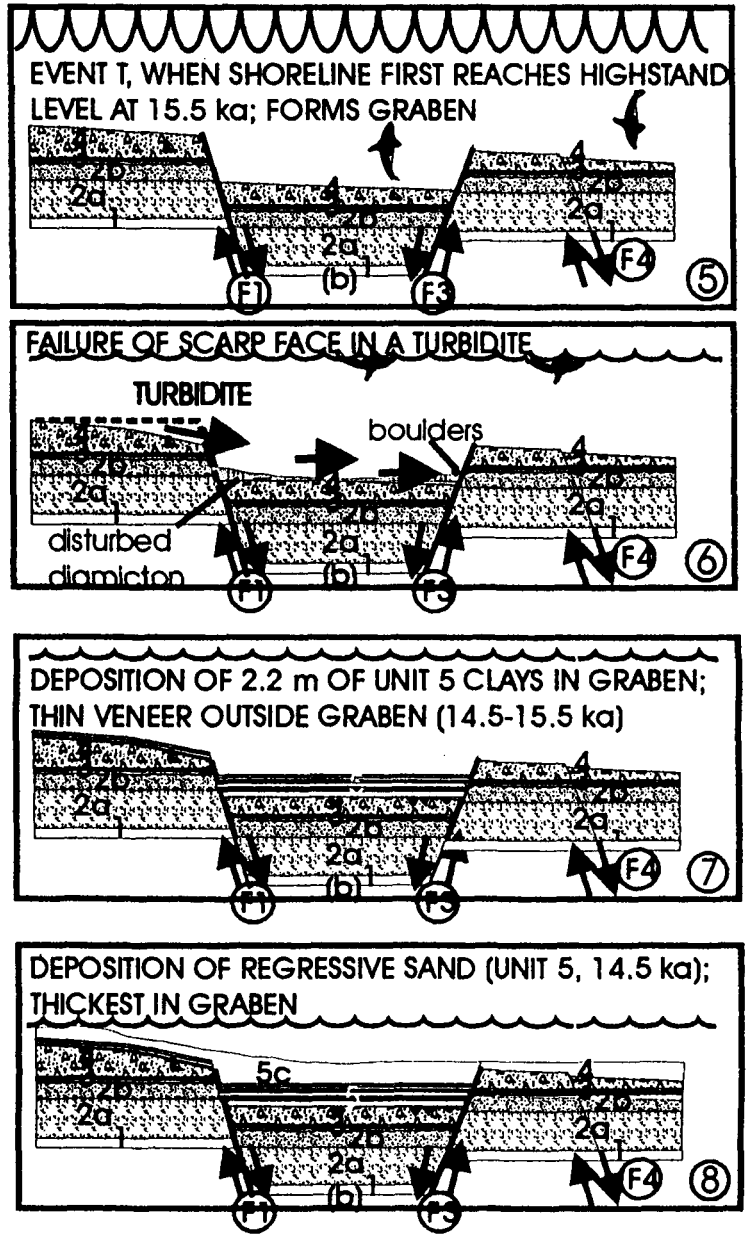

Fig. 11 (b) Steps 8-15, 14.5 ka to ca. 7 ka.

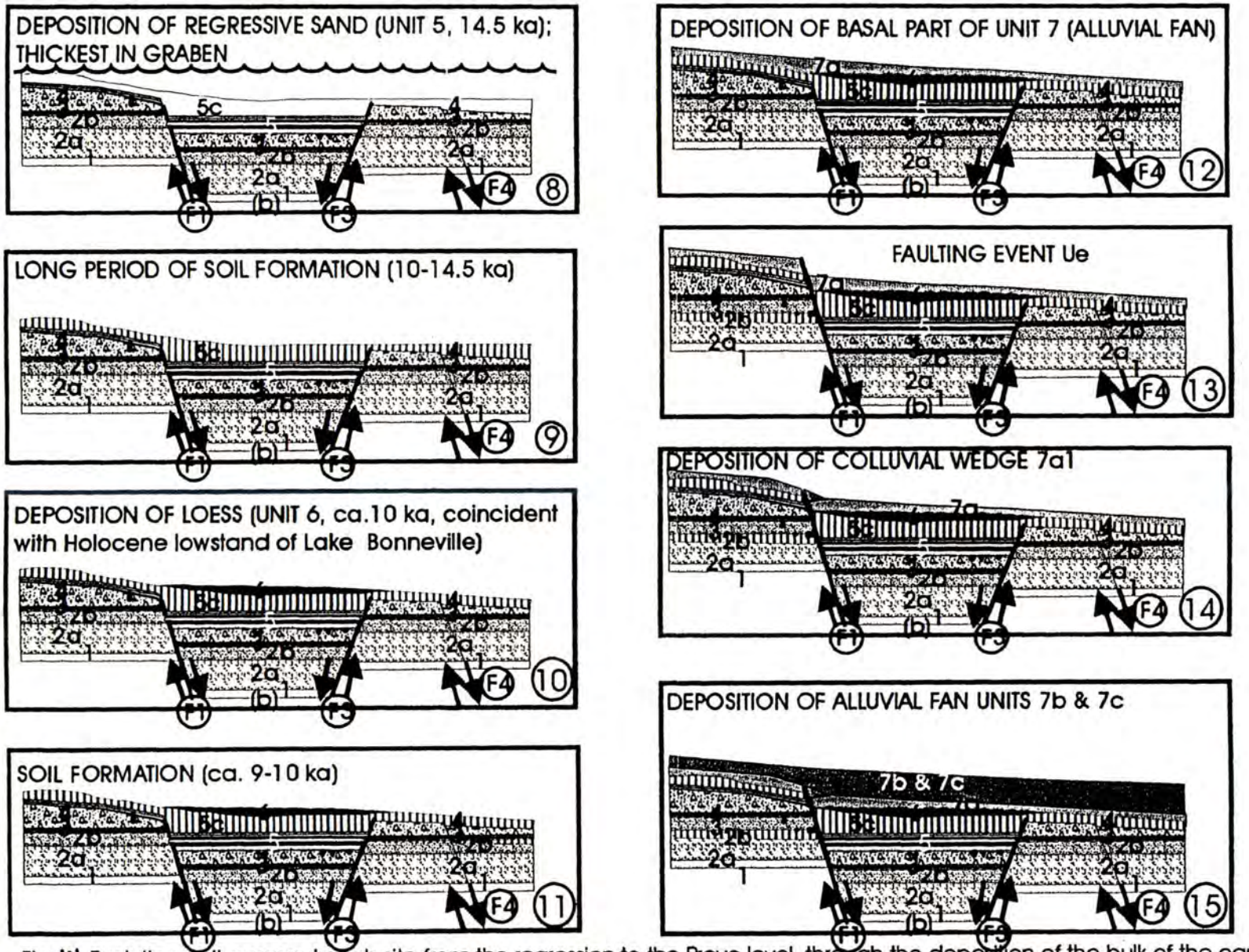

Fig. 11b Evolution of the megatrench site from the regression to the Provo level, through the deposition of the bulk of the early Holocene alluvial fan sediments (unit 7). Loess is presumed to have been deposited only in the early graben between faults F1 and F3. Unit 7 is assumed to have been deposited upslope of fault F1, but thinly compared to farther west.

Fig. 11 (c) Steps 16-21, ca. 7 ka to present.

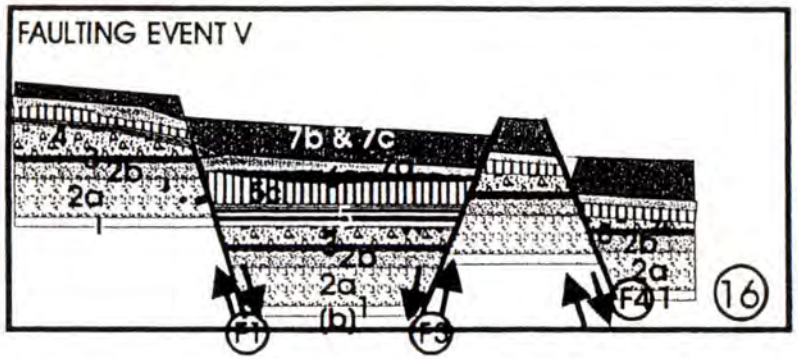

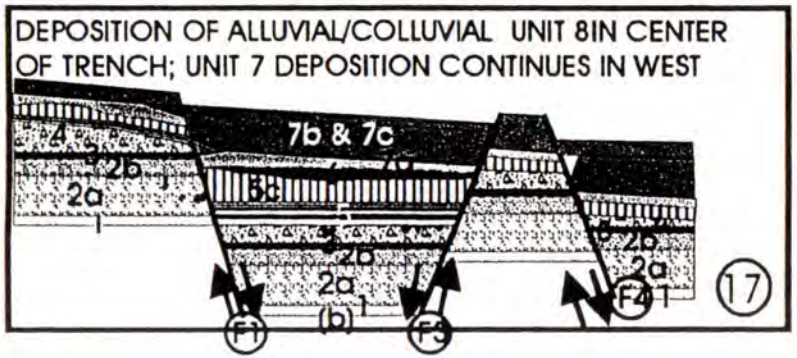

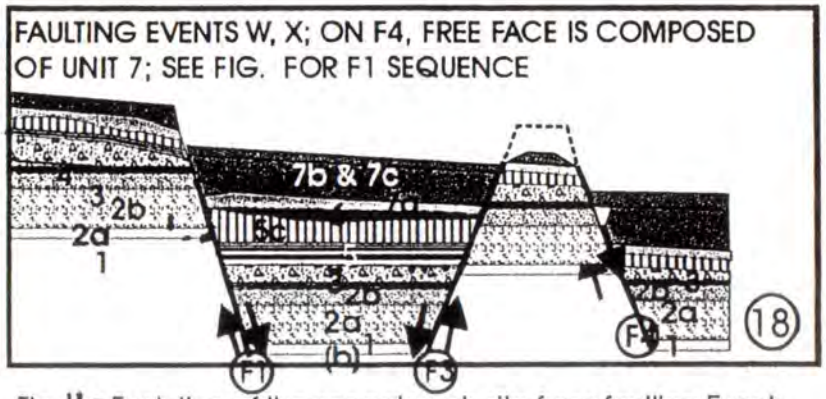

Fig. 11c Evolution of the megatrench site from faulting Event V to faulting Event Z, i.e. from ca. 8 ka to present. The main purpose of these diagrams is to show: 1) how unit 7 was eroded from atop the horst, and 2) how slip has successively shifted from F1 to F4 in the latest events. For detailed retro sequences of F1 and F4, see other figures.

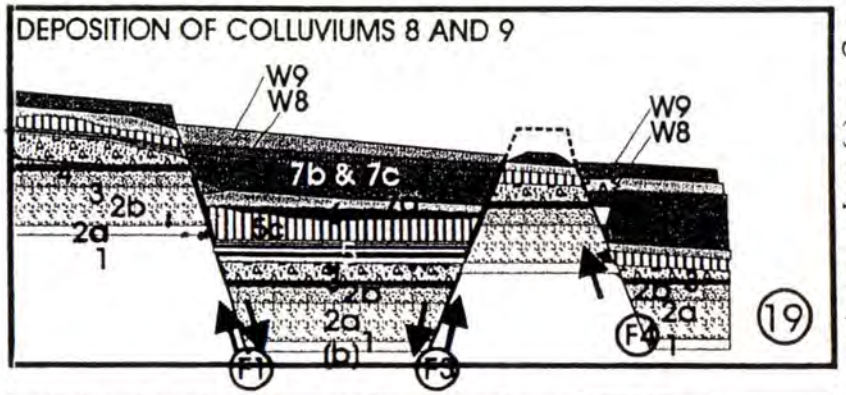

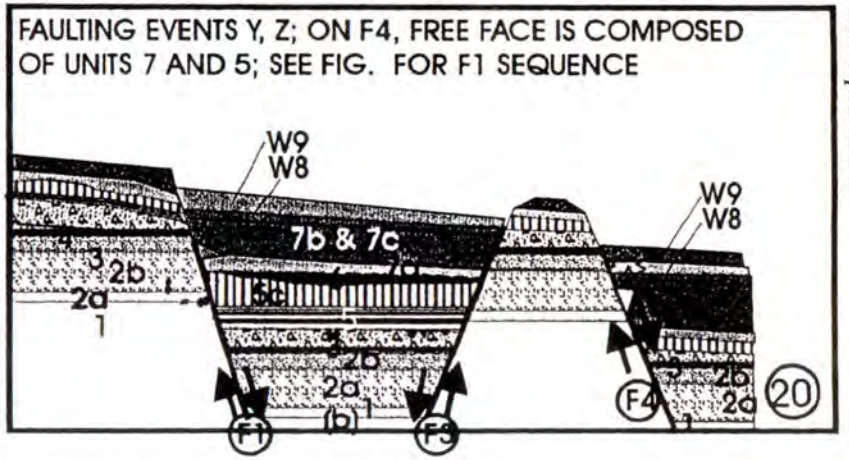

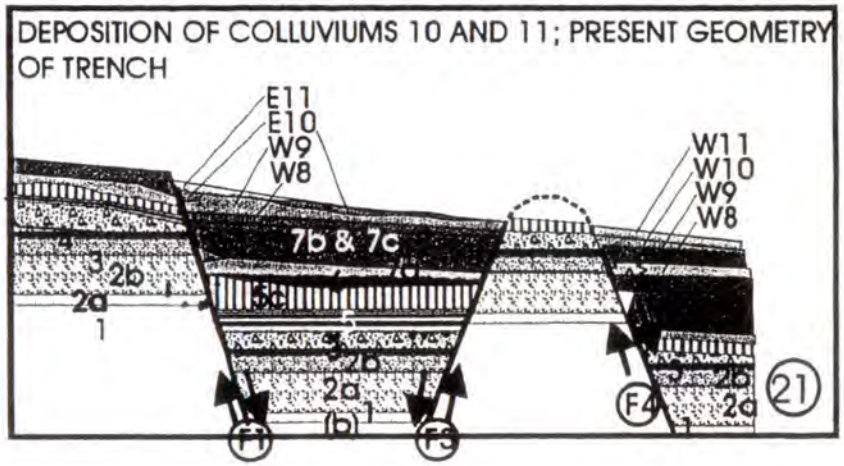

Table 3. Summary of age constraints on the latest four faulting events in fault zone F4.

Event	Colluvial Unit Formed	Min. Age	Max. Age (all ages in cal. yr BP)
Zw	W11	NA	925-1230
Yw	W10	NA	1080-1315 (bad date)
Xw	W9	NA	NA
Ww	W8	NA	7235-7815

8. CONCLUSIONS

7.1 Comparison of Previous Paleoearthquake Chronologies

The most detailed chronology of paleoearthquakes on the SLC segment prior to the megatrench was reported by Black et al. (1996), who dated four events in the past 5 ka (Table 3, Fig. 12) at the South Fork Dry Creek and Dry Gulch sites, roughly 5 km south of the megatrench site.

Table 4. Age estimates for paleoearthquakes on the SLC segment from Black et al. (1996).

Event	Min. Age	Preferred Age	Max. Age (all ages in cal. yr BP)
Z	1100	1300	1550
Y	2100	2450	2800
X	3500	3950	4500
W	4950	5300	5750

The Black et al. estimates formed the main basis for the age estimates of McCalpin and Nishenko (1996) in their compilation of paleoearthquake dates in the central five segments of the WFZ (Table 4, Fig. 12). For the SLC segment, McCalpin and Nishenko extracted the closest maximum limiting dates (i.e., one-sided age constraints) on the latest four paleoearthquakes, mainly from the data set of Black et al. (1996). Naturally, their results were very similar to Black et al.'s (Fig. 12), resulting in a very regular recurrence of ca. 1350 years among the latest four events.

By comparison to the Black et al. chronology, the current age constraints on the latest four events in the megatrench are not as closely limiting (Fig. 12). Partly this is due to the fact that organic matter in the megatrench could not always be found near paleoearthquake event horizons, and partly it is due to a budget insufficient to date more than half the samples collected. On fault zone F1, the two latest events (Ze, Ye) overlap the age ranges cited by Black et al. (1996), but the two older events (Xe, We) appear to be somewhat older than Black et al.'s events X and W. In fact, it could be argued that event Xe actually correlates with Black et al.'s event W. Part of the ambiguity on the ages of Events Xe and We stems from the fact that dated organics are from crack fills, rather than from soils buried by colluvial wedges. When a soil is buried by a colluvial wedge, the age of the soil constitutes a close maximum age on debris-facies colluvial deposition, and this on the age of the event. For organics in a crack fill, the origin of the organics is more ambiguous. The basal crack fill at the base of a free face is typically composed of intact blocks of material that fell off the scarp free face. These blocks could be parts of the surface soil, or parts of buried soils developed on previous colluvial wedges. Thus the age of organics could be older, even much older, than the age of the crack-forming event, even though the organics were deposited in the crack shortly after the cracking event.

Fig. 12 Space-time diagram of paleoearthquakes dated in previous studies, and in the megatrench.

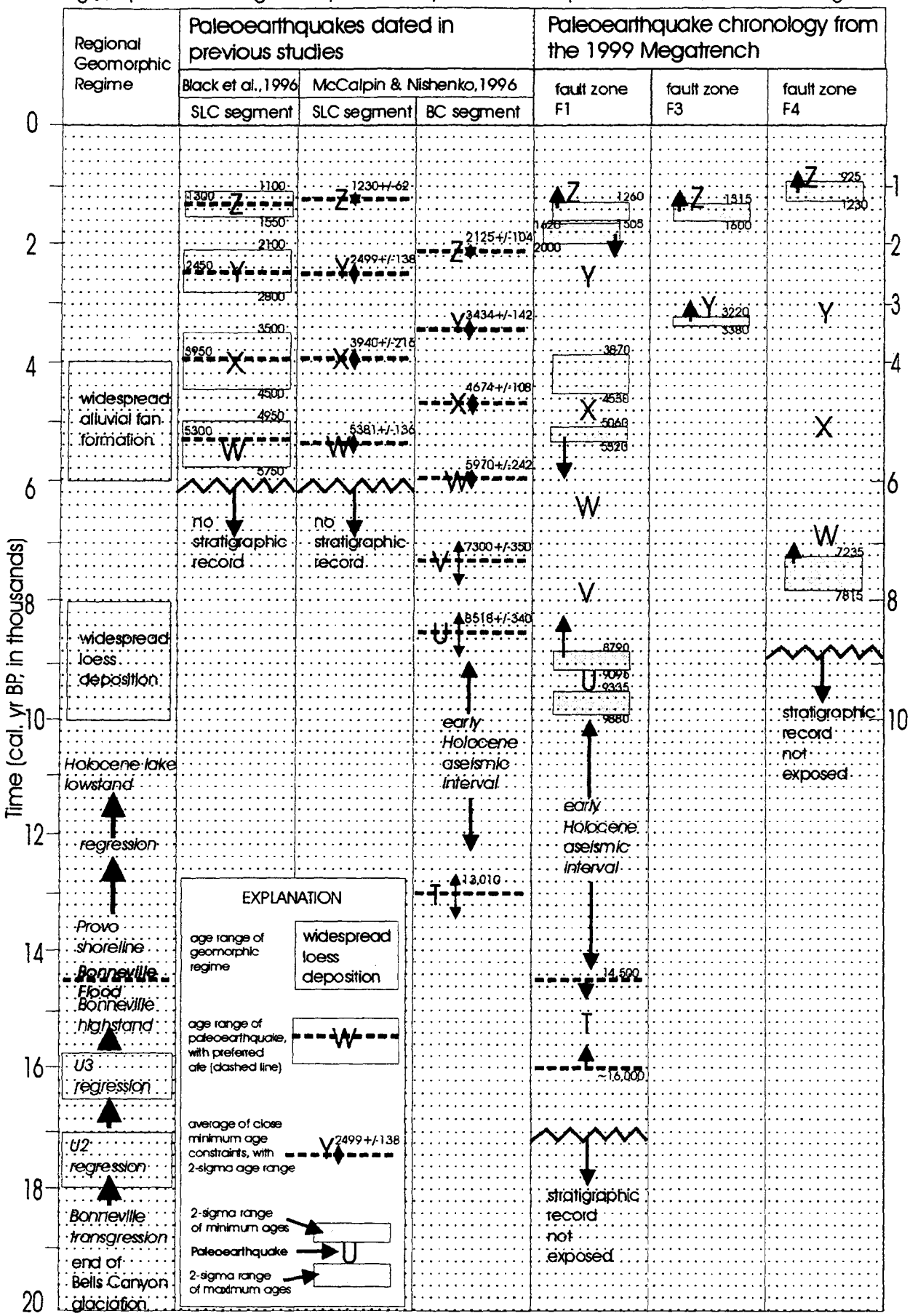

The ambiguity in correlating the latest four events in the megatrench does not affect the major goal of our investigation, that is, the chronology of paleoearthquakes between 6 ka and 15 ka. However, if our Event Xe actually correlates with Black et al.'s event W, then there have been four paleoearthquakes on fault zone F1 between ca. 6 ka and 15 ka, rather than the three otherwise inferred.

Another ambiguity in correlation exists on fault zone F4, where there have been four faulting events since 7.2 ka (Fig. 12). If the radiocarbon age of 7235-7815 cal yr BP is closely limiting on Event Ww, then that event is roughly 2000 years too old to correlate with Black et al.'s event W. That scenario then leaves only three recognizable faulting events on fault zone F4 in the past 6 ka, compared to the four recognized on the SLC segment by Black et al. (1996). Examination of Fig. 12 suggests that our Event Ww may actually correlate with our Event Ve. There are several possible explanations for this discrepancy: 1) one of Black et al.'s four post-6 ka events did not rupture this fault strand, 2) rupture did occur in all four events, but the proportion of displacement on fault F4 was so small in relation to that on fault F1 that no colluvial signature was generated, and 3) the 7235-7815 date is incorrect. However, we have confidence in the 7235-7815 date being correct, merely because it comes from strata deposited contemporaneously with the end of alluvial fan deposition, which was dated farther east in the trench as somewhat younger than 8790-9095 cal. yr BP.

In summary, the megatrench shows evidence for three paleoearthquakes in the same time period in which Black et al. (1996) inferred four paleoearthquakes. Our event Z correlates well with their event Z. For the earlier events, our age control is not tight enough to state which of Black et al.'s events is missing from the megatrench, but the pattern suggests that we have only one event to correlate with their events X and Y. In fact, the date from the basal crack fill of fault zone F3 falls almost exactly between the age estimates for Black et al.'s events X and Y (but see previous discussion of the limitation of crack fill dates). The more important conclusion in relation to our goals is that there is stratigraphic evidence for only three paleoearthquakes in the period 6 ka-15 ka, rather than the 6-7 events that would have occurred if 1350-year recurrence had continued throughout this 9000 year-long interval.

7.2 Physical Causes of Variable Earthquake Recurrence

We can calculate a rough pattern of recurrence between the 7 paleoearthquakes inferred from the megatrench from the dates presented in Fig. 12. The mean recurrence between the latest four paleoearthquakes, based on Black et al. (1996), ranges from 1150 years to 1500 years. The recurrence between our events U and V, and V and W, is roughly 2000 years in each case. However, the recurrence time between our Events T and U ranges from 4620 years to 7210 years (2 sigma range), with a mean value of 6035 years. This long period of landscape stability at the megatrench site is represented by the well-developed buried soils b4 and b5, developed on units 5 and 6, respectively, a time span during which no scarp-derived sediments or structures formed, even as close as 1 m to faults.

What would have caused such a long hiatus of faulting on the WFZ? The time window 9 ka to 15 ka coincides with the desiccation of Lake Bonneville, starting with the abrupt 100-m drop from the Bonneville highstand to Provo shorelines at 14.5 ka, and continuing to the Holocene lowstand of the lake (below the present level of the Great Salt Lake) at ca. 11 ka. This

desiccation removed an enormous weight of water from the hanging wall of the WFZ over a period of 4 ka. Could this desiccation have redistributed stress patterns on the hanging wall and footwall of the WFZ in a manner as to suppress fault movement? Conceptually, placing a load on the hanging wall of a normal fault and increasing the regional pore fluid pressure, such as would occur during a lake transgression, would tend to encourage slip on a normal fault. Conversely, a lake regression should have the opposite effect, that of suppressing fault slip.

An early Holocene aseismic interval was inferred by McCalpin and Forman (1991) and McCalpin and Nishenko (1996), based on trenching results on the Brigham City segment of the WFZ. Their 1991 trenching campaign on the Provo delta surface at Brigham City was one of the few trench studies that exposed the paleoearthquake record prior to the mid-Holocene. They found stratigraphic and geochronologic evidence that no faulting events had occurred between the occupation of the Provo Shoreline (ca. 13.5 ka) and about 8.5 ka. This quiescent period of 5 ka contrasts strongly with the subsequent 1200-1300 year recurrence between subsequent events (Fig. 12). Thus, the only two trench investigations (Brigham City, the megatrench) to deduce a detailed chronology of post-Bonneville paleoearthquakes both inferred a 5-6 ky early Holocene aseismic interval.

7.3 Implications of the Megatrench Results for Probability Estimates of Future Earthquakes on the SLC Segment

McCalpin and Nishenko (1996) calculated probabilities of M>7 earthquakes in the next 20, 50, and 100 years on the five central segments of the WFZ. Probabilities were calculated for both memoryless (Poisson) models of recurrence and also conditional probabilities assuming various renewal models of recurrence (lognormal and Weibull). For the SLC segment, Poisson probability in the next 100 years is 7%, compared to conditional probability estimates ranging from 6% to 56% (Table 5).

Table 5. Probability estimates of M>7 earthquakes in the next 100 years for the SLC segment. From McCalpin and Nishenko, 1996, Table 6.

Behavior Model	Recurrence Model	Mean Recurrence and Source[1] (years)	COV of Recurrence or Weibull shape parameter (B)	Probability of M>7 Earthquake in the Next 100 years[2]
memoryless	Poisson	NA	NA	7%
Renewal (memory)	Lognormal	1767, group	0.21	8%
Renewal (memory)	Lognormal	1767, group	0.5	8%
Renewal (memory)	Lognormal	1384, segment	0.21	22%
Renewal (memory)	Lognormal	1384, segment	0.5	11%
Renewal (memory)	Weibull	1775, group	B=3.36	6%
Renewal (memory)	Weibull	1328, short	B=17.8	57%

[1]- Source; "group" means derived from averaging all Holocene events on all five central segments; "segments" means derived just from the segment named; "short" refers to the group of short recurrences among the five central segments averaging 1328+/-104 years, as opposed to a separate group of "long" recurrences (dominantly observed

on the Provo and Nephi segments) averaging 2346+/-448 years. See McCalpin and Nishenko, 1996, p. 6248-6250 for detailed discussion.

[2]- All estimates assume an elapsed time of 1230+/-62 years.

What implications does the long paleoearthquake chronology from the megatrench have on the accuracy of these widely variable probability estimates? First, we have documented rather large departures in the latest Pleistocene/ early Holocene from the regular 1300-1400 year recurrence of the mid-late Holocene. However, we suspect that these longer recurrence times were strongly influenced by the unloading of the WFZ hanging wall during desiccation of Lake Bonneville. It appears that the unloading effect died out by the time of Event W, and that it has not affected the regular 1300-1400 year recurrence cycle since that time. Therefore, we do not propose to favor or disfavor any of McCalpin and Nishenko's recurrence models based on the long recurrence times observed while the lake was drying up.

However, we can apply the results of some more recent recurrence studies to the likelihood of the various recurrence models. For example, the highest 100-year conditional probability calculated by McCalpin and Nishenko (1996) was 57%, based on a Weibull model of recurrence with a mean of 1328 years and a COV of only 0.04. By comparison, conditional probabilities based on lognormal models with COVs of 0.21 and 0.5 indicated probabilities of 22% and 11%, respectively (Table 5). So, is the COV of long-term recurrence on the SLC segment closer to 0.04, 0.21, or 0.5?

McCalpin and Slemmons (1998) inventoried all published paleoseismic chronologies that contained 3 or more well-dated events. They found that, as a group, worldwide normal faults with a large span of slip rates and mean recurrences tended to have an average COV of recurrence of 0.35. The same data set for all fault types yielded an average COV of recurrence of 0.36. In addition, the more paleoearthquakes that had been dated at a local trench site, the closer the COV of that local recurrence series approached 0.36. McCalpin and Slemmons argued that a relatively short recurrence series at a site (say, containing only 3-4 events, or 2-3 recurrence intervals) could yield a wide possible range of recurrence COVs, ranging from ca. 0.04 to 0.8. However, the site chronologies with successively more events tended to have COVs that converged on the value 0.36. They further argued that, for the purposes of making conditional probability estimates, it would be preferable to use the value COV=0.36 rather than use an "apparent" COV value from a short (3-4 event) recurrence series.

Their conclusions suggest that we should probably not lend much weight to the probability estimate of 57% in Table 5, which is based on a COV=0.04 from only 4 events on the SLC segment. Instead, we should probably assume a long-term recurrence COV of 0.36 for the SLC segment. Note that 0.36 falls almost exactly halfway between the COVs of 0.21 and 0.5, which resulted in probability estimates of 22% and 11%, respectively, for the next 100 years. If we assume that conditional probability varies linearly with COV over this relatively small range, then an assumed recurrence COV=0.36 would imply a conditional probability of 16.5% for M>7 earthquakes in the next 100 years.

9. REFERENCES

Birkeland, P.W., 1999, Soils and geomorphology: Oxford University Press, 488 pp.

Black, B.D., Lund, W.R., Schwartz, D.P., Gill, H.E. and Mayes, B.H., 1996, Paleoseismic investigation on the Salt Lake City segment of the Wasatch fault zone at the South Fork Dry Creek and Dry Gulch sites, Salt Lake County, Utah: Utah Geol. Survey Spec. Study 92, Paleoseismology of Utah, Vol. 7, 22 p.

Machette, M.N., Personius, S.F. & Nelson, A.R. 1992. Paleoseismology of the Wasatch fault zone: a summary of recent investigations, interpretations, and conclusions, in Gori, P.L & Hays, W.W. (eds.) Assessment of Regional Earthquake Hazards and Risk Along the Wasatch Front, Utah. U.S. Geological Survey Professional Paper 1500, p. A1-A71.

McCalpin, J.P. and Berry, M.E., 1996, Soil catenas to estimate ages of movements on normal fault scarps, with an example from the Wasatch fault zone, Utah, USA: Catena 27:265-286.

McCalpin, J.P. and Niskenko, S.P., 1996, Holocene paleoseismicity, temporal clustering, and probabilities of future large (M>7) earthquakes on the Wasatch fault zone, Utah: Journal of Geophysical Research, v. 101(B4), p. 6233-6253.

McCalpin, J.P. and Slemmons, D.B., 1998, Statistics of paleoseismic data: unpublished Final Technical Report submitted to U.S. Geological Survey by GEO-HAZ Consulting, Inc., Contract 1434-HQ-96-GR-02752, March 20, 1998, 62 p.,

Oviatt, C.G., 1997, Lake Bonneville fluctuations and global climatic change: Geology, 25(2): 155-158.

Personius, S.F. and Scott, W.E., 1992, Surficial geologic map of the Salt Lake City segment and parts of adjacent segments of the Wasatch fault zone, Davis, Salt Lake, and Utah Counties, Utah: U.S. Geological Survey map I-2106, scale 1:50,000.

Schwartz, D.P. and Coppersmith, K.J., 1984, Fault behavior and characteristic earthquakes--Examples from the Wasatch and San Andreas fault zones: Journal of Geophysical Research, v. 89, p. 5681-5698.

Soil Conservation Service, 1994, Soil Taxonomy, 6th Edition: U.S. Department of Agriculture, Soil Conservation Service.

Swan, F.H. III, Schwartz, D.P. & Cluff, L.S. 1980. Recurrence of moderate to large magnitude earthquakes produced by surface faulting on the Wasatch fault, Utah. Bulletin of the Seismological Society of America, 70(5), 1431-1462.

Swan, F.H. III, Hanson, K.L., Schwartz, D.P., and Knuepfer, P.L.K., 1980 b, Study of earthquake recurrence intervals on the Wasatch Fault at the Little Cottonwood site, Utah: U.S. Geological Survey Open-File Report 81-450, 30p.

APPENDIX 1: Unit Descriptions, Wasatch Fault Megatrench

Units in the eastern 50 m of the trench

E11- Grayish brown (10YR5/2 d) gravelly silty sand; clasts average 2 cm diameter, max. 5-6 cm; moderately to poorly sorted; clasts are subangular; matrix is silty sand; matrix supported deposit; firm to hard; no bedding; downslope clast fabric;DEBRIS-FACIES COLLUVIAL WEDGE OF MOST RECENT EVENT (Event Ze) ON FAULT F1 (LATEST HOLOCENE).

E10b- Brown (19YR5/3 d) gravelly sand; clasts average 1 cm diameter, max. 10 cm; moderately to poorly sorted; clasts are angular; matrix is sand; matrix-supported deposit; hard; no bedding; downslope clast fabric; upper half of DEBRIS-FACIES COLLUVIAL WEDGE OF PENULTIMATE EVENT (Event Ye) ON FAULT F1 (LATE HOLOCENE).

E10a- Dark brown (10YR 3/3 d) gravelly sand; clasts average 1.5 cm diameter, max. 3 cm; moderately sorted; clasts subangular to subround; sand matrix; firm; downslope stratification, with beds 2-5 cm thick; downslope clast fabric; FLUVIAL CHANNEL ALONG BASE OF FAULT SCARP? (LATE HOLOCENE)

E9bAb1- Dark grayish brown (10YR4/2 d) gravelly silty sand; dominantly pea gravel to coarse sand; clasts average 1-2 cm, max. 5 cm; poorly to moderately sorted; clasts are angular; matrix is silty sand; firm to loose; unstratified; weak downslope clast fabric; SOIL A HORIZON DEVELOPED ON THE DEBRIS- and WASH-FACIES COLLUVIAL WEDGE OF THE ANTEPENULTIMATE EVENT (Event Xe) ON FAULT F1 (LATE HOLOCENE).

E8b- Brown (7.5YR5/4 d) gravelly silty sand; clasts average 2-3 cm diameter, max. 15 cm; poorly sorted; clasts are angular; matrix is silty sand; matrix supported deposit; hard to firm; unstratified; clasts generally random orientation, slight downslope fabric; CRACK FILL & DEFOMED COLLUVIAL WEDGE (?) OF ANTE-ANTEPENULTIMATE EVENT (Event We) ON FAULT F1 (MIDDLE HOLOCENE).

E7cA- Yellowish brown (19YR5/6 d) gravelly sand; clasts are pea gravel size, max. diameter 5 cm; poorly to moderately sorted, with some well-sorted stringers; clasts angular to subangular; matrix of silt to silty coarse sand; hard; matrix supported; no distinct bedding; weak downslope clast fabric; A HORIZON OF SURFACE SOIL, DEVELOPED ON DISTAL FAN ALLUVIUM/COLLUVIUM (HOLOCENE) ABOVE THE EASTERN SCARP.

Unit E10- Dark yellowish brown (10YR4/6 d) sand; dominantly coarse sand, with clasts up to 10 cm diameter; moderately sorted, with lenses well sorted; clasts are subangular to subround; matrix is coarse sand, quite hard; matrix supported deposit; bedding is lenticular, with well-sorted lenses averaging 10 cm thick and 100 cm long; DISTAL FAN ALLUVIUM/COLLUVIUM (HOLOCENE).

E9Ab1- Dark grayish brown (10YR4/2 d) gravelly silty sand; fine to coarse sand (40%), silt (25%), pebbles (20%) and gravel (15%); very poorly sorted and homogenous; gravels similar in lithology to Unit 8b but generally smaller and less abundant than in unit 8b; homogeneous, unstratified deposit; loose; soft, softer than unit 8b; undulatory contact with unit 8b; SOIL A HORIZON DEVELOPED ON UNIT 9, WASH-FACIES COLLUVIUM (HOLOCENE).

8b- Brown (10YR5/3 d) gravelly silty sand; fine to coarse sand (40-50%), silt (ca. 25%), and gravel (ca. 25%); very poorly sorted gravels; angular, average diameter 1-2 cm, max. 7 cm, dominantly green amphibolite, vein quartz, granodiorite; loose in upper 20 cm to moderately dense in lower part of unit; unstratified; lower 40 cm is darker brown (10YR4/3d), forms a slightly resistant bench below unit 9A; WASH-FACIES COLLUVIUM (HOLOCENE).

7c- Light olive brown (2.5Y5/6 d) sand; very fine sand with rare granitic cobbles (grussified, subround), max. diameter=18 cm; forms vermicular lenses 10-25 cm thick that interfinger with units 7a and 7b; GRABEN-FILL ALLVIUM (HOLOCENE).

7b- Light yellow brown (10YR6/4 d) gravelly sand; fine-medium gravel in matrix of medium-coarse sand; gravels subangular to subround, max, diameter 2-3 cm, quartzite with a few (grussified) granitic clasts; sands are subround in undulating (scour) contact with underlying unit 7a; GRABEN-FILL ALLVIUM (HOLOCENE).

7a- Light yellow brown (10YR6/4 d) sandy gravel; gravel with few cobbles in medium-coarse sand matrix; gravel clasts are angular to subangular; lithologies= quartzite (max. diameter=16 cm), diorite, amphibolite (max. diameter=6 cm); dominantly matrix-supported, poorly stratified; matrix is light yellow brown sand, subangular; GRABEN-FILL ALLUVIUM (HOLOCENE).

6- Yellowish brown (10YR5/4 d) silt; contains minor fine to medium sand; moderately dense; massive bedding ca. 75 cm thick; drapes underlying silty sand (unit 5c); LOESS (IMMEDIATELY POST-LAKE TO EARLY HOLOCENE).

5cACb5- Light yellowish brown (10YR6/4 d) to brownish yellow (10YR6/6 d) silty sand; very fine sand with ca. 30% silt and up to 25% medium sand, 15% coarse sand; lithology= granitic; subangular grains; moderately dense, density increases with silt content; loose where sand content is high; massively bedded ca. 50 cm thick; undulatory upper and lower contacts; AC HORIZON OF THE 5th BURIED SOIL, DEVELOPED ON UNIT 5c, REGRESSIVE LACUSTRINE SAND (ca. 15 ka).

5cC1oxb5- Light yellowish brown (10YR6/4 d) silty sand; fine to coarse sand (fine 10%, medium 40%, coarse 20%); poorly sorted, subround, moderately loose and soft; massive beds ca. 20 cm thick; lower contact with 5cC2 is gradational over ca. 5 cm and undulatory; C1ox HORIZON OF THE 5th BURIED SOIL, DEVELOPED ON UNIT 5c, REGRESSIVE LACUSTRINE SAND (ca. 15 ka).

5cC2oxb5- Yellow sand; medium to coarse grained, very clean, very loose; moderately sorted, subround; rare small gravel (granitic); poorly stratified with low angle foreset beds dipping 5-6

degrees west; C2ox HORIZON OF THE 5th BURIED SOIL, DEVELOPED ON UNIT 5c, REGRESSIVE LACUSTRINE SAND (ca. 15 ka).

5b- Olive yellow (2.5Y6/6 d) silt; sandy silt; well sorted; massively bedded; contains calcium carbonate tubes/nodules in irregular shapes; also contains occasional orange blobs; LACUSTRINE SILT (BONNEVILLE HIGHSTAND, ca. 14.5 ka?).

5a7- Pale olive (5Y6/4 d) silts and clays; alternating lenses of silts and silty clays; well sorted; breaks easily along bedding planes; dips 13-15 degrees east; LACUSTRINE SILT AND CLAY (BONNEVILLE HIGHSTAND, ca. 14.5 ka?).

5a6- Well-stratified fine sands and silts:(BONNEVILLE HIGHSTAND, ca. 14.5 ka?)

Subunit **5a61**- Pale yellow (5Y7/4 d) coarsening-upward package of silt to very fine sand; very fine sand is dominant; well sorted; grain size coarsens upward; well stratified; beds 0.5-2 cm thick; dips 8-9 degrees east; LACUSTRINE SILT AND SAND (BONNEVILLE HIGHSTAND, ca. 14.5 ka?).

Subunit **5a62**- Pale olive (5Y6/4 d) marker bed in unit 5a6; 2 cm thick bed of laminated silty clay; well sorted; dips 8-9 degrees east; upper and lower contacts slightly irregular; LACUSTRINE CLAY (BONNEVILLE HIGHSTAND, ca. 14.5 ka?).

Subunit **5a63**- Pale yellow (5Y7/4) silty sand; dominantly very fine sand; well sorted; well bedded; beds 1.5 cm thick; banded with brown layers; brown turns orange toward top of unit; dips 9-12 degrees east; LACUSTRINE SILT AND SAND (BONNEVILLE HIGHSTAND, ca. 14.5 ka?)

5a5- Olive (5Y5/3 d) silty clay; finely laminated; well sorted; slight orange- and brown-stained layers; beds typically <0.5 cm thick; dips 10-12 degrees east; LACUSTRINE CLAY (BONNEVILLE HIGHSTAND, ca. 14.5 ka?).

5a4- Pale yellow (5Y7/3 d) silty clay; hard, blocky, mottled green clay; well sorted; very hard; orange mottling; well stratified with orange-stained layers; beds <0.5 cm thick; dips east at 15 degrees; breaks in a platy fashion; will not scrape to a smooth surface; LACUSTRINE CLAY (BONNEVILLE HIGHSTAND, ca. 14.5 ka?).

5a3- Pale olive (5Y6/3 d) clay; massive green silty clay; very well sorted; very firm; massive unit with no internal bedding; discontinuous vertical orange stringers of unknown origin; LACUSTRINE CLAY (BONNEVILLE HIGHSTAND, ca. 14.5 ka?).

5a2- Pale yellow (5Y7/4 d) to strong brown (7.5YR5/8 d) silt; sequence of interbedded silt and very fine sand beds of variable colors; very well stratified; average fining-upward sequence is 1.5 cm thick; some layers are very oxidized (orange); quite firm, breaks along bedding planes; dip is 15 degrees east, rotated toward the main eastern fault zone; LACUSTRINE SILT AND SAND (BONNEVILLE HIGHSTAND, ca. 14.5 ka?).

5a1- Olive (5Y5/3 d) clayey silt; well sorted; firm; contains stringers of silt to very fine sand; stringers are discontinuous and very sinuous, possible result of liquefaction; in places vague

bedding is visible, but discontinuous; LACUSTRINE SILT (BONNEVILLE HIGHSTAND, ca. 14.5 ka?).

5b1- Light yellowish brown (2.5Y6/4 d) clayey silt; with occasional sand; moderately well sorted; massively bedded; contains large chunks of Unit 5a and 5b floating in it; most chunks congregate at the bottom of the unit; chunks range from 2x2cm, to 15x20 cm, to 30x50 cm; LACUSTRINE CLAY AND SILT SEVERELY DEFORMED BY SOFT-SEDIMENT DEFORMATION AND MECHANICALLY MIXED WITH ADJACENT UNITS.

4- White (5Y8/2 d) diamicton; upper half(unit 4b) contains clasts 10-50 cm on average, with max. diameter ca. 1 m; granitic; lower half (unit 4a) is more a sandy gravel; poorly sorted; clasts subangular to subrounded; upper half is matrix supported, with pale silt matrix (resembling Unit E9) between granite boulders lower half is a matrix-supported sandy gravel; firm consistence; no bedding in upper half; lower half contains some lenses of fine gravel 10-20 cm thick; carbonate rinds on clasts; DIAMICTON (LANDSLIDE DEPOSIT OF TILL INTO LACUSTRINE SILT?)

3d- Light gray (5Y7/2 d) sand; coarse sand with minor pea gravel; moderately sorted; grains subround; loose; grain supported; well stratified, with beds 1-5 cm thick; LACUSTRINE SANDS, PROBABLY FROM BONNEVILLE TRANSGRESSION (ca. 17 ka).

3c- Olive (5Y5/3 d) silt; well sorted; firm; matrix-supported; well stratified, with beds 1-2 cm thick; iron oxidation on some bedding planes; LACUSTRINE SILT (ca. 17 ka).

3b- Reddish yellow (7.5YR6/8 d) sand; coarse sand; well sorted; subrounded grains; firm; well stratified, with beds 1-2 cm thick; iron oxidation throughout, strongest at top of unit; LACUSTRINE SANDS, PROBABLY FROM BONNEVILLE TRANSGRESSION (ca. 17 ka).

3a- Light olive brown (2.5Y5/4 d) fine silt; well sorted; firm; matrix supported; well stratified, bedding thickness of 1 cm; finer mm-scale horizontal laminations; some beds are oxidized; LACUSTRINE SILT.

2b (EASTERN END OF TRENCH)- Gray (2.5Y6/0 d) to light gray (2.5Y5/0 d) sand; dominantly coarse sand, with rare clasts up to 20 cm; well sorted; clasts are subround to round; sand matrix, loose; matrix supported; well stratified, with beds averaging 2 cm thick; contains horizontal gravel beds throughout, 2-3 cm thick; some layers oxidized; LACUSTRINE SAND, PROBABLY FROM BONNEVILLE TRANSGRESSION (ca. 17 ka).

2a- Gray (5YR6/1 d) cobbly sandy gravel; cobbles average 10 cm in diameter, max. = 18 cm; lithologies= quartzite, diorite, and metamorphic green amphibolite (Little Willow series, ca. 1.8 by); quartz-mica schist; clasts are subangular to subround; no apparent imbrication; no carbonate coats; sands are clean, poorly sorted, medium-coarse grained, subround-round, very loose; LACUSTRINE BEACH GRAVEL, PROBABLY FROM THE BONNEVILLE TRANSGRESSION (ca. 17 ka).

Units in the western 15 m of the trench

2b - Gray (5YR6/1 d) gravelly sand; upward-fining sequence of interbedded clean gravelly sand, sandy gravel, and sands;
Lower 2 m= gravelly sand with clasts 2-3 cm diameter (max. 6-8 cm); lithologies similar to those in unit 2a, subangular to subround; larger clasts form distinct pebble lines. This section fines upwards to gravelly coarse sand, moderate-well sorted, with clasts ca. 1 cm diameter; beds are 2.5-7.5 cm thick; uppermost part is a manganese-stained, very well sorted, loose gravel 4 cm thick.
Middle 0.3 m= thinly-bedded sands, medium to coarse grained, well sorted, subround to subangular, loose; very thin interbeds of very fine, dense, tan sand; moderately to well stratified, horizontally bedded.
Upper 2 m= fining-upwards sequence of cobbly sand (25 cm thick) with medium- to thick-bedded, moderately well stratified, medium to coarse sand.
LACUSTRINE BEACH GRAVEL, PROBABLY FROM THE BONNEVILLE TRANSGRESSION (ca. 17 ka).

1- Light brownish gray (10YR6/2 d) to light gray (5Y7/1) sand; fine to coarse, laminated to thinly bedded (up to 12 cm thick) with few crossbeds; well sorted, subangular (coarse sand) to round (fine sand); iron oxide staining; LACUSTRINE NEARSHORE SANDS, PROBABLY FROM THE BONNEVILLE TRANSGRESSION (ca. 17 ka).

APPENDIX 2: Graphs showing calibration of radiocarbon age to calendar years

CALIBRATION OF RADIOCARBON AGE TO CALENDAR YEARS

(Variables: est. C13/C12=-25:lab. mult=1)

Laboratory number:	**Beta-139242**
Conventional radiocarbon age[1]:	**1440±70 BP**
2 Sigma calibrated result: (95% probability)	**Cal AD 445 to 690 (Cal BP 1505 to 1260)**

[1] C13/C12 ratio estimated

Intercept data

Intercept of radiocarbon age with calibration curve:	Cal AD 630 (Cal BP 1320)
1 Sigma calibrated result: (68% probability)	Cal AD 560 to 660 (Cal BP 1390 to 1290)

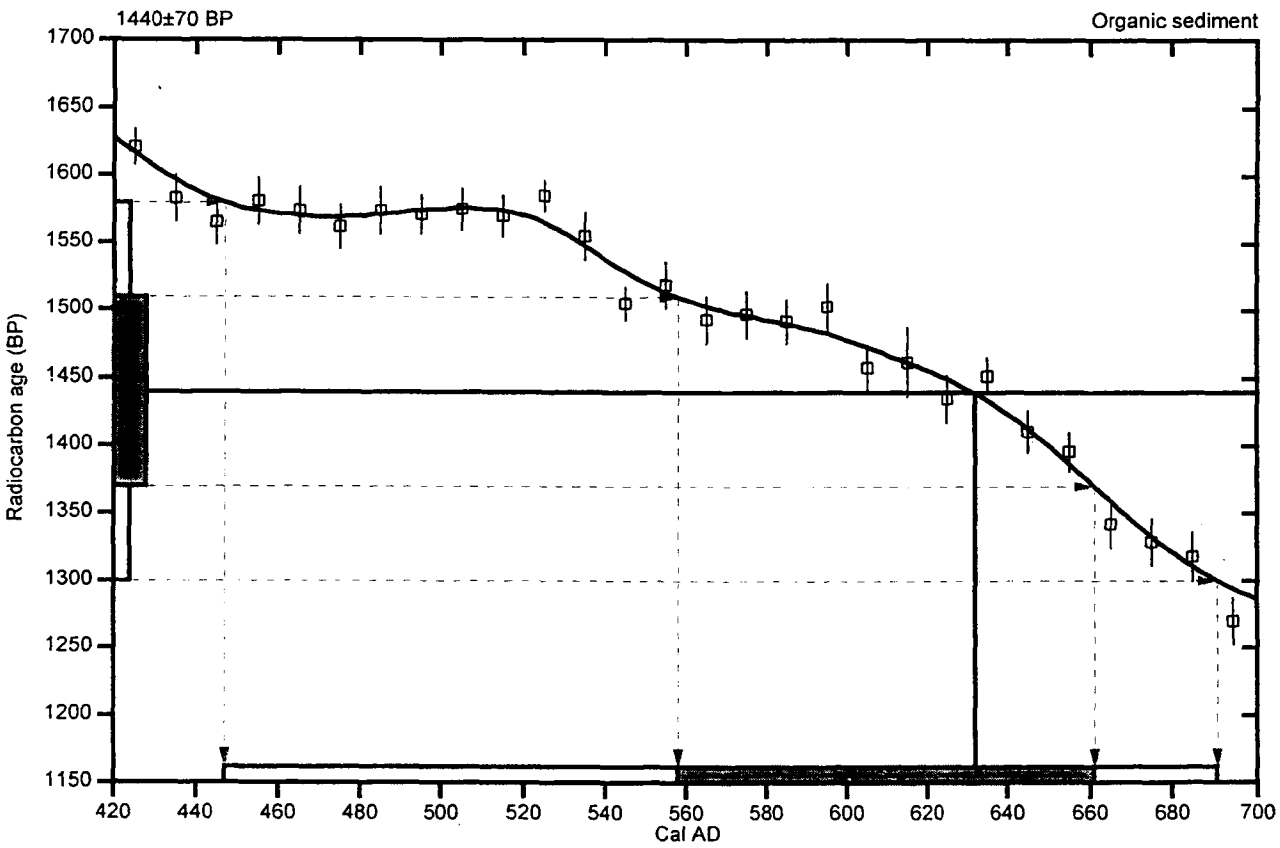

References:

Database used
INTCAL98
Calibration Database
Editorial Comment
Stuiver, M., van der Plicht, H., 1998, Radiocarbon 40(3), pxii-xiii
INTCAL98 Radiocarbon Age Calibration
Stuiver, M., et. al., 1998, Radiocarbon 40(3), p1041-1083
Mathematics
A Simplified Approach to Calibrating C14 Dates
Talma, A. S., Vogel, J. C., 1993, Radiocarbon 35(2), p317-322

Beta Analytic Radiocarbon Dating Laboratory

4985 S.W. 74th Court, Miami, Florida 33155 • Tel: (305)667-5167 • Fax: (305)663-0964 • E-mail: beta@radiocarbon.com

CALIBRATION OF RADIOCARBON AGE TO CALENDAR YEARS

(Variables: est. C13/C12=-25:lab. mult=1)

Laboratory number: **Beta-139243**

Conventional radiocarbon age[1]: ***1890±80 BP***

2 Sigma calibrated result: (95% probability) **Cal BC 50 to Cal AD 330 (Cal BP 2000 to 1620)**

[1] C13/C12 ratio estimated

Intercept data

Intercept of radiocarbon age with calibration curve: Cal AD 115 (Cal BP 1835)

1 Sigma calibrated result: (68% probability) Cal AD 45 to 230 (Cal BP 1905 to 1720)

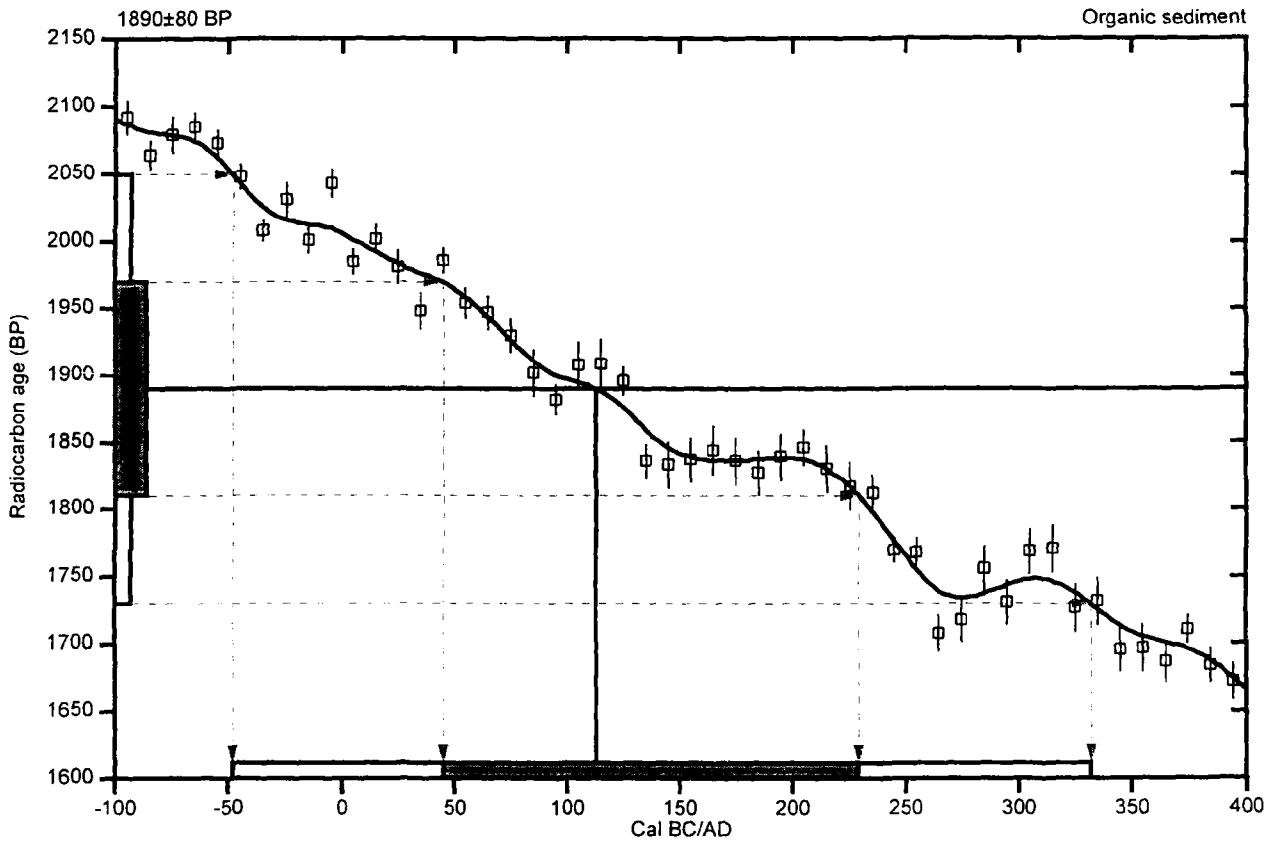

References:

Database used

INTCAL98

Calibration Database

Editorial Comment

Stuiver, M., van der Plicht, H., 1998, Radiocarbon 40(3), pxii-xiii

INTCAL98 Radiocarbon Age Calibration

Stuiver, M., et. al., 1998, Radiocarbon 40(3), p1041-1083

Mathematics

A Simplified Approach to Calibrating C14 Dates

Talma, A. S., Vogel, J. C., 1993, Radiocarbon 35(2), p317-322

Beta Analytic Radiocarbon Dating Laboratory

4985 S.W. 74th Court, Miami, Florida 33155 • Tel: (305)667-5167 • Fax: (305)663-0964 • E-mail: beta@radiocarbon.com

CALIBRATION OF RADIOCARBON AGE TO CALENDAR YEARS

(Variables: est. C13/C12=-25:lab. mult=1)

Laboratory number: **Beta-139244**

Conventional radiocarbon age[1]: **920±60 BP**

2 Sigma calibrated result: (95% probability) **Cal AD 1005 to 1250 (Cal BP 945 to 700)**

[1] C13/C12 ratio estimated

Intercept data

Intercepts of radiocarbon age with calibration curve: Cal AD 1055 (Cal BP 895) and
Cal AD 1085 (Cal BP 865) and
Cal AD 1150 (Cal BP 800)

1 Sigma calibrated result: (68% probability) Cal AD 1025 to 1195 (Cal BP 925 to 755)

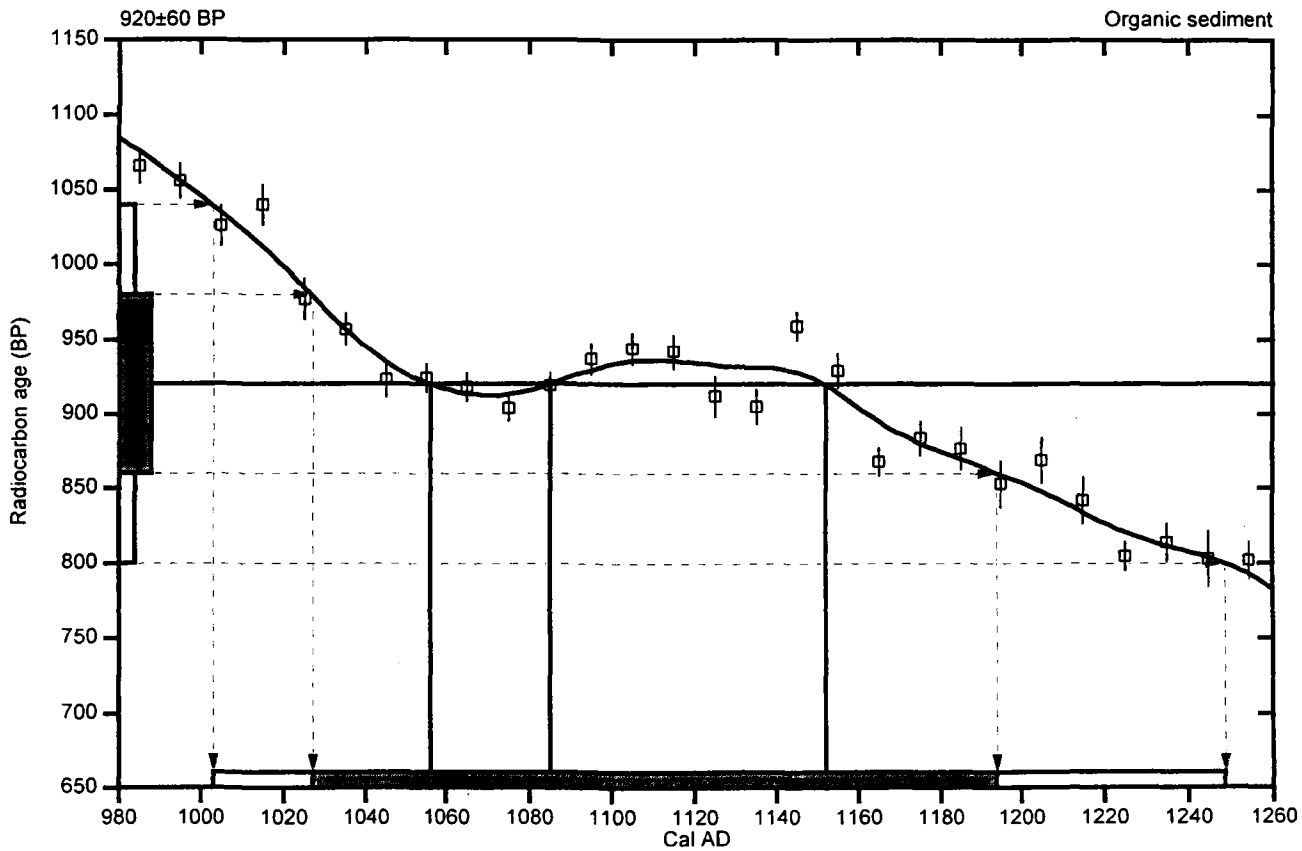

References:

Database used
INTCAL98
Calibration Database
Editorial Comment
Stuiver, M., van der Plicht, H., 1998, Radiocarbon 40(3), pxii-xiii
INTCAL98 Radiocarbon Age Calibration
Stuiver, M., et. al., 1998, Radiocarbon 40(3), p1041-1083
Mathematics
A Simplified Approach to Calibrating C14 Dates
Talma, A. S., Vogel, J. C., 1993, Radiocarbon 35(2), p317-322

Beta Analytic Radiocarbon Dating Laboratory

4985 S.W. 74th Court, Miami, Florida 33155 • Tel: (305)667-5167 • Fax: (305)663-0964 • E-mail: beta@radiocarbon.com

CALIBRATION OF RADIOCARBON AGE TO CALENDAR YEARS

(Variables: est. C13/C12=-25:lab. mult=1)

Laboratory number: **Beta-139245**

Conventional radiocarbon age[1]: **3820±120 BP**

2 Sigma calibrated result: **Cal BC 2580 to 1920 (Cal BP 4530 to 3870)**
(95% probability)

[1] *C13/C12 ratio estimated*

Intercept data

Intercept of radiocarbon age with calibration curve: Cal BC 2280 (Cal BP 4230)

1 Sigma calibrated results: Cal BC 2460 to 2120 (Cal BP 4410 to 4070) and
(68% probability) Cal BC 2085 to 2050 (Cal BP 4035 to 4000)

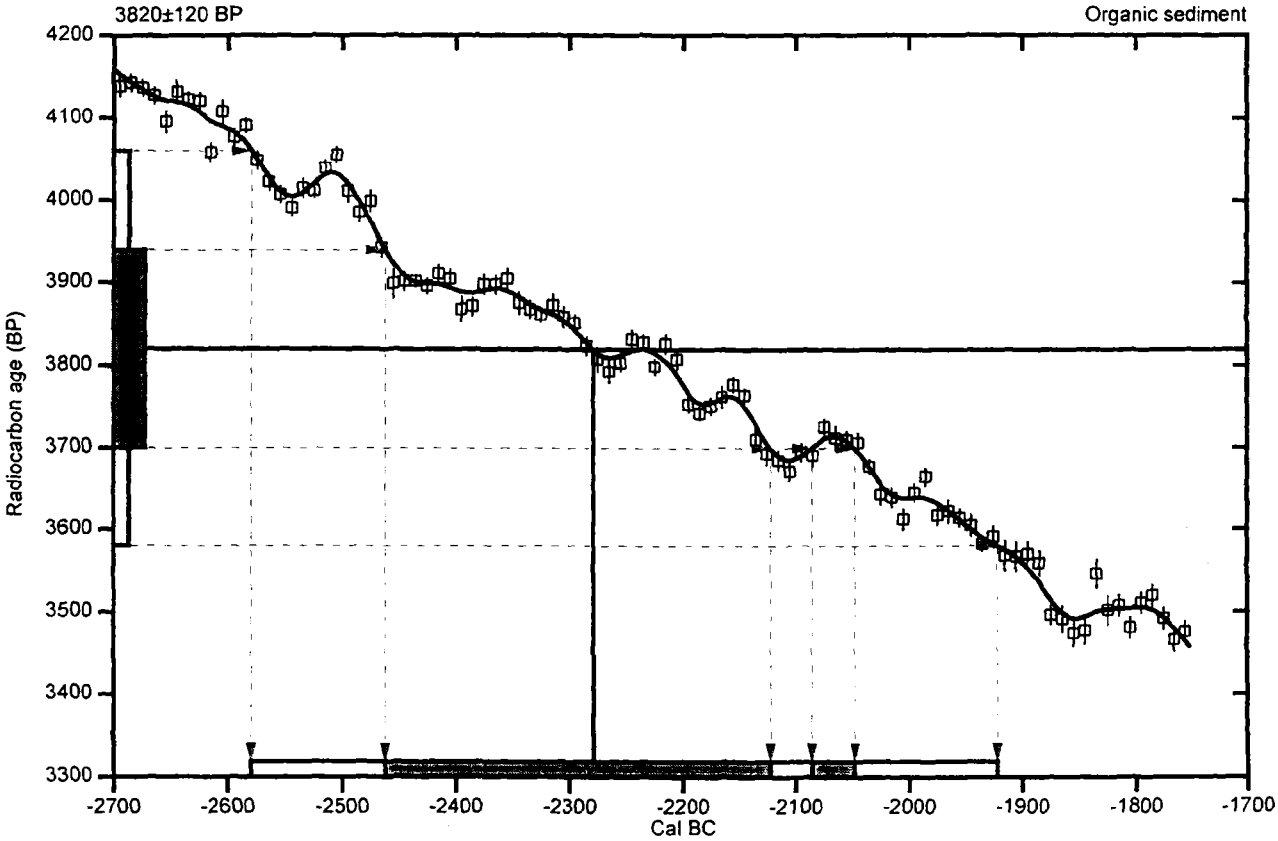

References:

Database used
INTCAL98
Calibration Database
Editorial Comment
Stuiver, M., van der Plicht, H., 1998, Radiocarbon 40(3), pxii-xiii
INTCAL98 Radiocarbon Age Calibration
Stuiver, M., et. al., 1998, Radiocarbon 40(3), p1041-1083
Mathematics
A Simplified Approach to Calibrating C14 Dates
Talma, A. S., Vogel, J. C., 1993, Radiocarbon 35(2), p317-322

Beta Analytic Radiocarbon Dating Laboratory

4985 S.W. 74th Court, Miami, Florida 33155 • Tel: (305)667-5167 • Fax: (305)663-0964 • E-mail: beta@radiocarbon.com

CALIBRATION OF RADIOCARBON AGE TO CALENDAR YEARS

(Variables: C13/C12=-25.1:lab. mult=1)

Laboratory number:	**Beta-139246**
Conventional radiocarbon age:	**4560±40 BP**
2 Sigma calibrated results: (95% probability)	**Cal BC 3485 to 3475 (Cal BP 5435 to 5425) and Cal BC 3370 to 3275 (Cal BP 5320 to 5225) and Cal BC 3240 to 3110 (Cal BP 5190 to 5060)**

Intercept data

Intercept of radiocarbon age with calibration curve:	Cal BC 3350 (Cal BP 5300)
1 Sigma calibrated results: (68% probability)	Cal BC 3360 to 3335 (Cal BP 5310 to 5285) and Cal BC 3205 to 3195 (Cal BP 5155 to 5145)

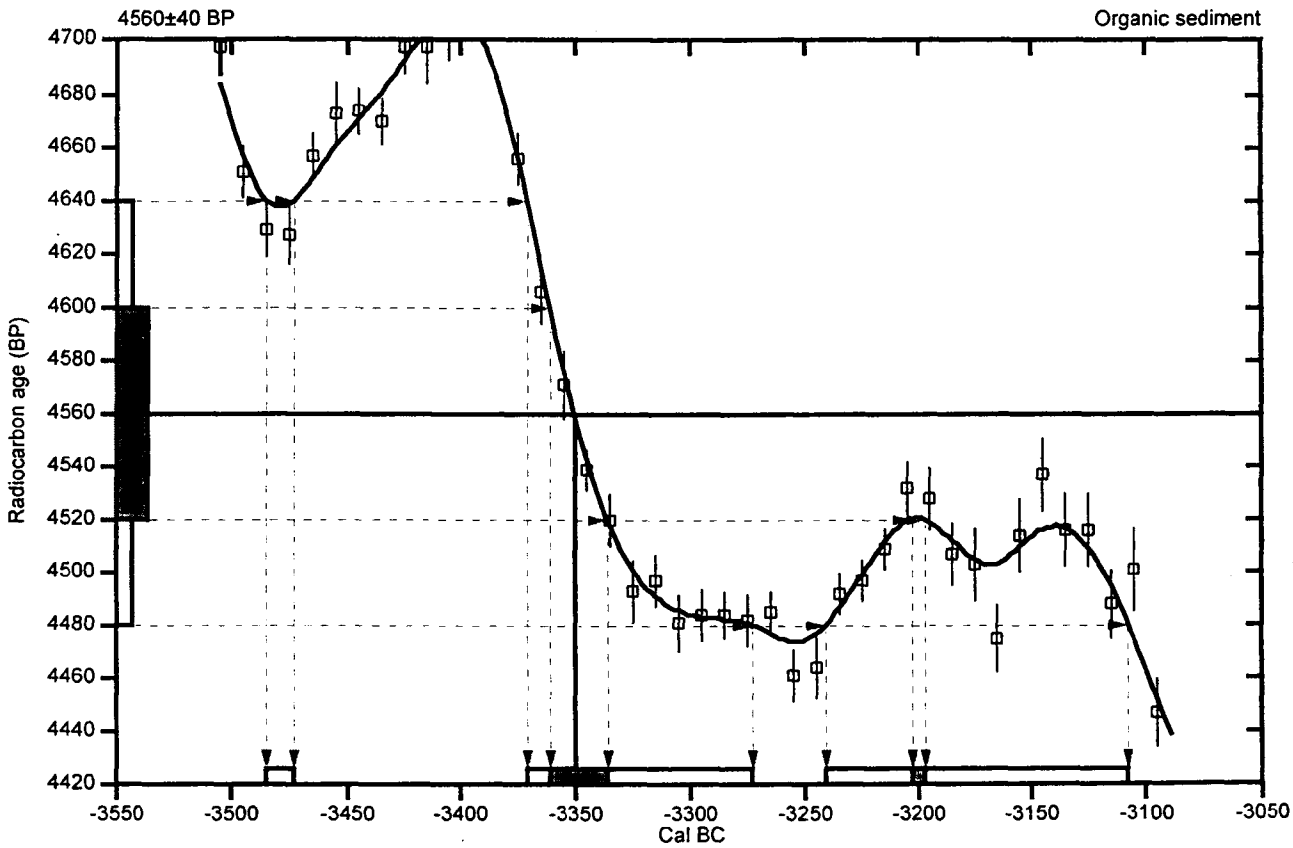

References:

Database used

INTCAL98

Calibration Database

Editorial Comment

Stuiver, M., van der Plicht, H., 1998, Radiocarbon 40(3), pxii-xiii

INTCAL98 Radiocarbon Age Calibration

Stuiver, M., et. al., 1998, Radiocarbon 40(3), p1041-1083

Mathematics

A Simplified Approach to Calibrating C14 Dates

Talma, A. S., Vogel, J. C., 1993, Radiocarbon 35(2), p317-322

Beta Analytic Radiocarbon Dating Laboratory

4985 S.W. 74th Court, Miami, Florida 33155 • Tel: (305)667-5167 • Fax: (305)663-0964 • E-mail: beta@radiocarbon.com

CALIBRATION OF RADIOCARBON AGE TO CALENDAR YEARS

(Variables: est. C13/C12=-25:lab. mult=1)

Laboratory number:	**Beta-139248**
Conventional radiocarbon age[1]:	**1130±70 BP**
2 Sigma calibrated results: (95% probability)	**Cal AD 720 to 745 (Cal BP 1230 to 1205) and Cal AD 760 to 1025 (Cal BP 1190 to 925)**

[1] C13/C12 ratio estimated

Intercept data

Intercept of radiocarbon age with calibration curve:	Cal AD 900 (Cal BP 1050)
1 Sigma calibrated results: (68% probability)	Cal AD 815 to 840 (Cal BP 1135 to 1110) and Cal AD 855 to 995 (Cal BP 1095 to 955)

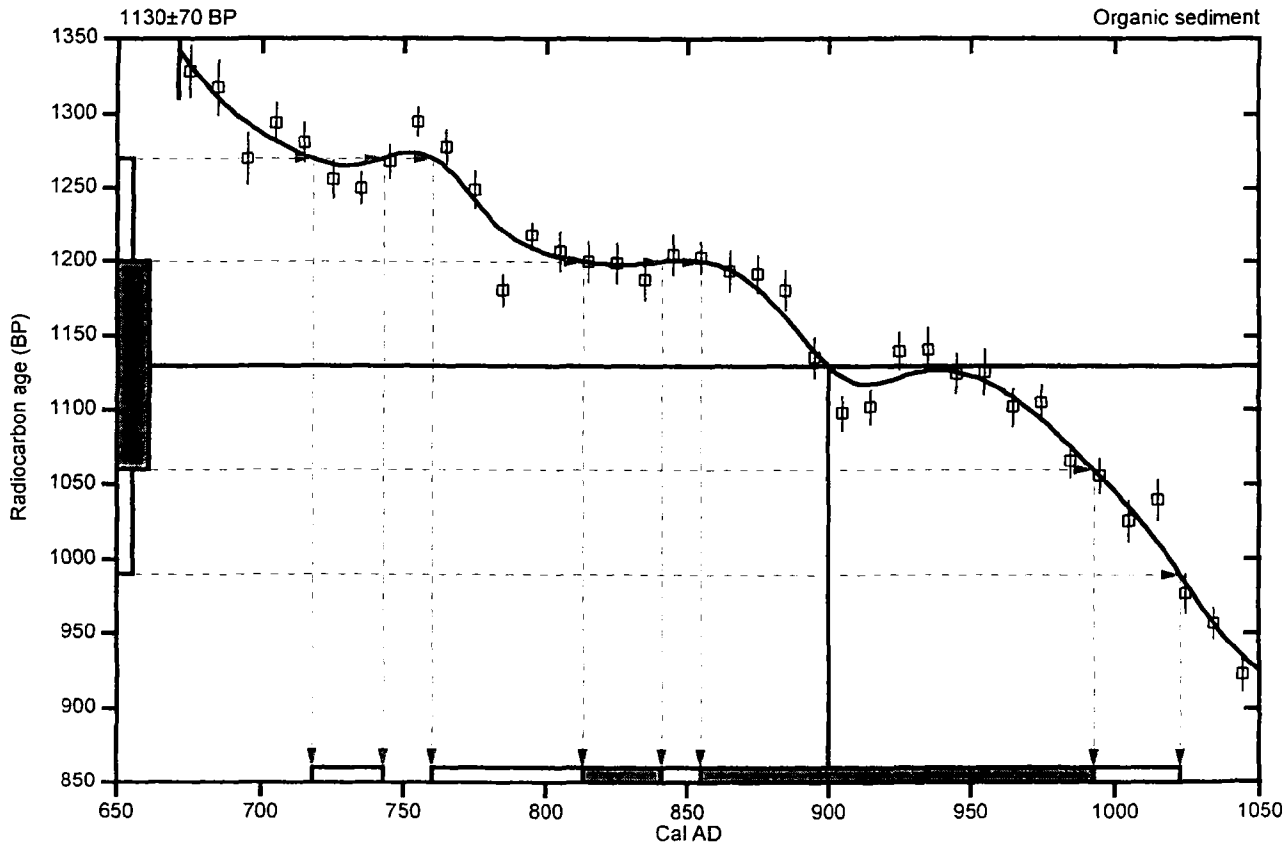

References:

Database used
INTCAL98
Calibration Database
Editorial Comment
Stuiver, M., van der Plicht, H., 1998, Radiocarbon 40(3), pxii-xiii
INTCAL98 Radiocarbon Age Calibration
Stuiver, M., et. al., 1998, Radiocarbon 40(3), p1041-1083
Mathematics
A Simplified Approach to Calibrating C14 Dates
Talma, A. S., Vogel, J. C., 1993, Radiocarbon 35(2), p317-322

Beta Analytic Radiocarbon Dating Laboratory

4985 S.W. 74th Court, Miami, Florida 33155 • Tel: (305)667-5167 • Fax: (305)663-0964 • E-mail: beta@radiocarbon.com

CALIBRATION OF RADIOCARBON AGE TO CALENDAR YEARS

(Variables: est. C13/C12=-25:lab. mult=1)

Laboratory number: **Beta-139249**

Conventional radiocarbon age[1]: **1310±60 BP**

2 Sigma calibrated result: (95% probability) **Cal AD 635 to 870 (Cal BP 1315 to 1080)**

[1] C13/C12 ratio estimated

Intercept data

Intercept of radiocarbon age with calibration curve: Cal AD 685 (Cal BP 1265)

1 Sigma calibrated result: (68% probability) Cal AD 660 to 770 (Cal BP 1290 to 1180)

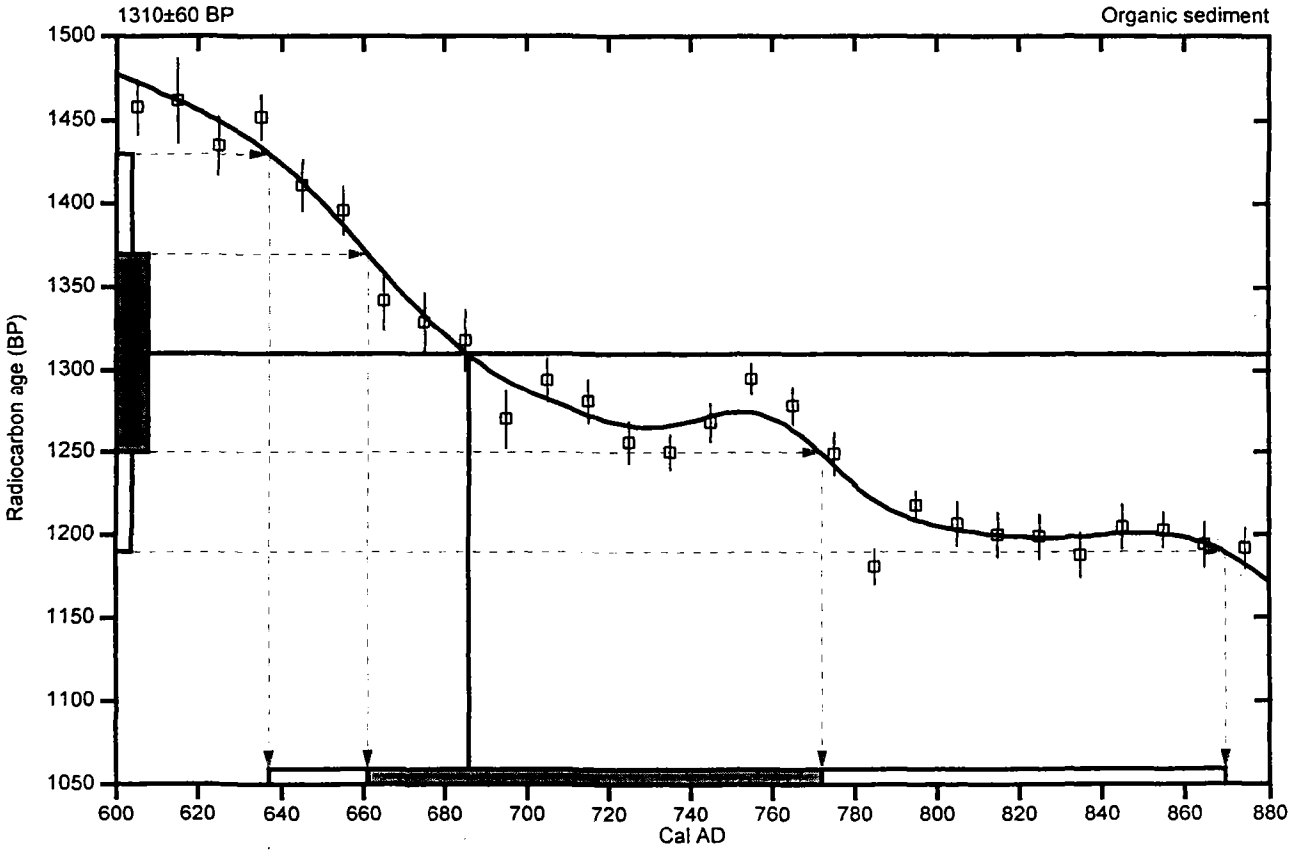

References:

Database used
INTCAL98
Calibration Database
Editorial Comment
Stuiver, M., van der Plicht, H., 1998, Radiocarbon 40(3), pxii-xiii
INTCAL98 Radiocarbon Age Calibration
Stuiver, M., et. al., 1998, Radiocarbon 40(3), p1041-1083
Mathematics
A Simplified Approach to Calibrating C14 Dates
Talma, A. S., Vogel, J. C., 1993, Radiocarbon 35(2), p317-322

Beta Analytic Radiocarbon Dating Laboratory

4985 S.W. 74th Court, Miami, Florida 33155 • Tel: (305)667-5167 • Fax: (305)663-0964 • E-mail: beta@radiocarbon.com

CALIBRATION OF RADIOCARBON AGE TO CALENDAR YEARS

(Variables: est. C13/C12=-25:lab. mult=1)

Laboratory number:	**Beta-139250**
Conventional radiocarbon age[1]:	**6640±180 BP**
2 Sigma calibrated result: (95% probability)	**Cal BC 5865 to 5285 (Cal BP 7815 to 7235)**

[1] C13/C12 ratio estimated

Intercept data

Intercepts of radiocarbon age with calibration curve:	Cal BC 5600 (Cal BP 7550) and Cal BC 5585 (Cal BP 7535) and Cal BC 5565 (Cal BP 7515)
1 Sigma calibrated result: (68% probability)	Cal BC 5710 to 5465 (Cal BP 7660 to 7415)

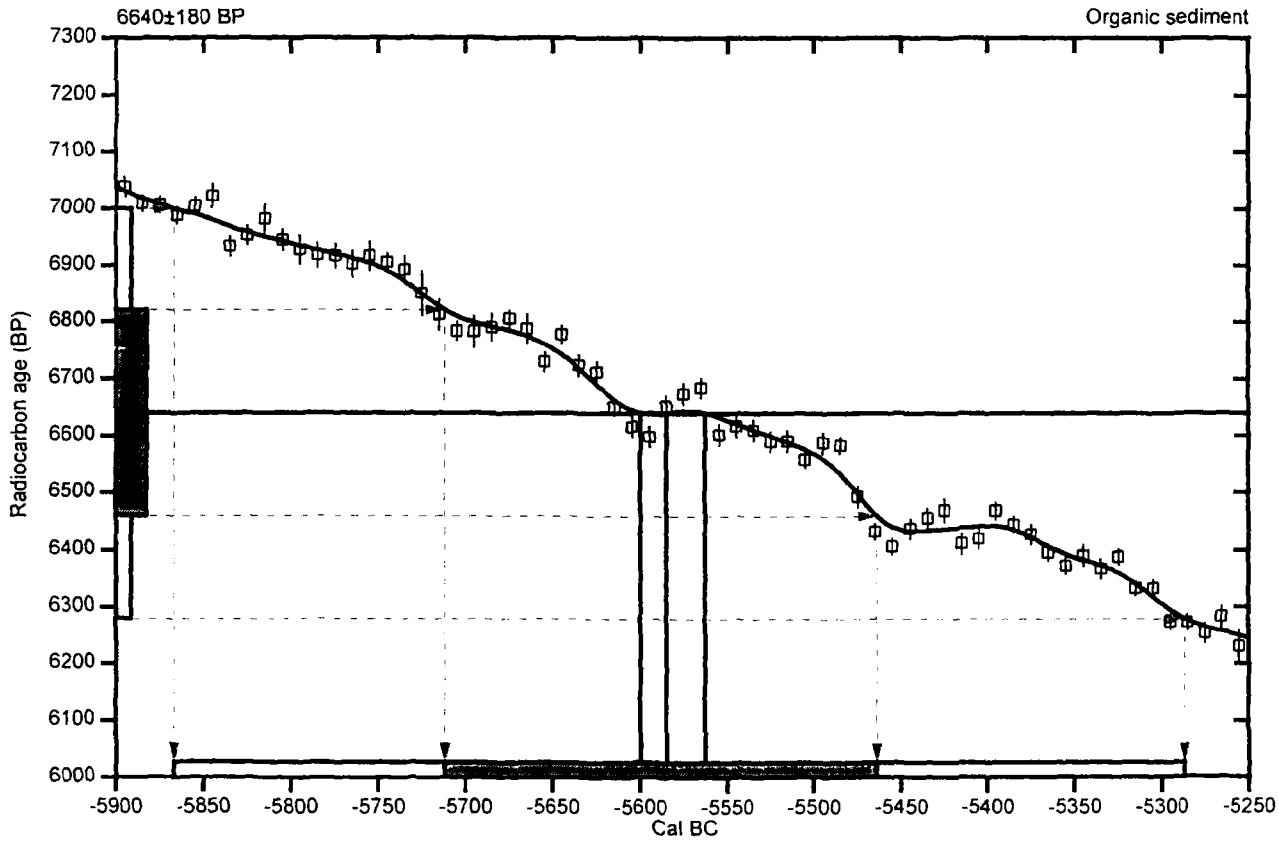

References:

Database used
INTCAL98
Calibration Database
Editorial Comment
Stuiver, M., van der Plicht, H., 1998, Radiocarbon 40(3), pxii-xiii
INTCAL98 Radiocarbon Age Calibration
Stuiver, M., et. al., 1998, Radiocarbon 40(3), p1041-1083
Mathematics
A Simplified Approach to Calibrating C14 Dates
Talma, A. S., Vogel, J. C., 1993, Radiocarbon 35(2), p317-322

Beta Analytic Radiocarbon Dating Laboratory

4985 S.W. 74th Court, Miami, Florida 33155 • Tel: (305)667-5167 • Fax: (305)663-0964 • E-mail: beta@radiocarbon.com

CALIBRATION OF RADIOCARBON AGE TO CALENDAR YEARS

(Variables: est. C13/C12=-25:lab. mult=1)

Laboratory number: **Beta-139251**

Conventional radiocarbon age[1]: **1570±70 BP**

2 Sigma calibrated result: (95% probability) **Cal AD 350 to 635 (Cal BP 1600 to 1315)**

[1] C13/C12 ratio estimated

Intercept data

Intercepts of radiocarbon age with calibration curve: Cal AD 465 (Cal BP 1485) and
Cal AD 480 (Cal BP 1470) and
Cal AD 520 (Cal BP 1430)

1 Sigma calibrated result: (68% probability) Cal AD 415 to 570 (Cal BP 1535 to 1380)

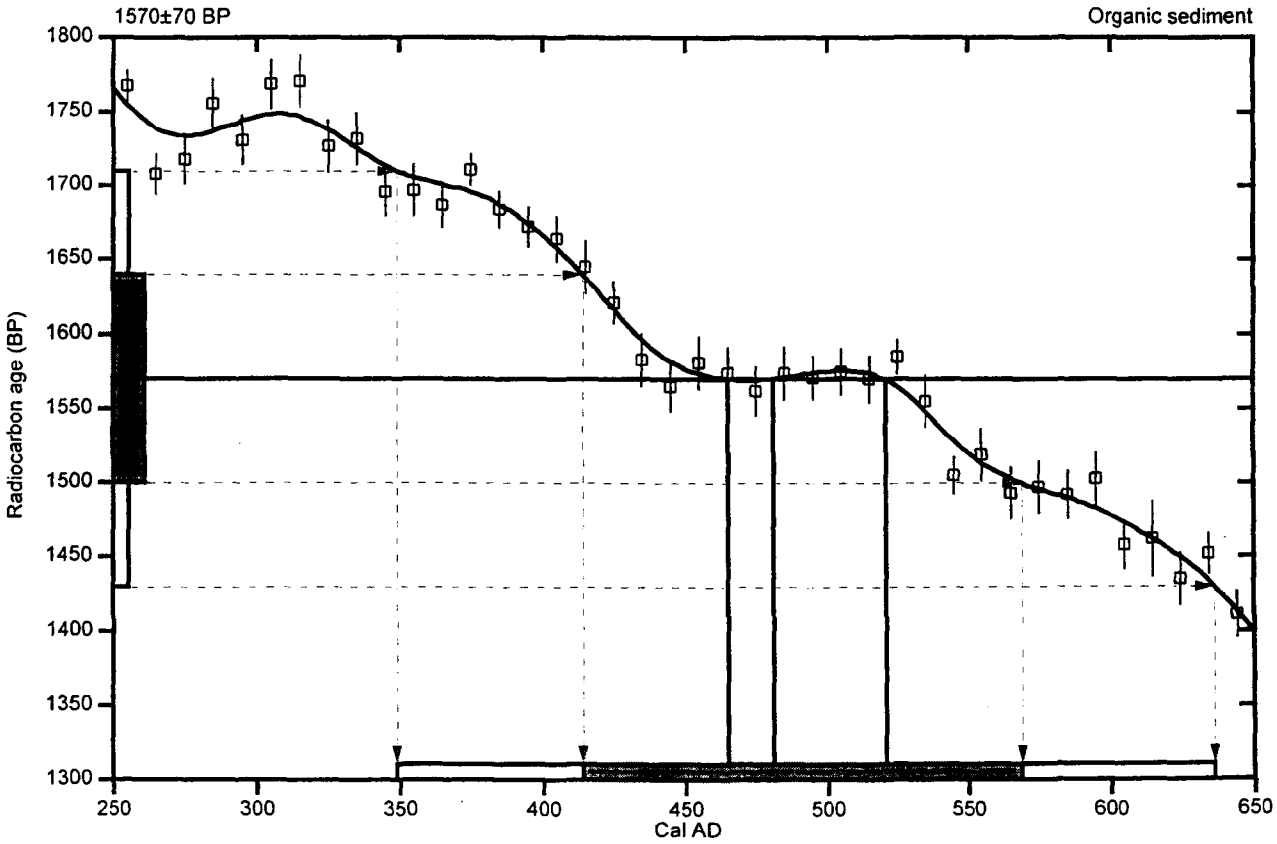

References:

Database used
INTCAL98
Calibration Database
Editorial Comment
Stuiver, M., van der Plicht, H., 1998, Radiocarbon 40(3), pxii-xiii
INTCAL98 Radiocarbon Age Calibration
Stuiver, M., et. al., 1998, Radiocarbon 40(3), p1041-1083
Mathematics
A Simplified Approach to Calibrating C14 Dates
Talma, A. S., Vogel, J. C., 1993, Radiocarbon 35(2), p317-322

Beta Analytic Radiocarbon Dating Laboratory

4985 S.W. 74th Court, Miami, Florida 33155 • Tel: (305)667-5167 • Fax: (305)663-0964 • E-mail: beta@radiocarbon.com

CALIBRATION OF RADIOCARBON AGE TO CALENDAR YEARS

(Variables: C13/C12=-25.2:lab. mult=1)

Laboratory number:	**Beta-139252**
Conventional radiocarbon age:	**3090±40 BP**
2 Sigma calibrated result: (95% probability)	**Cal BC 1430 to 1270 (Cal BP 3380 to 3220)**

Intercept data

Intercept of radiocarbon age with calibration curve:	Cal BC 1390 (Cal BP 3340)
1 Sigma calibrated result: (68% probability)	Cal BC 1410 to 1305 (Cal BP 3360 to 3255)

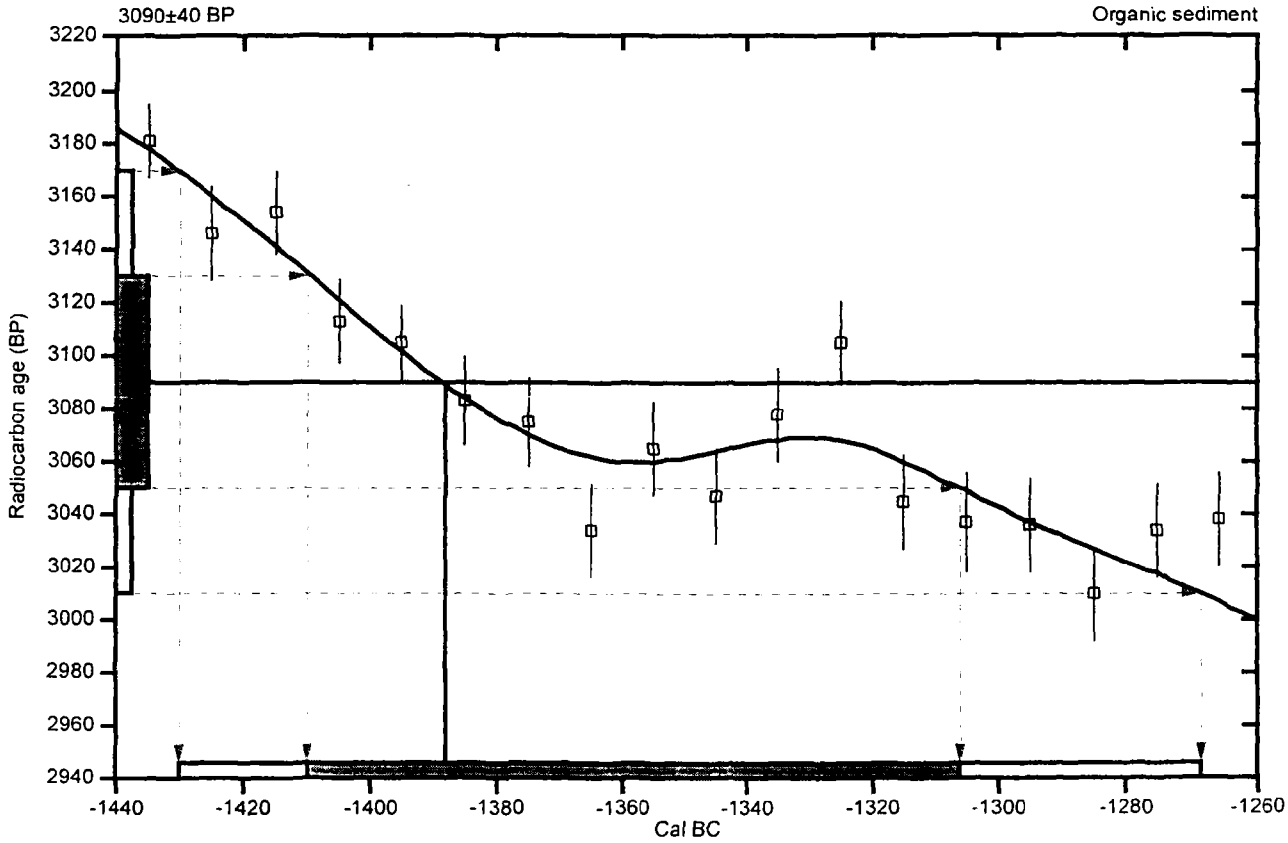

References:

Database used

INTCAL98

Calibration Database

Editorial Comment

Stuiver, M., van der Plicht, H., 1998, Radiocarbon 40(3), pxii-xiii

INTCAL98 Radiocarbon Age Calibration

Stuiver, M., et. al., 1998, Radiocarbon 40(3), p1041-1083

Mathematics

A Simplified Approach to Calibrating C14 Dates

Talma, A. S., Vogel, J. C., 1993, Radiocarbon 35(2), p317-322

Beta Analytic Radiocarbon Dating Laboratory

4985 S.W. 74th Court, Miami, Florida 33155 • Tel: (305)667-5167 • Fax: (305)663-0964 • E-mail: beta@radiocarbon.com

CALIBRATION OF RADIOCARBON AGE TO CALENDAR YEARS

(Variables: C13/C12=-24:lab. mult=1)

Laboratory number:	**Beta-139253**
Conventional radiocarbon age:	**8070±50 BP**
2 Sigma calibrated results: (95% probability)	**Cal BC 7145 to 7020 (Cal BP 9095 to 8970) and Cal BC 6965 to 6915 (Cal BP 8915 to 8865) and Cal BC 6880 to 6840 (Cal BP 8830 to 8790)**

Intercept data

Intercept of radiocarbon age with calibration curve:	Cal BC 7060 (Cal BP 9010)
1 Sigma calibrated result: (68% probability)	Cal BC 7075 to 7045 (Cal BP 9025 to 8995)

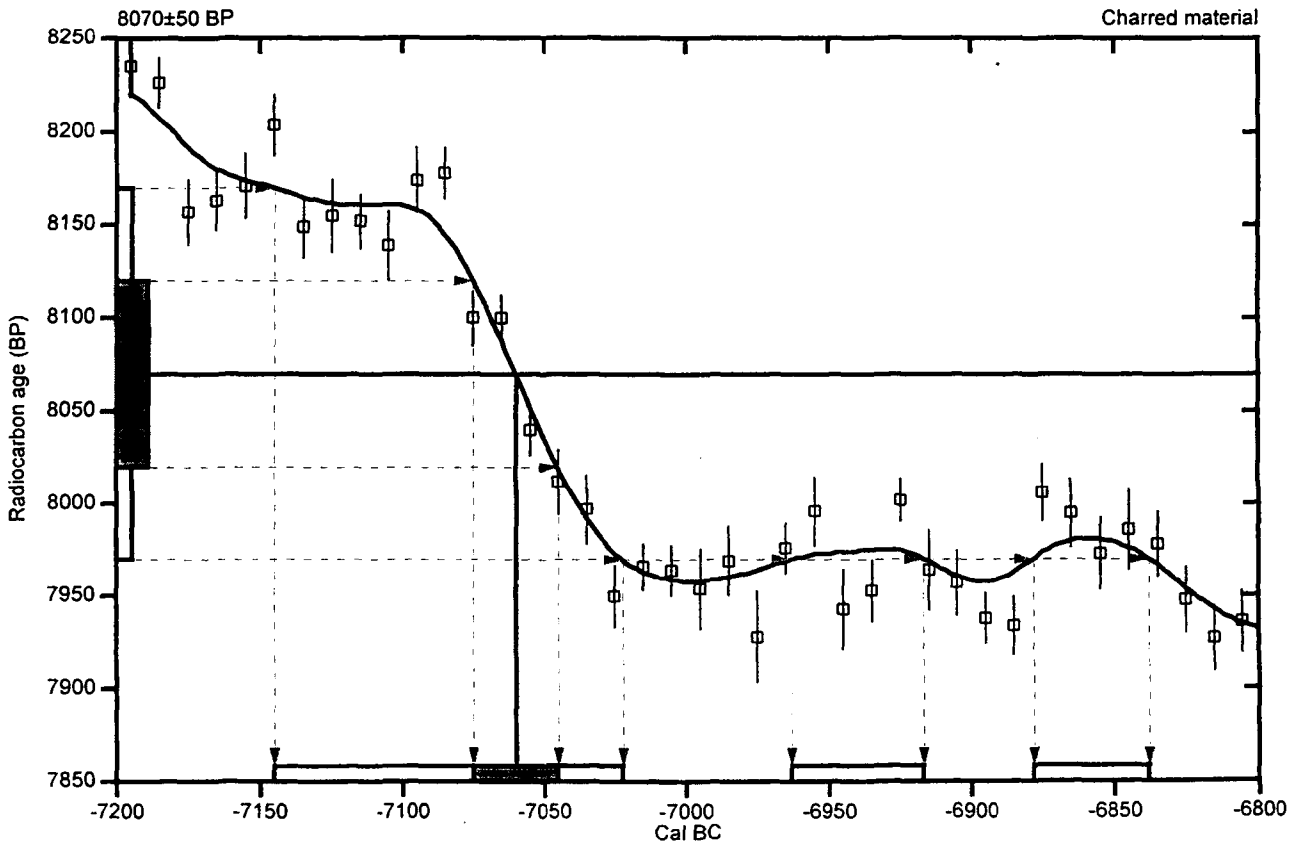

References:

Database used
INTCAL98
Calibration Database
Editorial Comment
Stuiver, M., van der Plicht, H., 1998, Radiocarbon 40(3), pxii-xiii
INTCAL98 Radiocarbon Age Calibration
Stuiver, M., et. al., 1998, Radiocarbon 40(3), p1041-1083
Mathematics
A Simplified Approach to Calibrating C14 Dates
Talma, A. S., Vogel, J. C., 1993, Radiocarbon 35(2), p317-322

Beta Analytic Radiocarbon Dating Laboratory

4985 S.W. 74th Court, Miami, Florida 33155 • Tel: (305)667-5167 • Fax: (305)663-0964 • E-mail: beta@radiocarbon.com

CALIBRATION OF RADIOCARBON AGE TO CALENDAR YEARS

(Variables: C13/C12=-24.9:lab. mult=1)

Laboratory number:	**Beta-139254**
Conventional radiocarbon age:	**8680±60 BP**
2 Sigma calibrated result: (95% probability)	**Cal BC 7930 to 7585 (Cal BP 9880 to 9535)**

Intercept data

Intercept of radiocarbon age with calibration curve:	Cal BC 7630 (Cal BP 9580)
1 Sigma calibrated result: (68% probability)	Cal BC 7760 to 7600 (Cal BP 9710 to 9550)

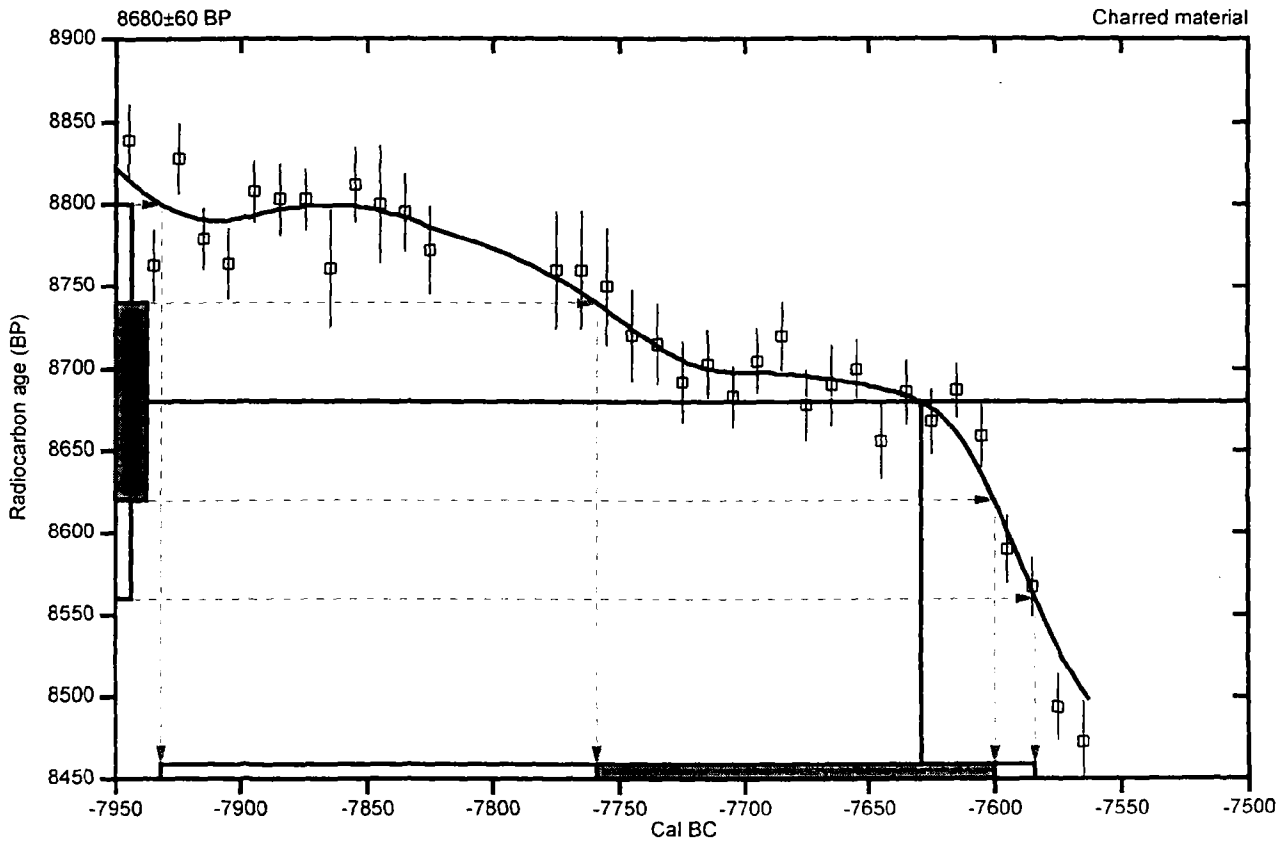

References:

Database used
INTCAL98
Calibration Database
Editorial Comment
Stuiver, M., van der Plicht, H., 1998, Radiocarbon 40(3), pxii-xiii
INTCAL98 Radiocarbon Age Calibration
Stuiver, M., et. al., 1998, Radiocarbon 40(3), p1041-1083
Mathematics
A Simplified Approach to Calibrating C14 Dates
Talma, A. S., Vogel, J. C., 1993, Radiocarbon 35(2), p317-322

Beta Analytic Radiocarbon Dating Laboratory

4985 S.W. 74th Court, Miami, Florida 33155 • Tel: (305)667-5167 • Fax: (305)663-0964 • E-mail: beta@radiocarbon.com

CALIBRATION OF RADIOCARBON AGE TO CALENDAR YEARS

(Variables: C13/C12=-25.5:lab. mult=1)

Laboratory number:	**Beta-139255**
Conventional radiocarbon age:	**10320±60 BP**
2 Sigma calibrated results: (95% probability)	**Cal BC 10815 to 10795 (Cal BP 12765 to 12745) and Cal BC 10705 to 10510 (Cal BP 12655 to 12460) and Cal BC 10450 to 9915 (Cal BP 12400 to 11865)**

Intercept data

Intercepts of radiocarbon age with calibration curve:	Cal BC 10345 (Cal BP 12295) and Cal BC 10280 (Cal BP 12230) and Cal BC 10180 (Cal BP 12130)
1 Sigma calibrated results: (68% probability)	Cal BC 10625 to 10565 (Cal BP 12575 to 12515) and Cal BC 10420 to 9965 (Cal BP 12370 to 11915)

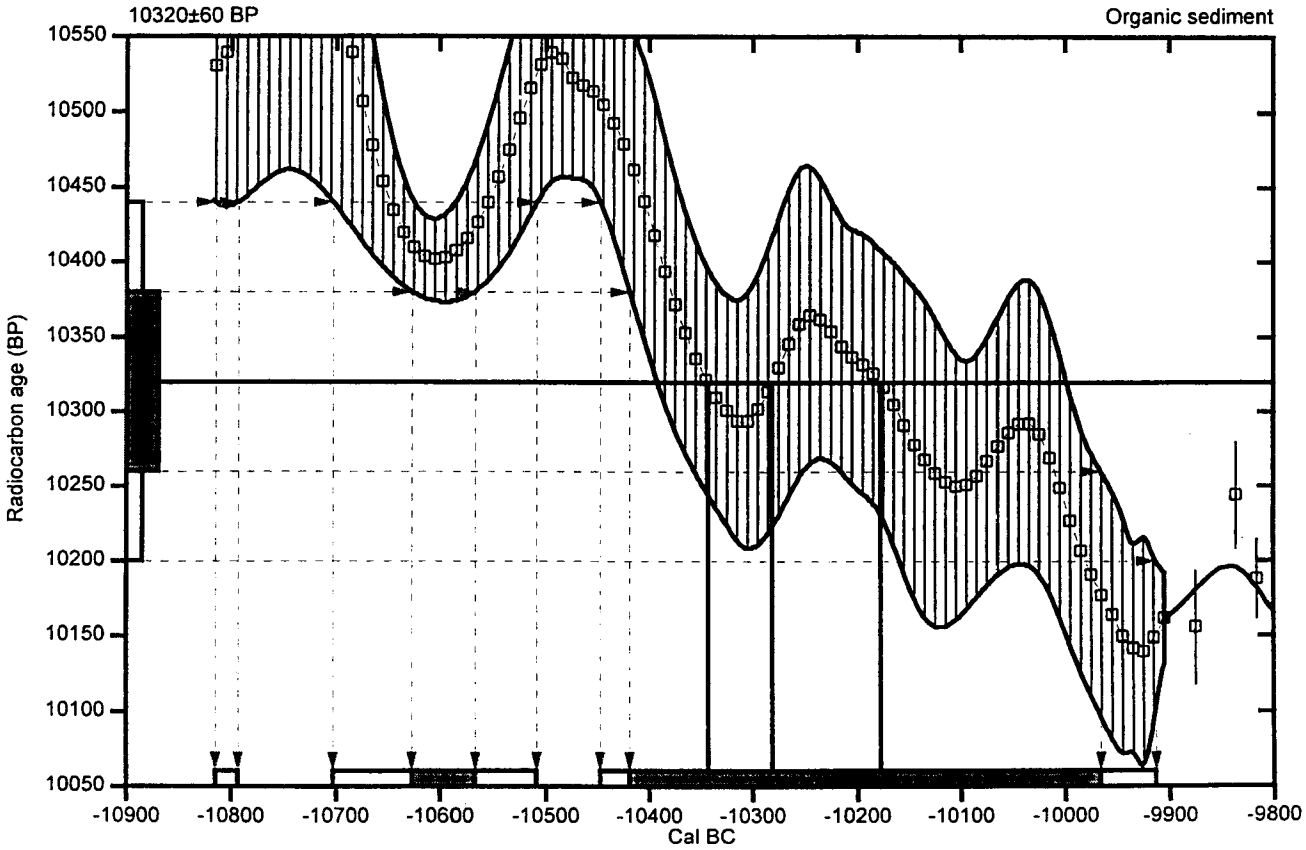

References:

Database used
INTCAL98
Calibration Database
Editorial Comment
Stuiver, M., van der Plicht, H., 1998, Radiocarbon 40(3), pxii-xiii
INTCAL98 Radiocarbon Age Calibration
Stuiver, M., et. al., 1998, Radiocarbon 40(3), p1041-1083
Mathematics
A Simplified Approach to Calibrating C14 Dates
Talma, A. S., Vogel, J. C., 1993, Radiocarbon 35(2), p317-322

Beta Analytic Radiocarbon Dating Laboratory

4985 S.W. 74th Court, Miami, Florida 33155 • Tel: (305)667-5167 • Fax: (305)663-0964 • E-mail: beta@radiocarbon.com

CALIBRATION OF RADIOCARBON AGE TO CALENDAR YEARS

(Variables: est. C13/C12=-25:lab. mult=1)

Laboratory number:	**Beta-139256**
Conventional radiocarbon age[1]:	**10260±330 BP**
2 Sigma calibrated results: (95% probability)	**Cal BC 11050 to 9130 (Cal BP 13000 to 11080) and Cal BC 8985 to 8920 (Cal BP 10935 to 10870)**

[1] C13/C12 ratio estimated

Intercept data

Intercepts of radiocarbon age with calibration curve:	Cal BC 10125 (Cal BP 12075) and Cal BC 10080 (Cal BP 12030) and Cal BC 10010 (Cal BP 11960)
1 Sigma calibrated result: (68% probability)	Cal BC 10900 to 9320 (Cal BP 12850 to 11270)

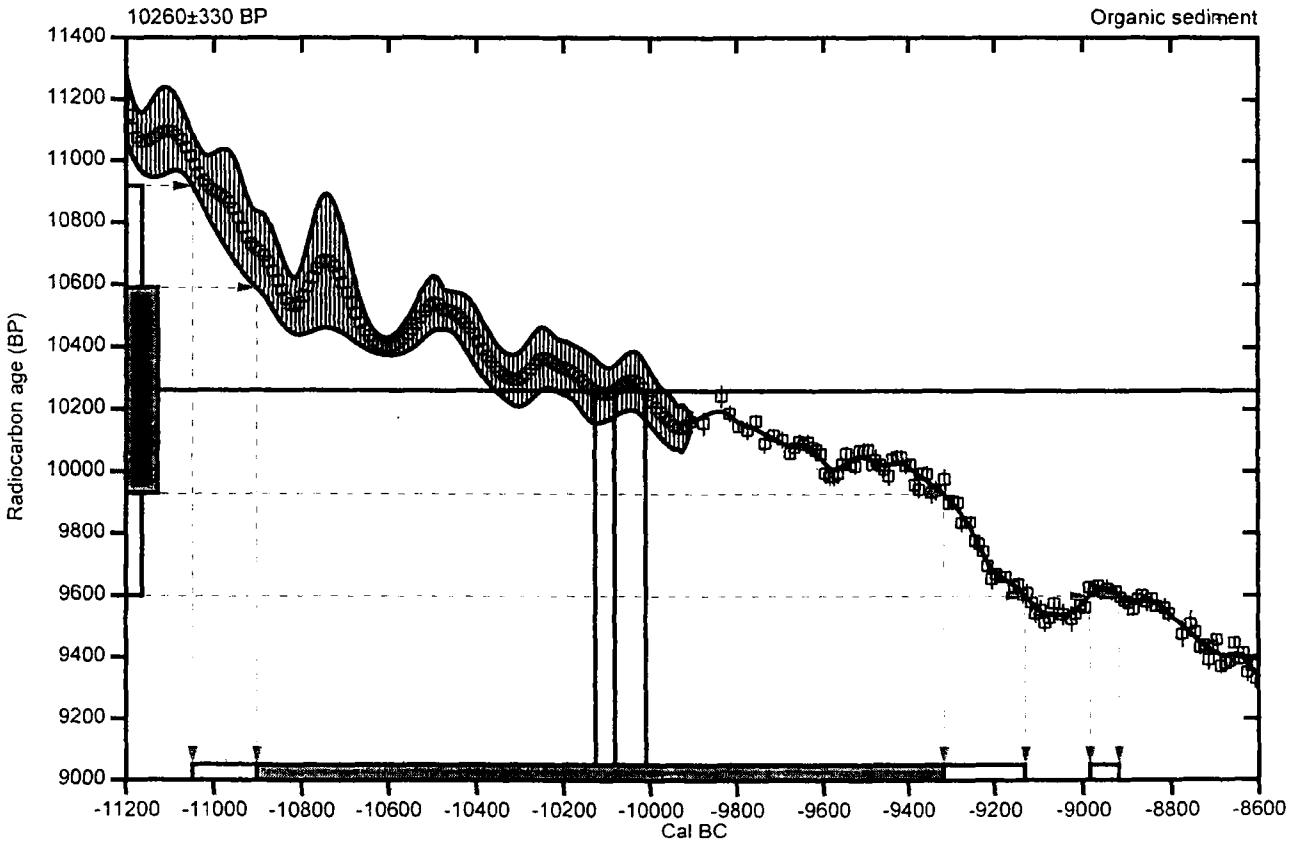

References:

Database used
INTCAL98
Calibration Database
Editorial Comment
Stuiver, M., van der Plicht, H., 1998, Radiocarbon 40(3), pxii-xiii
INTCAL98 Radiocarbon Age Calibration
Stuiver, M., et. al., 1998, Radiocarbon 40(3), p1041-1083
Mathematics
A Simplified Approach to Calibrating C14 Dates
Talma, A. S., Vogel, J. C., 1993, Radiocarbon 35(2), p317-322

Beta Analytic Radiocarbon Dating Laboratory

4985 S.W. 74th Court, Miami, Florida 33155 • Tel: (305)667-5167 • Fax: (305)663-0964 • E-mail: beta@radiocarbon.com